



GREEN 2016

The First International Conference on Green Communications, Computing and
Technologies

ISBN: 978-1-61208-524-1

July 24 - 28, 2016

Nice, France

GREEN 2016 Editors

Birgit Gersbeck-Schierholz, Leibniz Universität Hannover, Germany

Guillaume Habault, Télécom Bretagne, France

GREEN 2016

Forward

The First International Conference on Green Communications, Computing and Technologies (GREEN 2016), held between July 24-28, 2016 in Nice, France, was an inaugural event focusing on current green solutions, stringent requirements for further development, and evaluations of potential directions. The event targets are bringing together academia, research institutes, and industries working towards green solutions.

Expected economic, environmental and society wellbeing impact of green computing and communications technologies led to important research and solutions achievements in recent years. Environmental sustainability, high-energy efficiency, diversity of energy sources, renewable energy resources contributed to new paradigms and technologies for green computing and communication.

Economic metrics and social acceptability are still under scrutiny, despite the fact that many solutions, technologies and products are available. Deployment at large scale and a long term evaluation of benefits are under way in different areas where dedicated solutions are applied.

The conference had the following tracks:

- Green computing and communication technologies
- Smart greed
- Energy awareness

We take here the opportunity to warmly thank all the members of the GREEN 2016 technical program committee, as well as all the reviewers. The creation of such a high quality conference program would not have been possible without their involvement. We also kindly thank all the authors that dedicated much of their time and effort to contribute to GREEN 2016. We truly believe that, thanks to all these efforts, the final conference program consisted of top quality contributions.

Also, this event could not have been a reality without the support of many individuals, organizations and sponsors. We also gratefully thank the members of the GREEN 2016 organizing committee for their help in handling the logistics and for their work that made this professional meeting a success.

We hope GREEN 2016 was a successful international forum for the exchange of ideas and results between academia and industry and to promote further progress in the field of green communications, computing and technology. We also hope that Nice, France provided a pleasant environment during the conference and everyone saved some time enjoy the beautiful French Riviera.

GREEN 2016 Advisory Committee

Steffen Fries, Siemens AG, Germany

Carlos Becker Westphall, Federal University of Santa Catarina - Florianópolis, Brazil

Daisuke Mashima, Advanced Digital Sciences Center, Singapore

Bo Nørregaard Jørgensen, University of Southern Denmark, Denmark

Enrique Romero-Cadaval, University of Extremadura, Spain

Camille Salinesi, Université Paris 1 Panthéon - Sorbonne, France

Sotirios Ziavras, New Jersey Institute of Technology, USA

GREEN 2016 Special Area Chairs

Green Computing and Internet of Things

Sandra Sendra Compte, University of Granada, Spain

GREEN 2016

Committee

GREEN 2016 Advisory Committee

Steffen Fries, Siemens AG, Germany
Carlos Becker Westphall, Federal University of Santa Catarina - Florianópolis, Brazil
Daisuke Mashima, Advanced Digital Sciences Center, Singapore
Bo Nørregaard Jørgensen, University of Southern Denmark, Denmark
Enrique Romero-Cadaval, University of Extremadura, Spain
Camille Salinesi, Université Paris 1 Panthéon - Sorbonne, France
Sotirios Ziavras, New Jersey Institute of Technology, USA

GREEN 2016 Special Area Chairs

Green Computing and Internet of Things

Sandra Sendra Compte, University of Granada, Spain

GREEN 2016 Technical Program Committee

Daniel Ahlin, PDC, KTH, Sweden
Ayşe Başar Bener, Ryerson University, Canada
Carlos Becker Westphall, Federal University of Santa Catarina - Florianópolis, Brazil
Lamya Belhaj, Icam / IREENA, France
Siegfried Benkner, University of Vienna, Austria
Aoued Boukelif, University of SBA, Algeria
Massimo Canonico, University of Piemonte Orientale, Italy
Yuen Chau, Singapore University of Technology and Design, Singapore
Ruzanna Chitchyan, University of Leicester, UK
David (Bong Jun) Choi, SUNY Korea, South Korea
Fabrice Dupros, BRGM, France
Wilfried Elmenreich, University of Klagenfurt, Austria
Steffen Fries, Siemens AG, Germany
Holger Fröning, University of Heidelberg, Germany
Roberto Gioiosa, Pacific Northwest National Laboratory, USA
Chris Gniady, University of Arizona, USA
Marco Guazzone, University of Piemonte Orientale, Italy
Sekhar Kondepudi, National University of Singapore, Singapore
Anna Magdalena Kosek, Technical University of Denmark, Denmark
Erwin Laure, Royal Institute of Technology (KTH), Sweden
Zhenhua Liu, Stony Brook University, USA
Zheng Ma, University of Southern Denmark, Denmark
Daisuke Mashima, Advanced Digital Sciences Center, Singapore
Jean-Marc Menaud, Mines Nantes | INRIA | LINA, France

M^a Ángeles Moraga, University of Castilla-La Mancha, Spain
Masayuki Murata, Osaka University, Japan
Bruce Nordman, Lawrence Berkeley National Laboratory, USA
Bo Nørregaard Jørgensen, University of Southern Denmark, Denmark
Wolfgang Reif, University of Augsburg, Germany
Enrique Romero-Cadaval, University of Extremadura, Spain
Camille Salinesi, Université Paris 1 Panthéon - Sorbonne, France
Mat Santamouris, National and Kapodistrian University of Athens, Greece
Sandra Sendra Compte, University of Granada, Spain
Heikki Seppä, VTT, Finland
Vinod Kumar Sharma, Italian National Agency for New Technologies, Energy and Sustainable Economic Development (ENEA), Italy
Sabu M. Thampi, Indian Institute of Information Technology and Management - Kerala (IIITM-K), India
Chresten Træholt, Technical University of Denmark, Denmark
Zita A. Vale, ISEP/IPP, Portugal
Sotirios Zivarras, New Jersey Institute of Technology, USA

Copyright Information

For your reference, this is the text governing the copyright release for material published by IARIA.

The copyright release is a transfer of publication rights, which allows IARIA and its partners to drive the dissemination of the published material. This allows IARIA to give articles increased visibility via distribution, inclusion in libraries, and arrangements for submission to indexes.

I, the undersigned, declare that the article is original, and that I represent the authors of this article in the copyright release matters. If this work has been done as work-for-hire, I have obtained all necessary clearances to execute a copyright release. I hereby irrevocably transfer exclusive copyright for this material to IARIA. I give IARIA permission to reproduce the work in any media format such as, but not limited to, print, digital, or electronic. I give IARIA permission to distribute the materials without restriction to any institutions or individuals. I give IARIA permission to submit the work for inclusion in article repositories as IARIA sees fit.

I, the undersigned, declare that to the best of my knowledge, the article does not contain libelous or otherwise unlawful contents or invading the right of privacy or infringing on a proprietary right.

Following the copyright release, any circulated version of the article must bear the copyright notice and any header and footer information that IARIA applies to the published article.

IARIA grants royalty-free permission to the authors to disseminate the work, under the above provisions, for any academic, commercial, or industrial use. IARIA grants royalty-free permission to any individuals or institutions to make the article available electronically, online, or in print.

IARIA acknowledges that rights to any algorithm, process, procedure, apparatus, or articles of manufacture remain with the authors and their employers.

I, the undersigned, understand that IARIA will not be liable, in contract, tort (including, without limitation, negligence), pre-contract or other representations (other than fraudulent misrepresentations) or otherwise in connection with the publication of my work.

Exception to the above is made for work-for-hire performed while employed by the government. In that case, copyright to the material remains with the said government. The rightful owners (authors and government entity) grant unlimited and unrestricted permission to IARIA, IARIA's contractors, and IARIA's partners to further distribute the work.

Table of Contents

Enabling Green Heterogeneous Wireless Networks <i>Muhammad Ismail, Erchin Serpedin, and Khalid Qaraqe</i>	1
Path Loss Analysis and Verification by Ray-Tracing for 3.5GHz Outdoor Environments <i>Seoungwoo Kim, Byungjin Lee, and Kyungseok Kim</i>	7
Channel Measurement and Characteristics Analysis on 3.5GHz Outdoor Environment <i>Bong-Gu Yeo, Byung Jin Lee, and Kyung-Seok Kim</i>	11
Indirect Demand Side Management Program Under Real-Time Pricing in Smart Grids Using Oligopoly Market Model <i>Poria Poria Hasanpor Divshali and Bong Jun Choi</i>	15
Simulation of Electric Vehicle Battery Behaviour for Frequency Regulation Use: Profitability Versus Mobility Constraints and Grid Needs <i>Lamy Abdeljalil Belhaj, Antoine Aubineau, Antoine Cannieux, Salome Rioult, Isabel Praca, and Zita Vale</i>	22
Outsourcing Electric Vehicle Smart Charging on the Web of Data <i>Maxime Lefrancois, Guillaume Habault, Caroline Ramondou, and Eric Francon</i>	29
Hypergraph of Massive Digital Traces as Representation of Human Activities: A Way to Reduce Energy Consumption by Identifying Sustainable Practices <i>Eddie Soulier and Philippe Calvez</i>	36
SWIM: Social Welfare Maximizing Incentive Mechanism for Smart Meter Data Aggregation <i>Duin Back and Bongjun Choi</i>	42
Channel Allocation Plan for DAB and DRM+ Systems in VHF Band III <i>Youngjae Kim, Sanglim Ju, and Kyungseok Kim</i>	49

Enabling Green Heterogeneous Wireless Networks

Muhammad Ismail

Department of Electrical and
Computer Engineering
Texas A&M University at Qatar
Doha, Qatar

email: m.ismail@qatar.tamu.edu

Erchin Serpedin

Department of Electrical and
Computer Engineering
Texas A&M University
College Station, USA

email: serpedin@ece.tamu.edu

Khalid Qaraqe

Department of Electrical and
Computer Engineering
Texas A&M University at Qatar
Doha, Qatar

email: khalid.qaraqe@qatar.tamu.edu

Abstract—This paper focuses on a significant research topic “green/energy efficient wireless networks” that has drawn huge attention due to important environmental, financial, and quality-of-experience (QoE) considerations. We mainly target energy efficiency in a heterogeneous wireless medium with overlapped coverage due to the co-existence of different cells (macro, micro, pico, and femto), networks (cellular networks, wireless local areas networks, wireless metropolitan area networks), and technologies (radio frequency (RF) and visible light communications (VLC)). This paper summarizes the authors’ research work in green networking via radio resource and network management solutions. First, we present green multi-homing radio resource management mechanisms in downlink and uplink for both RF and RF-VLC heterogeneous networks. These techniques can be adopted at high call traffic load conditions. Then, we present balanced dynamic planning framework that can be adopted at low call traffic load conditions.

Keywords—Green networking; multi-homing resource allocation; dynamic planning.

I. INTRODUCTION

The increasing demand for wireless communications services during the past decade has led to a wide deployment of wireless access networks [1]. From the network operator point of view, the base station (BS) is the main source of energy consumption in the wireless access network (with almost 57% of the operator total power consumption) [2] [3] [4]. From the user perspective, high energy is consumed by mobile terminals (MTs) in video and data calls. This high energy consumption of BSs and MTs has raised environmental, financial, and quality-of-experience (QoE) concerns.

From an environmental perspective, the telecommunications industry contributes by 2% of the total CO₂ emissions worldwide, and such a percentage is expected to double by 2020 [5]. In addition, the expected lifetime of the MT rechargeable batteries is approximately 2–3 years and results in 25,000 tons of disposed batteries annually [6]. Moreover, the high energy consumption in wireless networks presents a source of high heat dissipation and electronic pollution [7]. From a financial point of view, technical reports have demonstrated that the cost of energy bills of service providers ranges from 18% (in mature markets in Europe) to 32% (in India) of the operational expenditure (OPEX) [8] [9] and reach up to 50% of the OPEX for cellular networks outside the power grid [10] [11]. From a user QoE perspective, reports indicate that over 60% of mobile users complain about their limited battery capacity due to the increasing gap between the MT

offered battery capacity and the mobile user demand for energy [12].

Such concerns have motivated an increasing demand for energy efficient (green) solutions in wireless access networks. The research efforts carried out in this regard are referred to as green network solutions. The main objectives of such a paradigm are: 1) reducing energy consumption of communication devices (e.g., BSs and MTs) and 2) taking into account the environmental impacts of the proposed solutions. In this paper, we present our most recent research efforts in this direction for both high and low call traffic load conditions. At a high call traffic load condition, radio resource (e.g., power and bandwidth allocation) management techniques are adopted, while network management solutions (e.g., dynamic planning) are applied.

The rest of this paper is organized as follows. Section II reviews the related work in green networks at both high and low call traffic load conditions. Section III summarizes our research contributions for green solutions at a high call traffic load condition via a multi-homing radio resource allocation. Section IV summarizes our research contributions at a low call traffic load condition via a balanced dynamic planning approach. Finally, Section V presents conclusions and future research directions.

II. GREEN SOLUTIONS: STATE-OF-THE-ART

This section reviews state-of-the-art green networking solutions and analytical models from network operator and mobile user perspectives at different traffic load conditions. Overall, two categories can be distinguished for the green networking solutions based on the call traffic load condition. Scheduling techniques are adopted at a high and/or continuous call traffic load, while resource on-off switching techniques are implemented at a low and/or bursty call traffic load [13].

Different scheduling techniques are employed at a high call traffic load condition. BSs can save energy via a margin adaptive strategy where the objective is to minimize the transmission power consumption while ensuring an acceptable service quality for mobile users [14]. Furthermore, in a heterogeneous wireless medium with overlapped coverage from different BSs, energy saving can be achieved by assigning MTs to the BSs that consume the least transmission power [15]. On the other hand, MTs can save energy through sub-carrier allocation and carrier aggregation techniques in orthogonal frequency division multiple access (OFDMA) networks [16],

while in time division multiple access (TDMA) networks, MTs save energy by opportunistic transmission [17]. Moreover, BSs and MTs can save energy in a heterogeneous wireless medium through multi-homing resource allocation. In this case, the MT simultaneously connects to multiple BSs and aggregates the offered resources from these BSs to achieve the required data rate. BSs can save energy in the downlink by coordinating their transmission power for different radio interfaces of the MT [18]. Similarly, MTs can save energy in the uplink through efficient transmission power allocation to different radio interfaces. In addition, small cell deployment can save energy for both BSs and MTs by dividing the cell into several tiers of smaller cells, and hence, reducing the transmission range for BSs and MTs [19]. In this context, cell-on-edge deployment can achieve more energy saving than uniform cell deployment [19]. The main research challenge here is how to deal with cross-tier interference between macro and small cells [20]. Another approach that reduces the transmission range for BSs and MTs and hence achieves energy saving relies on relays or device-to-device (D2D) communications. When fixed relays are deployed for energy saving, two research issues must be handled, namely, optimal relay placement and relay selection for minimum transmission power consumption [21]. Employing MTs as relays necessitates adopting incentive techniques to motivate selfish mobile users to participate in data forwarding [22]. In D2D communications, mobile nodes in close proximity communicate directly with each other without going through a BS. In this context, interference issues with cellular users should be tackled for in-band underlay D2D communications [23], while efficient radio resource partitioning should be adopted for in-band overlay D2D communications [24], and coordination techniques should be employed for out-band D2D communications [25]. Moreover, BSs and MTs can save energy through efficient scheduling among multiple energy sources. For instance, the network operator can rely on multiple electricity retailers and decides how much electricity to procure from each retailer to power the BSs using minimum cost and CO₂ emissions [26]. Also, using a mixture of on-grid and green energy sources can lead to energy saving by maximizing the utilization of green energy [27]. In this case, complementary renewable sources (e.g., solar cells and wind turbines) can be used to power the BSs [28]. For MTs, multiple batteries can be employed where energy efficiency is improved due to the batteries recovery effect [29].

At a low and/or bursty call traffic load condition, resource on-off switching is adopted for energy saving. Specifically, dynamic planning can be adopted where BSs with low call traffic load can be switched off and the remaining active BSs can support the ongoing calls [30]. Dynamic planning mainly involves two phases, namely, user association and BS operation. In user association, MTs are concentrated in a few BSs to enable switching off lightly loaded BSs [31]. However, such a problem is highly complex due to its mixed-integer nature. Consequently, greedy algorithms are adopted to enable a suboptimal switching decision. In this context, greedy algorithms can be based on user-BS distance decision criterion [32], network impact decision criterion [33], and coverage hole avoidance decision criterion [34]. Following the user association phase, three tasks should be carried out in the BS operation phase, namely, accommodating future traffic loads via bandwidth reservation [5], determining BS wake-

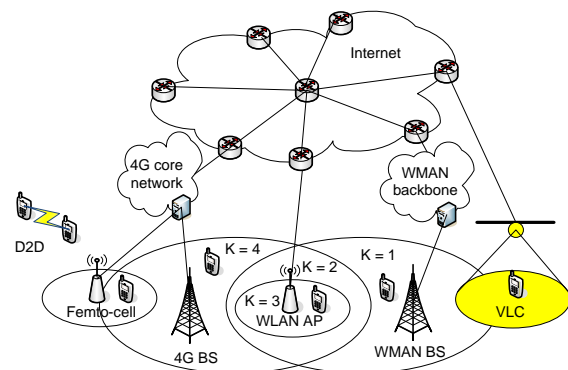


Figure 1. Illustration of a heterogeneous wireless network [30].

up instants [35], and implementing the BS on-off switching decision via BS wilting and blossoming [36]. For MTs, energy saving can be achieved by on-off switching of the MT radio interface according to traffic load condition. For downlink traffic, the MT switches off its radio interface when no data packets are available for the MT at the serving BS [37]. To further elongate the sleep duration, and hence, save more energy, traffic shaping techniques can be adopted either at the MT side [38] or at the BS side [39] to enable a more bursty traffic. For uplink traffic, the MT performs joint optimization of radio interface on-off switching, transmission power control, and modulation and coding scheme selection [40]. In presence of bi-directional traffic, a finite general Markov background process is employed to model the uplink and downlink traffic activity [41].

III. GREEN MULTI-HOMING RESOURCE ALLOCATION

Currently, the wireless communication medium is a heterogeneous environment with overlapped coverage from different cells (macro, micro, pico, and femto), networks (cellular networks, wireless local area networks (WLANs), and wireless metropolitan area networks (WMANs)), and technologies (radio frequency (RF) and visible light communication (VLC)), as shown in Figure 1.

In a multi-homing access, the MT connects to all available BSs of different networks, and radio resources (e.g., bandwidth and power) are allocated to improve energy efficiency in the networking environment. In the following, we highlight our recent research efforts in green multi-homing resource allocation for uplink and downlink scenarios and for RF and RF-VLC inter-networking environments.

A. Green Uplink Multi-homing

One limitation with the existing mechanisms is that they focus mainly on optimal power allocation to the MT different radio interfaces, assuming an allocated bandwidth. These research efforts aim to exploit the diversity in fading channels and propagation losses between the MT and different BSs to improve the uplink energy efficiency. Further improvement can be achieved due to the disparity in available bandwidth at the BSs of different networks. This necessitates a joint optimization framework for bandwidth and power allocation to maximize uplink energy efficiency. Moreover, the existing aggregation schemes deal with a situation where all radio resources are operated by the same service provider. Thus,

centralized radio resource allocation mechanisms can be employed. In a heterogeneous networking environment, the aggregated resources belong to different service providers. As a result, novel decentralized mechanisms should be investigated to enable coordination among MTs and BSs of different networks to satisfy the required QoS in an energy efficient manner. One challenge that faces implementing such a decentralized mechanism is the associated high computational complexity. Finally, the existing research deals with a single-user system where the objective is to maximize energy efficiency for a given mobile user. In practice, multi-user systems exist where multiple mobile users compete on the available bandwidth to satisfy their target service quality in an energy efficient manner. In this context, maximizing the total (sum) energy efficiency of all MTs may not be a good choice since the sum energy efficiency can be maximized while some MTs achieve very low energy efficiency.

In our research [42], we investigate the problem of joint uplink bandwidth and power allocation to maximize energy efficiency of a set of MTs with multi-homing capabilities. In such a multi-user system, the objective is to maximize the performance of the MT that achieves the minimum energy efficiency in the geographical region. For each MT, energy efficiency is defined as the ratio of the total achieved data rate to the total power consumption. The total achieved data rate for each MT is the summation of the data rates achieved on each radio interface of the MT. Power consumption of the MT accounts for both circuit and transmission power consumption, and circuit power consumption has two parts, namely, fixed power consumption and dynamic (bandwidth scaling) power consumption. The resource allocation framework should satisfy the minimum required data rate for each MT and should respect the power consumption constraint for each MT and the bandwidth availability constraint for each BS. The optimization problem in [42] is shown to be a max-min concave-convex fractional program. Through a parametric approach, the problem is transformed into a convex optimization problem. The optimal solution can be obtained using an iterative Dinkelbach-type algorithm. For each step, the convex optimization problem should be solved to determine the joint bandwidth and power allocation that satisfy the aforementioned constraints for a given parameter. The decomposition theory is applied to solve the optimization problem, which is decomposed into a power allocation sub-problem and a bandwidth-allocation sub-problem. Through Lagrangian multipliers, the two sub-problems are iteratively solved to satisfy the minimum required data rate. Due to computational complexity, a sub-optimal framework is designed, which is based on determining the optimal Lagrangian multipliers for maximizing the minimum average energy efficiency while satisfying the average data rate constraint. Such Lagrangian multipliers are then used in an online phase to allocate radio resources to MTs according to the current channel conditions.

Simulation results in [42] have indicated an improved energy efficiency performance over a power only allocation benchmark, as shown in Figure 2, along with an improved satisfaction index for the mobile users.

B. Green Downlink Multi-homing

Cooperative multi-homing radio resource allocation mechanisms can achieve higher energy saving compared with the

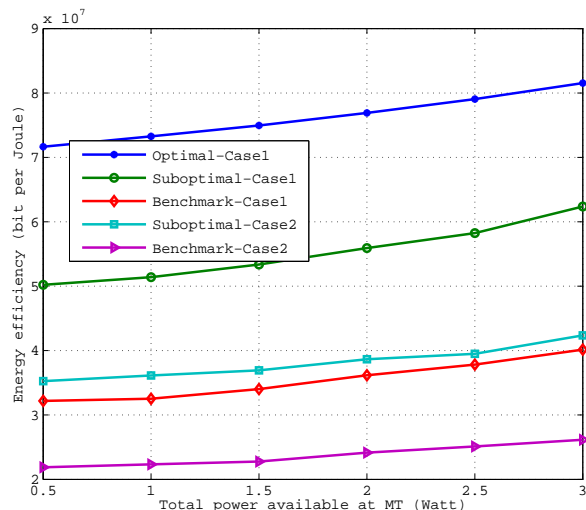


Figure 2. Average achieved energy efficiency versus total power available at each MT [42].

single-network radio resource allocation mechanisms thanks to the disparity in wireless channels and available radio resources. However, the main limitation with the existing cooperative mechanisms is the assumption that different networks are willing to cooperate unconditionally so as to minimize the total (sum) power consumption in the geographical region. While this assumption can be true when different networks are operated by the same service provider, however, in presence of multi-service providers, cooperation is adopted only if mutual benefits can be achieved. In addition, existing research relies mainly on power allocation to minimize the consumption, and hence, employs solely the disparity in channel conditions. Finally, decentralized radio resource allocation mechanisms should be adopted in such a multi-operator environment.

In our research [43], we investigate developing a win-win cooperative joint radio resource (e.g., bandwidth and power) allocation mechanism that ensures mutual power saving for all cooperating network operators. The problem is formulated as a Nash bargain game that maximizes energy saving for cooperating networks (compared with the non-cooperative case) while ensuring that mutual power saving is achieved for all participants. An asymmetric Nash bargain game is employed to enable different networks to have different influence (bargain power) to affect the resulting power saving for each network. The rationale behind such an approach is to account for the fact that some networks may have more capabilities (e.g., available bandwidth) than other networks and this factor should be accounted for in the problem formulation. The joint bandwidth and power allocation framework should satisfy the minimum required data rate of mobile users and the total bandwidth and power consumption constraints for the BSs. The Nash bargain game in [43] is shown to have a unique bargain point, and the problem is transformed into an equivalent convex optimization program. Using the decomposition theory, the joint bandwidth and power allocation framework is decomposed into two sub-problems for bandwidth allocation and power allocation that are iteratively solved until the minimum required data rate is satisfied.

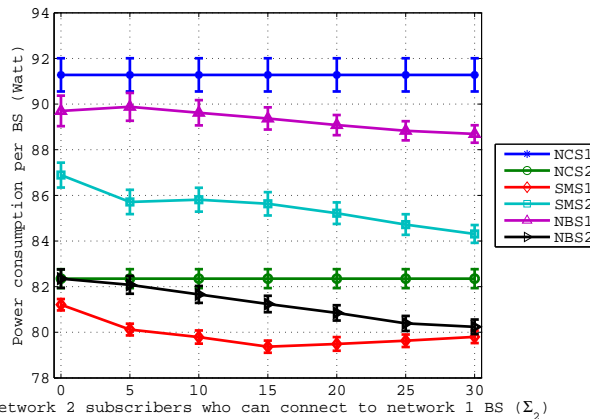


Figure 3. Power consumption for each BS versus the number of network 2 subscribers who can connect to the BSs of both networks [43].

Simulation results in [43] have demonstrated the effectiveness of the proposed win-win cooperative approach. While more power saving can be obtained using the sum minimization solution (SMS) as compared with both the Nash bargain solution (NBS) and the non-cooperative solution (NCS), the NBS is more practical as it provides incentives to network operators to participate in a cooperative framework. As shown in Figure 3, the SMS for the second network (SMS2) is always higher than the non-cooperative solution (NCS2), indicating that it is not beneficial for network 2 to cooperate with network 1 under the SMS framework. On the other hand, the NBS2 is always less than or equal to the NCS2, indicating mutual benefits (power saving) for both network operators.

C. RF-VLC Inter-networking

Most of the existing research in heterogeneous networks is based on RF network integration as in WLAN and cellular networks and macro-femto cells. One challenging issue in such scenario is spectrum congestion in RF networks. On the other hand, VLC is introduced as a promising technology that uses visible light for communications, and hence, offers larger spectrum availability and can achieve high data rates. More importantly, VLC consumes almost no transmission power since VLC uses illumination energy, which is already used for lighting, for communications. However, VLC suffers from reliability issue in absence of line-of-sight (LoS) component and cannot support uplink transmission. Such limitations of VLC networks motivates RF-VLC network integration to exploit the potential benefits of both networks and address their limitations. In literature several Rf-VLC integration objectives are investigated, namely, load balancing, throughput maximization, and uplink support. However, the existing research does not investigate Rf-VLC network integration for energy efficient (green) communications.

In our research [44], we investigate energy efficient integration of a VLC access point (AP) with a femto AP. MTs aggregate the offered resources from both APs to satisfy the required data rate using the multi-homing capability. The achieved data rate from each AP is averaged over the LoS availability probability mass function. For the RF network, the MT experiences LoS and non-LoS (NLoS) channels with

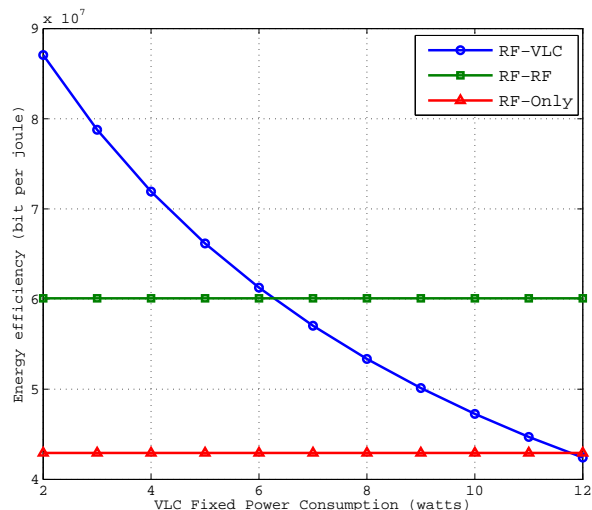


Figure 4. Energy efficiency against the fixed power of the VLC system [44].

probabilities κ_1 and $(1 - \kappa_1)$, respectively. On the other hand, for the VLC network, the MT do not receive any data rate for NLoS channel (with probability $1 - \kappa_2$) and receives data rate only for LoS channel (with probability κ_2). For each MT, the total achieved data rate is the summation of the average data rate achieved using VLC and femto APs, which should satisfy a minimum required data rate. The total communication power consumption for the APs has two components, namely, VLC and femto AP power consumption. The VLC component mainly includes a fixed power consumption that captures the consumed power for signal processing, since no power is consumed in data transmission. For the femto AP, both transmission and fixed power consumption components are accounted for. The objective in [44] is to maximize the total energy efficiency (i.e., a ratio of total achieved throughput to total power consumption) in the geographical region through joint bandwidth and power allocation. The total allocated bandwidth and power for each AP should satisfy the maximum available bandwidth and power. The problem is shown to be a fractional concave-convex program that can be transformed into a convex optimization problem using a parametric approach. Using a Dinkelbach-type algorithm and decomposition theory, the optimal joint resource allocation can be obtained.

Simulation results have demonstrated the improved energy efficiency performance for the RF-VLC network compared with multi-homing among RF only networks and in absence of multi-homing. Such an improved performance mainly depends on the amount of VLC fixed power consumption as shown in Figure 4.

IV. BALANCED DYNAMIC PLANNING FRAMEWORK

At a low call traffic load condition, network operators can save energy by switching off lightly loaded BSs and the traffic is supported by the remaining active cells. The existing research mainly focus on improving energy saving for network operators (i.e., in the downlink) with no investigation on the incurred energy consumption in the uplink and its impact on service quality deterioration for uplink mobile users. Specifically, the existing dynamic planning mechanisms switch off

the BSs that can balance energy saving for network operators with service quality of downlink mobile users. However, such an approach can lead to inefficient MT-BS association in the uplink (i.e., from mobile user perspective) due to switching off nearby BSs resulting in larger transmission distances for uplink mobile users. Consequently, MTs suffer from battery drain at a faster rate leading to call dropping, i.e., deterioration of service quality for uplink users. As a result, a balanced dynamic planning approach is required to account for energy saving and service quality both in the downlink and uplink.

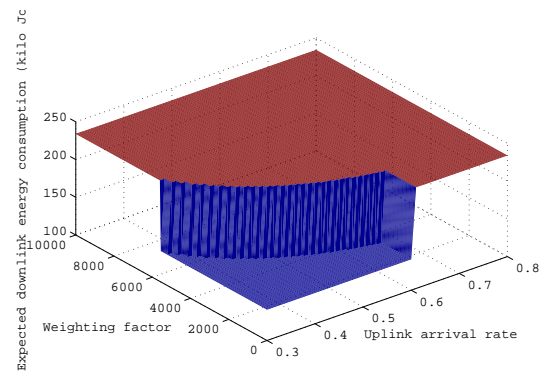
In our research [45], we present a balanced dynamic planning framework that is based on a two-timescale decision problem. Consider a cluster of two BSs with overlapped coverage. Since BS operation (i.e., on-off switching) does not occur at same rate as the MT association, time is partitioned into two timescales. The BS operation occurs at a slow rate (with scale of hours) according to temporal fluctuations in call traffic load density. On the other hand, the MT association occurs at a faster rate (with scale of minutes) according to user arrivals and departures. The slow timescale system state represents the uplink and downlink call traffic load densities, which can be inferred from historical traffic load patterns. Based on the slow timescale state, the slow timescale decision specifies the BS operation mode while satisfying a target call blocking probabilities in the uplink and downlink. The fast timescale state represents the number of mobile users in the uplink and downlink. Two *Geo/Geo/M/M* queues captures temporal fluctuations in number of MTs in the uplink and downlink. Following the fast timescale state and the slow timescale decision, the fast timescale decision controls the transmission powers of the BSs and MTs. The decision problem objective is to balance the expected uplink and downlink energy consumption based on a weighting factor. Such a weighting factor captures the significance of uplink energy consumption and its impact on uplink service quality degradation.

Simulation results have demonstrated the effectiveness of the balanced dynamic planning approach compared with traditional approaches that accounts only for downlink service quality. Unlike the traditional approaches, the balanced approach switching decision depends on the uplink arrival rate and the weighting factor, as shown in Figures 5a, which leads to improved energy saving for the MTs, as shown in Figures 5b.

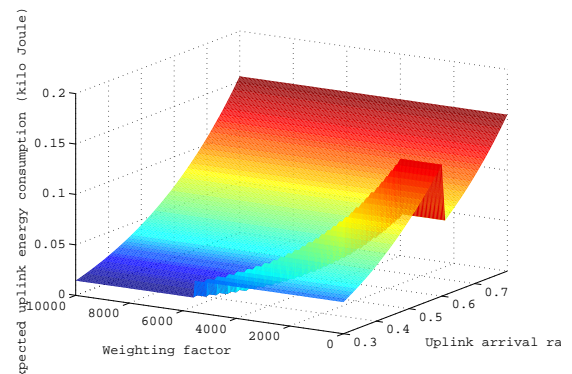
V. CONCLUSIONS AND FUTURE RESEARCH

Radio resource scheduling techniques are adopted at a high call traffic load condition to improve energy efficiency for network operators and mobile users. Green multi-homing techniques in the uplink, downlink, and for RF-VLC inter-networking have been investigated. Emphasis is given to decentralized joint bandwidth and power allocation to maximize energy efficiency. At a low call traffic load condition, balanced dynamic planning can be implemented to achieve energy saving for network operators while not jeopardizing service quality for uplink users due to high energy consumption in the uplink.

While most existing research focus on saving energy either for the network operators or the mobile users, future research directions should consider joint energy saving for network operators and mobile users. For instance, BSs and MTs can save energy at low call traffic load condition via on-off switching



(a) Downlink-Balanced Approach



(b) Uplink-Balanced Approach

Figure 5. The expected energy consumption versus the arrival rate of uplink users and the weighting factor [45].

mechanisms. The existing research allows an MT to switch off its radio interface for energy saving while dealing with buffer delay and/or overflow at the BS. However, the impact of BS on-off switching is not considered. In addition, the existing opportunistic scheduling mechanisms result in energy saving either for network operators or mobile users. However, opportunistic scheduling MTs with bidirectional traffic should ensure energy saving for both network operators and mobile users.

ACKNOWLEDGMENT

This publication was made possible by NPRP grant # NPRP 6-415-3-111 from the Qatar National Research Fund (a member of Qatar Foundation). The statements made herein are solely the responsibility of the authors.

REFERENCES

- [1] M. Ismail and W. Zhuang, "Cooperative networking in a heterogeneous wireless medium," Springer Briefs in Computer Science, New York, April 2013.
- [2] T. Chen, Y. Yang, H. Zhang, H. Kim, and K. Horneman, "Network energy saving technologies for green wireless access networks," *IEEE Wireless Commun.*, vol. 8, no. 5, Oct. 2011, pp. 30-38.
- [3] C. Han, T. Harrold, S. Armour, and I. Krikidis, "Green radio: radio techniques to enable energy-efficient wireless networks," *IEEE Commun. Magazine*, vol. 49, no. 6, June 2011, pp. 46-54.
- [4] Y. Chen, S. Zhang, S. Xu, and G. Y. Li, "Fundamental trade-offs on green wireless networks," *IEEE Commun. Magazine*, vol. 49, no. 6, June 2011, pp. 30-37.

- [5] M. Ismail and W. Zhuang, "Network cooperation for energy saving in green radio communications," *IEEE Wireless Commun.*, vol. 18, no. 5, Oct. 2011, pp. 76-81.
- [6] K. Pentikousis, "In search of energy-efficient mobile networking," *IEEE Commun. Magazine*, vol. 48, no. 1, Jan. 2010, pp. 95-103.
- [7] G. Miao, "Energy-efficient uplink multi-user MIMO," *IEEE Trans. Wireless Commun.*, vol. 12, no. 5, May 2013, pp. 2302-2313.
- [8] I. Humar et al. "Rethinking energy efficiency models of cellular networks with embodied energy," *IEEE Network*, vol. 25, no. 2, April 2011, pp. 40-49.
- [9] D. Feng et al. "A survey of energy-efficient wireless communications," *IEEE Commun. Surveys & Tutorials*, vol. 15, no. 1, 2013, pp. 167-178.
- [10] S. Tombaz, A. Vastberg, and J. Zander, "Energy- and cost-efficient ultra-high-capacity wireless access," *IEEE Wireless Commun.*, vol. 18, no. 5, Oct. 2011, pp. 18-24.
- [11] L. M. Correia, D. Zeller, O. Blume, and D. Ferling, "Challenges and enabling technologies for energy aware mobile radio networks," *IEEE Commun. Magazine*, vol. 48, no. 11, Nov. 2010, pp. 66-72.
- [12] G. Miao, N. Himayat, Y. Li, and A. Swami, "Cross-layer optimization for energy-efficient wireless communications: a survey," *Wiley J. Wireless Commun. and Mobile Computing*, vol. 9, March 2009, pp. 529-542.
- [13] M. Ismail, W. Zhuang, E. Serpedin, and K. Qaraqe, "A survey on green mobile networking: from the perspectives of network operators and mobile users," *IEEE Commun. Surveys & Tutorials*, vol. 17, no. 3, Nov. 2014, pp. 1535-1556.
- [14] H. Bogucka and A. Conti, "Degrees of freedom for energy savings in practical adaptive wireless systems," *IEEE Commun. Magazine*, vol. 49, no. 6, June 2011, pp. 38-45.
- [15] K. Ying, H. Yu, and H. Luo, "Inter-RAT energy saving for multicast services," *IEEE Commun. Letters*, vol. 17, no. 5, May 2013, pp. 900-903.
- [16] F. Liu, K. Zheng, W. Xiang, and H. Zhao, "Design and performance analysis of an energy-efficient uplink carrier aggregation scheme," *IEEE Journal Selected Areas Commun.*, to appear.
- [17] H. Kwon and B. G. Lee, "Energy-efficient scheduling with delay constraints in time-varying uplink channels," *Journal of Commun. and Networks*, vol. 10, no. 1, March 2008, pp. 28-37.
- [18] X. Ma, M. Sheng, and Y. Zhang, "Green communications with network cooperation: a concurrent transmission approach," *IEEE Commun. Letters*, vol. 16, no. 12, Dec. 2012, pp. 1952-1955.
- [19] M. Z. Shakir et al. "Green heterogeneous small-cell networks: toward reducing the CO₂ emissions of mobile communications industry using uplink power adaptation," *IEEE Commun.*, vol. 51, no. 6, June 2013, pp. 52-61.
- [20] L. B. Le, D. Niyato, E. Hossain, D. I. Kim, and D. T. Hoang, "QoS-aware and energy-efficient resource management in OFDMA femtocells," *IEEE Trans. Wireless Commun.*, vol. 12, no. 1, Jan. 2013, pp. 180-194.
- [21] Y. Li, X. Zhu, C. Liao, C. Wang, and B. Cao, "Energy efficiency maximization by jointly optimizing the positions and serving range of relay stations in cellular networks," *IEEE Trans. Vehicular Technology*, vol. 64, no. 6, July 2014, pp. 2551-2560.
- [22] Y. Li, C. Liao, and C. Wang, "Energy-efficient optimal relay selection in cooperative cellular networks based on double auction," *IEEE Trans. Wireless Commun.*, to appear.
- [23] M. Jung, K. Hwang, and S. Choi, "Joint mode selection and power allocation scheme for power-efficient Device-to-Device (D2D) communication," *Proc. IEEE VTC-Spring12*, May 2012, pp. 1-5.
- [24] G. Fodor et al. "Design aspects of network assisted device-to-device communications," *IEEE Commun. Magazine*, vol. 50, no. 3, March 2012, pp. 170-177.
- [25] A. Asadi and V. Mancuso, "Energy efficient opportunistic uplink packet forwarding in hybrid wireless networks," *Proc. 4th Intl Conf. Future Energy Systems*, 2013, pp. 261-262.
- [26] S. Bu, F. R. Yu, Y. Cai, and X. P. Liu, "When the smart grid meets energy-efficient communications: green wireless cellular networks powered by the smart grid," *IEEE Trans. Wireless Commun.*, vol. 11, no. 8, Aug. 2012, pp. 3014-3024.
- [27] T. Han and N. Ansari, "On optimizing green energy utilization for cellular networks with hybrid energy supplies," *IEEE Trans. Wireless Commun.*, to appear.
- [28] C. McGuire et al. "HopScotch-a low-power renewable energy base station network for rural broadband access," *EURASIP J. on Wireless Communications and Networking*, vol. 112, March 2012, pp. 1-12.
- [29] C. F. Chiasserini and R. R. Rao, "Energy efficient battery management," *IEEE J. Selected Areas Commun.*, vol. 19, no. 7, July 2001, pp. 1235-1245.
- [30] M. Ismail and W. Zhuang, "Green radio communications in a heterogeneous wireless medium," *IEEE Wireless Commun. Magazine*, vol. 21, no. 3, June 2014, pp. 128-135.
- [31] K. Son, H. Kim, Y. Yi, and B. Krishnamachari, "Base station operation and user association mechanisms for energy-delay tradeoffs in green cellular networks," *IEEE Journal Selected Areas Commun.*, vol. 29, no. 8, Sep. 2011, pp. 1525-1536.
- [32] T. Han and N. Ansari, "On greening cellular networks via multicell cooperation," *IEEE Wireless Commun.*, vol. 20, no. 1, Feb. 2013, pp. 82-89.
- [33] E. Oh, K. Son, and B. Krishnamachari, "Dynamic base station switching-on/off strategies for green cellular networks," *IEEE Trans. Wireless Commun.*, vol. 12, no. 5, May 2013, pp. 2126-2136.
- [34] C. Y. Chang, W. Liao, H. Y. Hsieh, and D. S. Shiu, "On optimal cell activation for coverage preservation in green cellular networks," *IEEE Trans. Mobile Computing*, to appear.
- [35] J. Wu, S. Zhou, and Z. Niu, "Traffic-aware base station sleeping control and power matching for energy-delay tradeoffs in green cellular networks," *IEEE Trans. Wireless Commun.*, vol. 12, no. 8, Aug. 2013, pp. 4196-4209.
- [36] A. Conte et al. "Cell wilting and blossoming for energy efficiency," *IEEE Wireless Commun.*, vol. 18, no. 5, Oct. 2011, pp. 50-57.
- [37] A. P. Azad, "Analysis and optimization of sleeping mode in WiMAX via stochastic decomposition techniques," *IEEE J. Selected Areas Commun.*, vol. 29, no. 8, Sep. 2011, pp. 1630-1640.
- [38] H. Yan et al. "Client-centered, energy-efficient wireless communication on IEEE 802.11b networks," *IEEE Trans. Mobile Computing*, vol. 5, no. 11, Nov. 2006, pp. 1575-1590.
- [39] R. Wang, J. Tsai, C. Maciocco, T. Y. C. Tai, and J. Wu, "Reducing power consumption for mobile platforms via adaptive traffic coalescing," *IEEE J. Selected Areas Commun.*, vol. 29, no. 8, Sep. 2011, pp. 1618-1629.
- [40] Y. Jin, J. Xu, and L. Qiu, "Energy-efficient scheduling with individual packet delay constraints and non-ideal circuit power," *J. Commun. and Networks*, vol. 16, no. 1, Feb. 2014, pp. 36-44.
- [41] K. D. Turck, S. D. Vuyst, D. Fiems, S. Wittevrongel, and H. Brueneel, "Performance analysis of sleep mode mechanisms in the presence of bidirectional traffic," *Computer Networks*, vol. 56, March 2012, pp. 2494-2505.
- [42] M. Ismail et al. "Uplink decentralized joint bandwidth and power allocation for energy-efficient operation in a heterogeneous wireless medium," *IEEE Trans. Commun.*, vol. 63, no. 4, April 2015, pp. 1483-1495.
- [43] M. Ismail, K. Qaraqe, and E. Serpedin, "Cooperation incentives and downlink radio resource allocation for green communications in a heterogeneous wireless environment," *IEEE Trans. Vehicular Technology*, vol. 65, no. 3, March 2015, pp. 1627-1638.
- [44] M. Kashaf, M. Ismail, M. Abdallah, K. Qaraqe, and E. Serpedin, "Energy efficient resource allocation for mixed RF/VLC heterogeneous wireless networks," *IEEE J. Selected Areas Commun.*, vol. 34, no. 4, March 2016, pp. 883-893.
- [45] M. Ismail, M. Kashaf, E. Serpedin, K. Qaraqe, "On balancing energy efficiency for network operators and mobile users in dynamic planning," *IEEE Commun. Magazine*, vol. 53, no. 11, Nov. 2015, pp. 158-165.

Path Loss Analysis and Verification by Ray-Tracing for 3.5GHz Outdoor Environments

Sungwoo Kim, Byungjin Lee, Kyungseok Kim
Radio & Communications Engineering
Chungbuk National University
Cheongju, Chungbuk, 361-763, Korea

E-mail: onlyparadise@nate.com, byung2487@naver.com, kseokkim@cbnu.ac.kr

Abstract— This paper presents the channel propagation characteristics analysis in 3500MHz outdoor environments and verification by Ray-Tracing simulations. Because we are studying small cell hot spot environment, we use 3500MHz. We describe a computer program to predict radio propagation in buildings, based on site-specific information, such as wall locations and building materials. Line-of-sight, specularly transmitted, specularly reflected, and non-specularly transmitted and reflected rays are included in the model. Actually, we considered two places, each one with different environmental conditions: one was Dunsan-dong and the second was the Electronics and Telecommunications Research Institute (ETRI). We measured the path loss and, to verify our measurement results, we compared them with Ray-Tracing results.

Keywords- path loss; outdoor path analysis; Ray-Tracing.

I. INTRODUCTION

The purpose of the experiment is to analyze the channel propagation characteristics. Currently, the rapid increase in demand for wireless communication and the explosive growth of the mobile communication service require optimization of the next generation mobile communication system. The development of efficient frequency use and study of competitive next generation radio transmission technology are based on the exact identification of the radio channel characteristics. Path loss is one of the many channel parameters that can represent radio channel characteristics. Also, microcellular path loss can be predicted from the Ultra High Frequency (UHF) [1]. Finally, the experiment was difficult to execute because of poor meteorological conditions such as rain, preventing the progress of the experiment.

In this paper, we present results that were obtained in the ETRI and Dunsan-dong outdoor environments. We used a isotropic antenna with 3500MHz frequency. Many people claim that 3500MHz is the frequency of 5G. For this reason, we decided to analyze the 3500MHz. The power was different in the two locations: for ETRI, it was 0.974W and for Dunsan-dong it was 2W. We focused on propagation characteristics, which are important for the development and validation of a realistic channel model. No experiment was performed in bad weather, so there were difficulties or obstacles in that regard. We compared the measurement

results and simulation results from the Ray-Tracing 3D simulator to verify our data. This paper is structured into 4 sections. In Section II, we explain the measurement environments. In Section III, we perform channel characteristic analysis and in Section IV we deal with verification of path loss analysis using Ray-Tracing. We conclude in Section V.

II. MEASUREMENT ENVIRONMENTS

The measurements were performed in 2 places in Daejeon using an antenna array mounted on a car. These places are shown in Figure 1. We used a 1-by-1 antenna, i.e, Single-Input Single-Output (SISO) and the wideband radio channel measurement system was the channel sounder.



(a) Dunsan-dong



(b) ETRI

Figure 1. Measurement area

As shown in Figure 1, the measurement scenarios consist of 2 different Tx locations and Rx routes. Dunsandong Tx is inside a building and ETRI is in stadium. During the measurements, the Tx was stationary at each site, while the Rx was driven along the measurement routes. TABLE I shows the detailed information of the measurement places.

TABLE I. THE DETAILED INFORMATION OF MEASUREMENT PLACES

Location	Feature
Dunsandong	· High-rise buildings (above 10 floors) and many lanes road , heavy traffic
ETRI	· Low-rise buildings (above 6 floors) and many lanes road , light traffic

Antenna was located in the middle of the rooftop on the motor vehicle at a base station (BS) with the antenna height of 7.3 m. The mobile station (MS)'s antenna with the antenna height of 2 m was set on the end of the rooftop on the motor vehicle because we could ignore the reflection since the absorber was installed on the rear surface of the vehicle. TABLE II shows the information related to the channel sounder system.

TABLE II. CHANNEL SOUNDER SYSTEM

Item	Specification
Center Frequency	3.5 GHz
PN Length (Pseudo Random Noise Swquence)	32768 chips
Number of Antenna	Tx : 1, Rx : 1
Antenna Height	Tx : 7.3 m, Rx : 2 m
RX ADC	Sampling : 209MSa/s
Tx Output Power	Max. +33dBm
Tx/Rx Antenna Gain	5.82dBi

The measurement frequency was 3.5 GHz and PN length was 32768 chips. The sample data was the transmission of two million per second, the maximum transmit power of 33dBm in Tx. SISO was the antenna that we used.

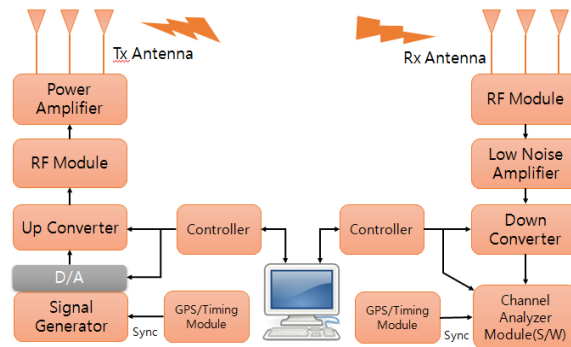


Figure 2. Measurement system configuration

Figure 2 shows our measurement system. The transmission data consisted of 209×10^6 samples, and the communication took place via an antenna through the RF (Radio Frequency) module and the Power Amp.

III. CHANNEL CHARACTERISTIC ANALYSIS

Path loss is a major element in planning cell coverage. In the UHF (Ultra High Frequency) band case, there are many existing models. For example, Kronrcker model, Weichelberger model, etc. But, there are few studies on peer to peer signal attenuation at 700 MHz frequency. The propagation of energy from the transmitter to the receiver occurs in various modes. Because of this, it is important to recognize the path loss dependence. The path loss is extracted from the measurements and comparisons are made with the results [2][3].

The distance-dependent part of the path loss is modeled to be a function of the geometrical distance, d , as

$$P_L(d) = L_0 - 10n \log_{10} \left(\frac{d}{d_{ref}} \right) + X_{\sigma}, \quad [\text{dB}] \quad (1)$$

where L_0 is the initial value at the reference distance d_{ref} and n is the path loss index, and X_{σ} is standard deviation. The measured received power values indicate that the path loss decreases when the receiving vehicle moves because that path loss is reduced in a logarithmic form [4].

Measurement was performed at each place per 100 m, and over 100 times of each test point. Path loss occurs when the signal passes through a radio channel. Figure 3 shows the path loss that occurs when the car moves 10m~500m .

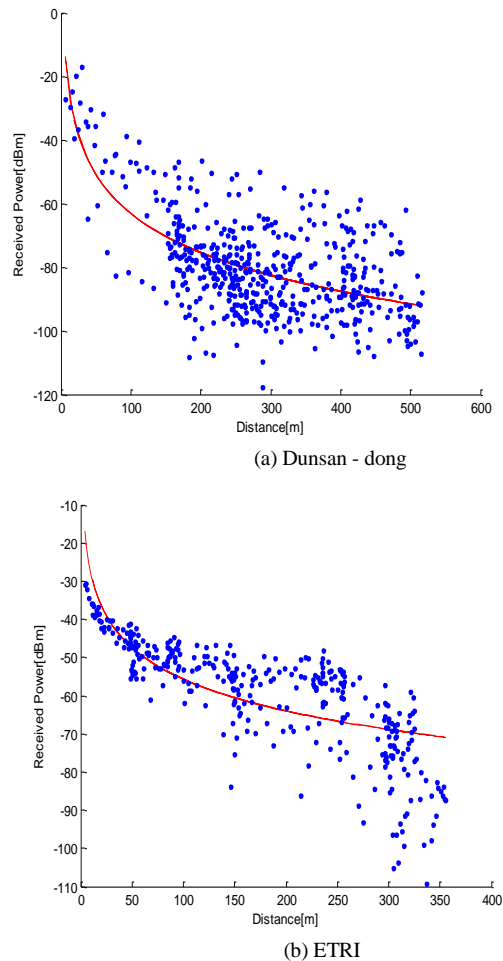


Figure 3. Received level of our measured data

Comparing the two measurement areas, we can see that the Dunsan - dong has a large power attenuation. It means that, when the radio wave moves in the wireless channel, lots of elements interrupt the flow of the radio wave. Actually, high rise buildings, large pedestrian population and vehicles added a lot more distractions. Table 3 shows the measurement environment by a constant value.

TABLE III. COMPARE THE MEASUREMENT ENVIRONMENT BY A CONSTANT VALUE

Measurement conditions					Path loss (P_L)		
Area	$f(\text{GHz})$	$h_b(\text{m})$	$h_m(\text{m})$	$d_{ref}(\text{m})$	l_0	n	$X_s(dB)$
ETRI	3.5	7.5	2.0	20	4.36	3.4	11.2
Dunsan-dong					-	4.2	8.91

According to the above results, path loss characteristic is distance-dependent. Dunsan-dong PL Initial Value and PL index are much bigger than ETRI. But the result of standard deviation is different; ETRI is bigger than Dunsan – dong.

IV. VERIFICATION OF PATH LOSS ANALYSIS USING RAY-TRACING METHOD

A. Ray-Tracing simulation configuration

To verify the validity of the measurement results, we made a simulation based on the ETRI and Dunsan-dong cases. Then, we compared the simulation results with our measurements. We made a 3D model similar to the real environment for Ray-Tracing simulation. In the Ray-Tracing we used quality of the material. A software application has been written to implement the model as an automated propagation prediction tool. The program uses Ray –Tracing to account for all possible propagation paths. Ray-Tracing is commonly used for computer image rendering and for computer animation. Ray-Tracing is used instead of electromagnetic image theory so various channel geometries can be considered. Image theory is cumbersome when randomly oriented objects or multiple reflections are considered. As computation times increase, Ray-Tracing acceleration techniques are employed to combat the computational requirements of Ray-Tracing. In Ray-Tracing we set up some materials [5].

Floor and buildings are concrete, forest and trees are wood, and finally, tennis court is sandy soil. Figure 4 and 5 show the Ray-Tracing simulation configuration for ETRI and Dunsan – dong, respectively.

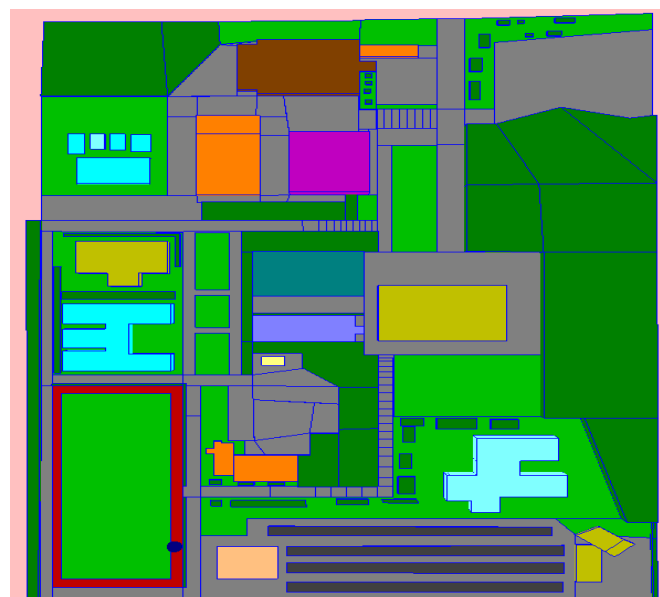


Figure 4. Simulation configuration of ETRI case

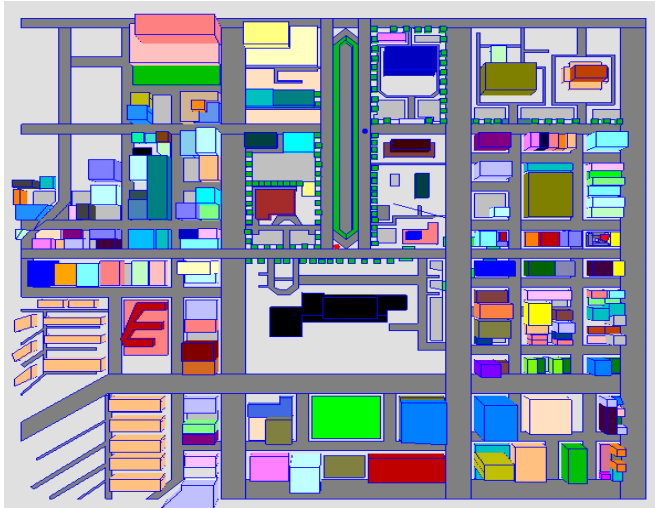


Figure 5. Simulation configuration of Dunsan - dong case

B. Verification of our measurement result

Figure 6 shows a comparison between Ray-Tracing and our measurement data. The red line represents the measurement results and the blue line is the Ray-Tracing simulation result. In ETRI, the result of Ray-Tracing and measurement are little bit different. The reason is that, in ETRI, there are many hills and it is very difficult to express that in Ray-Tracing. This is this reason why the graph is not perfect match. But, in Dunsan-dong, the 2 graphs are similar.

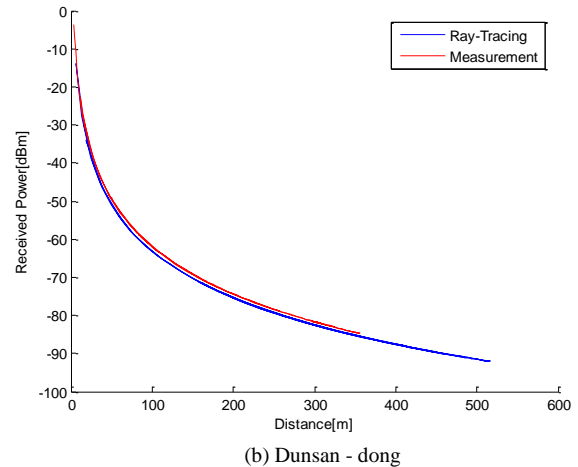
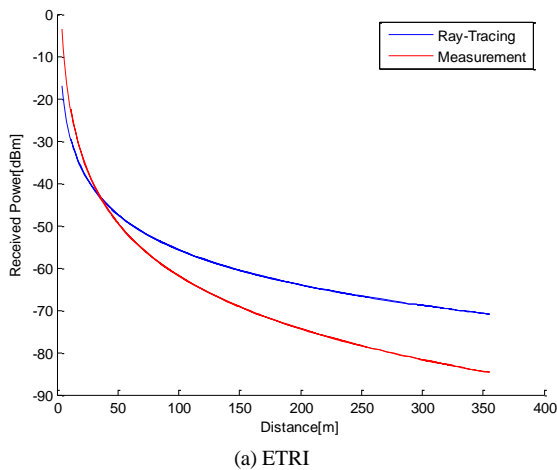


Figure 6. Comparison between Ray-Tracing and measurement

V. CONCLUSION

We presented a measurement system, and measured the characteristics of the wave propagation in the outdoor environment at 3500MHz. We deduced path characteristics for SISO wireless mobile communication systems in the outdoor environments from the measured data. Also, we compared path characteristics with simulation results obtained by Ray-Tracing. From the comparison results, we conclude that there is little difference in path characteristics. Path loss characteristics have different trend in the Dunsan-dong and ETRI case. In ETRI, there are many different materials so, the graph is a little different. So, we need to make a new path loss model for new mobile communication system. Finally, to verify the validity of the analysis results, the measurement data is compared to simulation results. The measurement data and simulated data show similar inclination, which leads us to believe that our measurements are correct.

REFERENCES

- [1] M.W. Jong, et al., "Path Loss Characteristics for New Wireless Mobile Communication System in Outdoor Environments", Radar Conference (EuRAD), 2012 9th European, pp. 545-550, 2012.
- [2] Kurt R. Schaubach, Nathaniel J. Dvis IV, Theodore S. Rappaport, "A Ray Tracing Method for Predicting Path Loss and Delay Spread in Microcellular Environments", Vehicular Technology Confenece, vol. 2, pp. 932-935, 1992.
- [3] Scott Y. Seidel, Theodore S. Rappaport, "A Rqy Tracing Technique to Predict Path Loss and Delay Spread Inside Uildings", Global Telecommunications Conference, vol. 2, pp. 649-653, 1992.
- [4] A. Bhuvaneshwari, R. Hemalatha, T. Satyasavithri, 'Path Loss Prediction Analysis by Ray Tracing Approach for NLOS Indoor Propagation", Signal Processing And Communication Engineering Systems (SPACES),pp. 486-491,2015.
- [5] Y. Oda, K. Tsunekawa, "Advanced LOS path-loss model in microcellular mobile communications," *IEEE Trans. Veh. Technol.*,vol49,no. 6,pp. 56-61,Nov.,2000.

Channel Measurement and Characteristics Analysis on 3.5GHz Outdoor Environment

Bong-Gu Yeo, Byung Jin Lee, Kyung-Seok Kim

Radio & Communications Engineering

Chungbuk National University

Cheongju, Chungbuk, 361-763, Korea

E-mail: vinss200@cbnu.ac.kr, byung2487@naver.com, kseokkim@cbnu.ac.kr

Abstract— If the channel characteristics of an outdoor cell are known, it makes it possible to use the optimal frequency and to optimize the system design. This paper presents the correlations between channel parameter Path Loss (PL), root mean square Delay Spread (DS), and K-factor established based on channel measurements. The channel measurements were performed in a 3.5 GHz Non-Line of Sight (NLOS) environment. We measured the channel characteristics in Dunsan area in Korea using a channel sounder and 1×1 antennas. The correlations between channel parameters show that the wireless channel characteristics can be determined and effective communication system design can be produced for use in similar environments.

Keywords-Channel parameter; Mobile communication; Correlation coefficients.

I. INTRODUCTION

It is important to analyze the radio channel parameters from the latest high-speed wireless communication [1]. A sharp demand for wireless communications requires the development and optimization of the next generation mobile communication system. Development of efficient frequency use and study of a wireless transmission technology having high competitiveness is based on the understanding of the correct radio channel characteristics. Radio channel characteristics are based on the channel parameter analysis. Channel parameter analysis is helpful in understanding the characteristics of the propagation channel space and have a significant impact on the design of the mobile system. Current wireless channel models were established through measurement of a wide range of channel 800MHz ~ 2.5GHz band. Typically, it is used to establish, based on the channel model for the International Telecommunication Union (ITU) standard channel model [2]. Propagation Modeling and Analysis for the current below 6GHz band is being studied in major countries such as the United States, Europe, Japan progress. In addition, the international standards organization [ITU, Institute of Electrical and Electronics Engineers (IEEE), 3rd Generation Partnership Project (3GPP), WINNER] has proposed a standard and modeling results of the analysis method [3].

Recently, many countries and international standardization organizations are working to examine the next-generation mobile (5G) wireless communication system using a range of frequencies below 6GHz. Therefore, it is

determined that the prior studies of the same frequency band are necessary in Korea. International standards organizations have classified bandwidth utilization as high as 3GHz ~ 4GHz frequency among the next generation of mobile communications. In this paper, the selection of a 3.5GHz band and the analysis of the propagation characteristics of the channel parameters are measured and presented based on the correlation between the parameters. Analysis of the channel in such an environment will facilitate the system design of future communication systems.

This paper is organized as follows. Section 2 is an introduction section; Section 3 presents the channel characteristic parameters and correlation analysis with related measurement data; Section 4 provides a summary and conclusions of the this paper.

II. MEASUREMENT SYSTEM

A. System environments

This study analyzes the propagation characteristics in the frequency band of 3.5GHz for a 5-generation wireless mobile communication system. We focused on the primary channel characterization of the physical channel. Hence, we constructed a measurement system to analyze the propagation characteristics.

We took our measurements on the Dunsan area using 1×1 antennas and a channel sounder from the Korea Electronics and Telecommunications Research Institute (ETRI). We were using the channel sounder to the system. Further details are shown in Table 1.

Table I. CHANNEL SOUNDER SYSTEM

Item	Specification
Center Frequency	3.5 GHz
PN Length	32768 chips
Number of Antenna	Tx : 1, Rx : 1
Antenna Height	Tx : 7.3 m, Rx : 2 m
RX ADC	Sampling : 209 MSa/s
Tx Output Power	Max. +33dBm
Tx/Rx Antenna Gain	5.82dBi

The measurement frequency was 3.5 GHz and Pseudo Random Noise Sequence (PN Codes) was using 32768 chips. The sample data was the transmission of two million per second, the maximum transmit power of 33dBm is Tx.

Antenna gain is 5.82dBi in one. We used a 1-by-1 antenna, i.e, Single-Input Single-Output (SISO).

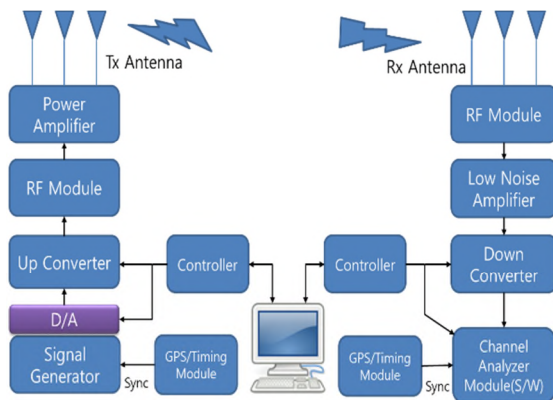


Figure 1. Measurement system configuration

Figure 1 presents our measurement system. Transmission is sent using 209×10^6 samples of data, and the communication takes place via an antenna through the RF module and the Power Amp. Align the synchronization via GPS and Timing Module. In the receiver, the signal is received via the IQ Data RF Module. Also, the channel parameters are derived from the S/W.

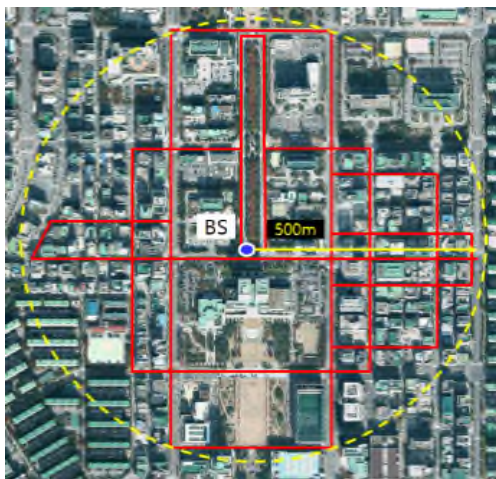


Figure 2. Dunsan measuring area

B. Measurement Scenario

In this study, we measured the propagation characteristics. Our selected area was Dunsan, characterized by an urban environment within about 1 km. Figure 2 shows an aerial photograph of the building location and the area of the measurement region. A Base Station (BS), as shown in Table 1, is installed in the antenna height of 7.3m and a Mobile Station (MS) has been set on top of the roof of a car at 2m. MS is moving along a path within 500m around the BS, measuring the radio wave, and storing the measured data. We analyze the channel parameters based on the stored data.

III. CHANNEL CHARACTERISTIC ANALYSIS

A. Path Loss (PL)

Signal passing through a radio channel results in path loss. When the path loss is caused by the encounter, each reflection, diffraction, scattering will have a different value according to the surrounding environment and the distance between the transceiver. The power value changes according to the distance and has the following distribution [4].

$$P_L(d) = L_0 - 10n \log_{10} \left(\frac{d}{d_{def}} \right) + X_\sigma \quad (1)$$

where L_0 is the initial value, and n is the index of the path-loss. Figure 3 illustrates the received power according to the distance measured from Dunsan area.

The measured reception power value is reduced to a logarithmic function type according to distance. This is meant to increase their element to interrupt the flow of the radio wave according to the distance between the transmitter and the receiver. In fact, the high buildings and large floating population and vehicle were acting as impediments.

The received power value measured in the region Dunsan follows the following distribution.

$$P_{L_d}(d) = 20.06 - 4.204 \times 10 \log_{10} \left(\frac{d}{d_{def}} \right) + 8.91 \quad (2)$$

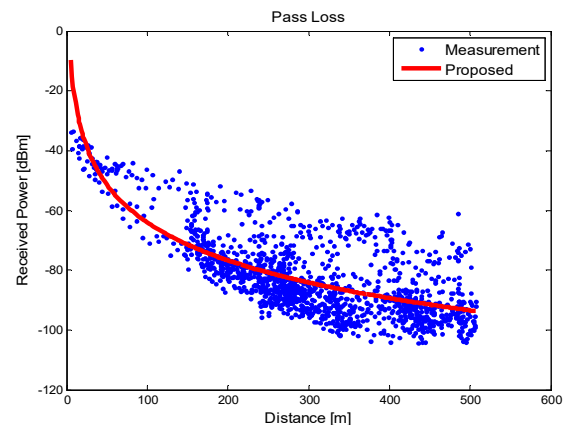


Figure 3. Path loss according to the distance

Figure 2 shows the distance away from the BS that tends to be much higher with respect to the number of buildings. Figure 3 shows the tendency on the received power distribution to increase with the distance; at 500m point, the power received shows a big difference of 40dbm.

B. Delay Spread (DS)

Delay spread is due to multipath reflections and influences the Inter Symbol Interference (ISI). Therefore, the maximum data rates on the communication applications could be limited by ISI.

Time delay spread is derived by calculating the signal level and the noise signal over a reference impulse signal. 1 sample corresponds to 0.48 us and multiplies the time and

power values of a fading signal to calculate the Mean Excess Delay value [5].

$$\bar{\tau} = \frac{\sum_k P(\tau_k)\tau_k}{\sum_k P(\tau_k)} \quad (3)$$

The RMS delay spread is defined as the square root of the second central moment of the Mean Excess Delay. Figure 4 shows the RMS delay spread in our scenario.

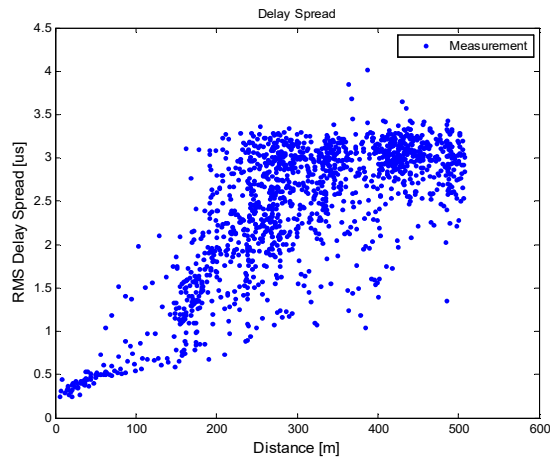


Figure 4. RMS Delay Spread according to the distance

As expected, the highest delay spreads are found mostly because of its high density of scattering.

C. K-factor

In many radio environments, the complex path gain consists of a fixed component plus a zero-mean fluctuating component. The ratio of the fixed and fluctuating power components is defined as the K-factor [6].

$$K[\text{dB}] = 10 \log_{10} \frac{c^2}{2\sigma^2} \quad (4)$$

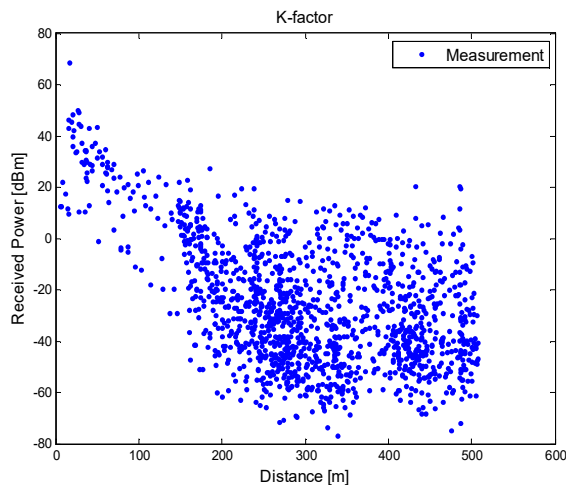


Figure 5. K-factor according to the distance

where c^2 is the power of the LOS component and $2\sigma^2$ is the power of the NLOS component. The K-factor is an important parameter in a wireless channel system since it defines the power probability of the LOS component. The results are shown in Figure 5; they are calculated by the measured data is K-factor and tend to be inversely proportional with the distance. This means that, according to the increasing distance, the LOS signal component is reduced.

D. Channel Capacity

To derive the channel capacitor of performance in a wireless channel, the channel capacity from SISO radio channel is calculated by the following formula [7].

$$C = \log_2(1 + \gamma) = \log_2 \left(1 + \frac{P_t}{\sigma_n^2} |h|^2 \right) \quad (5)$$

where γ denotes the total received signal-to-noise ratio and h represents the channel.

Figure 6 shows the cumulative distribution probability according to the channel capacity. Blue, red and black lines represent SNR 0, 10, 20dB, respectively. It can be seen that the channel capacitor is proportional to the SNR.

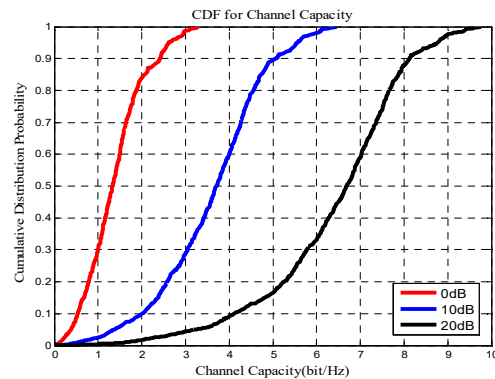


Figure 6. Cumulative Distribution Function for Channel Capacity

E. Correlation Channel Parameters

The correlation of the parameters observed in the measured data is reflected in joint power or probability distributions.

$$\rho_{xy} = \frac{c_{xy}}{\sqrt{c_{xx}c_{yy}}} \quad (6)$$

where C_{xy} is the cross-covariance of channel parameters x and y . The correlation between the different channel parameters is an important property when developing and evaluating channel models. The correlation coefficients for all of the combinations of the estimated channel parameters are shown in Figure 8. Figure 9 presents the analysis data from a similar environment at 300 MHz [8]. We can see a positive correlation in our scenario between the K-factor and DS in Figure 7.

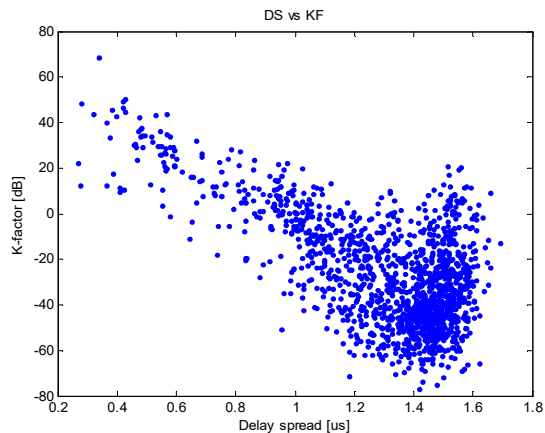


Figure 7. The Correlation for DS vs KF

	Distance	Path loss	DS	K-factor
Distance	1.0	-0.65	0.68	-0.44
Path loss	-0.65	1.0	-0.82	0.79
DS	0.68	-0.82	1.0	-0.63
K-factor	-0.44	0.79	-0.63	1.0
Correlation				
-1	0	0	0	1

Figure 8. Correlation Coefficients

	Distance	Path loss	DS	K-factor
Distance	1.0	-0.87	0.50	-0.03
Path loss	-0.87	1.0	-0.74	0.35
DS	0.50	-0.74	1.0	-0.54
K-factor	-0.03	0.35	-0.54	1.0
Correlation				
-1	0	0	0	1

Figure 9. Correlation Coefficients (300MHz)[8]

The correlation between the channel parameters is shown by the channel characteristic in the measured scenario. Generally, the DS values are observed to have a positive correlation, and the PL and K-factors are observed to have a negative correlation, according to the distance. The reduction of overall power explains the negative correlation of the PL and distance. The reduction of the LOS signal explains the negative correlation of the K-factor and distance. The strongest correlations between the distance and PL are observed in scenario. In this scenario, DS correlation value for PLs is -0.82. We can see a similar correlation between PLs and the DS when measured at 300MHz, -0.74. This means that the measurement environment seems similar

according to distance. However, the correlation between distance and PLs exposes the difference between the Korean environment and the Swedish environment, are -0.65 and -0.87, respectively. The difference in the two environments is closely associated with the landscape, surroundings, and temperature. The amplitude of the multipath components is frequency dependent, resulting in different fading characteristics in the channel and also the channel parameters.

IV. CONCLUSION AND FUTURE WORK

In this paper, we presented the correlation between channel parameters at 3.5GHz, which is an important frequency band for radio services and new mobile communication. It was measured according to a receiver path in an urban area environment. We derived channel parameters, such as path loss, delay spread and K-factor for SISO wireless system from the measured data. Also, the correlation coefficients of the channel parameters were derived for the urban environment. High negative correlations between DS and PL are observed in this urban scenario. It means the generation of a large path loss. Similar correlations can be found with measurements at 300 MHz. But, the correlation between distance and k-factor shows the difference between the Korean environment and the Swedish environment. This difference shows the measurement frequency band and the difference between Korean and Swedish environments. Generalizations should be explained from the environment structure, propagation mechanism, and the inclusion of other related measurement results, which should be done in the future.

REFERENCES

- [1] F. Wyne, A. F. Molisch, P. Almers, G. Eriksson, J. Karedal, and F. Tufvesson, "Outdoor-to-indoor office MIMO measurements and analysis at 5.2 GHz", IEEE Trans. Veh. Technol., vol. 57, no. 3, pp. 1374-1386, May 2008.
- [2] ITU-R M.2135-1, "Guidelines for evaluation of radio interface technologies for IMT-Advanced," Dec. 2009.
- [3] G. Eriksson et al., "Urban Peer-to-Peer MIMO Channel Measurements and Analysis at 300 MHz", IEEE Military Communications Conference, pp. 1-8, 2008.
- [4] V. Erceg et al., "An empirically based path loss model for wireless channels in suburban environments," IEEE J. Select Areas Commun., vol. 17, no. 7, July 1999, pp. 1205-1211.
- [5] Draft Revision of Recommendation ITU-R P.1407-5, "Multipath propagation and parameterization of its characteristics", 2013.
- [6] N. Shroff and K. Giridhar, "Biased Estimation of Rician K factor", IEEE Int. Conf., 2007, pp. 1-5.
- [7] A. J. Goldsmith and P. P. Varaiya, "Capacity, mutual information, and coding for finite-state Markov channels", IEEE Transactions on Information Theory., vol 42, no.3, May 1996., pp. 868-886.
- [8] N. Jalden, "Analysis of radio channel measurements using multiple base stations", Licenciate Thesis, Royal Institute of technology, Stockholm, Sweden, May 2007.

Indirect Demand Side Management Program Under Real-Time Pricing in Smart Grids Using Oligopoly Market Model

Poria Hasanpor Divshali^{1,2} and Bong Jun Choi^{1,2}

¹Department of Computer Science, The State University of New York (SUNY) Korea, Songdo, Incheon, Korea

²Department of Computer Science, Stony Brook University, New York, NY, USA

Email: poriahd@gmail.com, bjchoi@sunykorea.ac.kr

Abstract—The rise in electricity demand, environmental concerns, and economic issues have increased the importance of demand response in recent years. Among different incentive methods of demand side management (DSM) programs, real-time pricing (RTP) can adaptively control the electricity consumption while giving the decision authority to customers and satisfying the power system constraints. Although the existing RTP methods require a complicated computational process to determine the equilibrium point, this paper proposes a heuristic two-stage iterative method to quickly find the market equilibrium using the Cournot oligopoly competition model in a smart grid. The proposed method minimizes the cost for each customer by running a simple computational algorithm on each customer's smart meter while also satisfying the power system constraints. The effectiveness and feasibility of the proposed method is demonstrated by conducting simulations in the IEEE 37-bus test system with about 1500 customers using real data sets of loads. The results show that the proposed technique can better manage the elastic loads in terms of power and cost in comparison with the existing methods and is quick enough to run in real-time.

Keywords—Demand side management; Imperfect competition market; Indirect control; Real-time pricing; Smart grid; Smart meter.

I. INTRODUCTION

Demand response (DR) can be defined as any change in electric usage of end-use customers from their normal consumption patterns in response to incentive payments designed to induce lower electricity use at times of high cost of electricity supply [1]. Under this definition, the demand side management (DSM) programs include all activities that alters the consumer's demand profile to match the supply profile [2]. The idea of DSM is not new and it emerged in electrical systems in the 1970s and has evolved over the past four decades. The smart grid (SG), infrastructures such as two-way communication system are attracting more researchers to DSM concepts in recent years.

Implementing DSM leads to technical and economic benefits for utilities and customers, if the number of participants is large enough. Customer motivation methods in DSM have a major role in the customers' participation. The different motivation methods in DSM are surveyed into [3]. Generally, the motivation methods can be divided in two

main categories: incentive based methods and time based methods. The incentive based programs offer payments to customers who reduce their electricity usage during periods of system need or stress [4]. However, in order to determine the amount of reduction, a baseline load threshold must be calculated for each customer, which is a complicated and imprecise procedure [5].

In the time based programs, the price of consumption is varied based on the time of usage and can lead customers to transfer consumption to the off-peak period [6]. The time based program has two different subcategories. Some programs offer varying prices for different time periods but do not change prices based on customers' decisions, e.g., the time of use (TOU) method. Some other programs consider the effects of customers' decisions and change the price in real-time manner, e.g., real-time pricing (RTP) method.

The TOU method has a critical drawback; since the price of each time period is independent from customers' behavior and each customer decides individually, it is possible that all customers decide to simultaneously use in off peak period, causing a new "rebound" peak [7,8]. In order to solve this problem, retailers must determine the price of each time period based on the real-time consumption. Implementation of RTP method requires two-way real-time communication and complicated computational process for determining the optimum price [3]. This complication causes most of researchers employ direct methods to control demand, and minimize the total cost of the distribution grid by a central optimization technique [9,10]. However, using a direct control method takes away the decision authority from customers and produces adverse effects in the popularity and security of participants [11]. In addition, most of DSM methods do not pay attention to each customer's profit, and as a result, customers tend to contribute less in DSM. In order to solve this problem, the authors of [12] propose a multi-agent framework to minimize the electricity bill of each household while considering the piecewise linear function for each customer's cost. Still, the method neglects the correlation of loads with each other and cannot prevent rebounding peak.

Implementing the RTP-based indirect DSM program involves the electrical market models with an oligopoly competition instead of the perfect competition model. Typically, there are two competitive market models: the perfect competition and the imperfect competition

(oligopoly) model. The perfect competition model, which assumes that the decision of each participant in market has no effect in the market price, is relatively simpler and so it has gained popularity in the power market. Although in the power system, the consumption of each customer alone has negligible effect in the whole network; in indirect controlling, due to customers sometimes making similar decisions, it may have a big effect on the power system. In this case, the power market cannot be modeled by a perfect competition, and in order to consider the effect of real-time behavior of customers, an imperfect competition or oligopoly model is more suitable. The implementation of an imperfect competition is much more complicated than a perfect one. For modeling oligopoly energy productions, the Cournot competition model is widely used [13]. However, using this model on the customer side, with many participants, has more complexity. Since customers cannot neglect their energy consumption, they can only shift it to another time period; therefore, the energy consumption of each time depends on the consumption of other time periods. On the other hand, the energy price of different time periods depends on the total network consumption and loss in that time period. Consequently, in the Cournot model, the energy price of each time interval depends on the consumption of all customers in the present and the future time periods. The authors of [14] employ a Cournot competition to model a dynamic price for an intelligent building but they make some simplifying assumptions, such as linear inverse demand curve or having exclusive energy storage device to solve the problem, which limits the implementation of their technique.

Another weak point of existing research in DSM is that most of them do not consider the power system limits such as the electrical lines' overloading, power stability, power loss, and so on. A game-theoretic real-time price market to maximize the profit of each participant is proposed in [15]. However, their method does not have the ability to consider nonlinear power flow equations.

In this paper, we propose a new heuristic two-stage technique to implement indirect DSM program under RTP method. This technique can quickly find the optimum power of each customer in a decentralize manner to minimize their own cost while satisfying the technical constraints of the power system. The main contributions of this paper are summarized as follows:

- Proposes a dynamic RTP-based DSM program using a Cournot imperfect competition market model preventing rebound peak.
- Implements an indirect charging technique that gives the decision authority to all customers.
- Minimizes the cost of each customer individually instead of considering whole the network cost (all customers together).
- Proposes a heuristic two-stage iterative method to quickly find the market equilibrium point.
- Considers the power issues such as power loss or lines overload using nonlinear power flow equations.
- Solves systems with nonlinear constraints and non-convex cost function.

The rest of this paper is organized as follows. The mathematical modeling of the RTP-based indirect DSM is presented in Section II. A proposed heuristic method is explained in Section III. The simulation network and the simulation results are detailed in Section IV. Finally, we conclude in Section V.

II. RTP-BASED INDIRECT DSM MODEL

In this RTP-based indirect DSM program, each customer wants to schedule its appliances to minimize its cost by considering the influence of other customers based on the Cournot oligopoly model. It is assumed that each customer has two types of loads: inelastic loads, which cannot be shifted, such as lightings, and elastic loads, such as wet appliances, which can shift during a defined time period. When one appliance starts to operate it should continue its operation until the given task is done. In this case, each customer should determine the optimum time of turning elastic loads on, while satisfying the network and its own constraints. The objective function of this optimization problem is defined as follows:

$$\text{Min}_{t_{0,k}} \text{Obj} = \sum_{k=1}^{n_{e,i}} \sum_{t=t_{0,k}}^{t_{0,k}+t_{d,ik}} P_{e,ik}(t) \cdot \pi(t) \quad (1)$$

where $P_{e,ik}(t)$ is the active power of the i -th customer's k -th elastic appliance in time t ; $t_{0,ik}$ is the starting time of the k -th appliance; $t_{d,ik}$ is the time duration that the appliance need to finish its task; $n_{e,i}$ is the number of i -th customer's elastic appliances; $\pi(t)$ is the market price and it is updated based on the total real-time power consumption of the network in each time interval as follows:

$$\pi(t) = S \left(\sum_{i=1}^n \left(P_{ie,i}(t) + \sum_{k=1}^{n_{e,i}} P_{e,ik}(t) \right) + P_{loss}(t) \right), \quad (2)$$

where n is the number of customers, $P_{ie,i}(t)$ is the inelastic power of i -th customer; P_{loss} is the power loss of the electrical grid; and S is the power grid supply function calculated from supply side management (SSM) program or the supply curve giving the cost of the supplied energy for the power grid. The power loss of the network can be calculated as follows [16]:

$$P_{loss} = \sum_{i=1}^m \sum_{k=1}^m |V_i| |V_k| |Y_{ik}| \cos(\delta_i - \delta_k - \theta_{ik}), \quad (3)$$

where $|V_i|$ and δ_i are the magnitude and phase of i -th bus voltage, $|V_k|$ and δ_k are the magnitude and phase of k -th bus voltage, respectively; m is the number of network buses; and $|Y_{ik}|$ and θ_{ik} are the magnitude and phase of the grid admittance matrix, respectively. The voltage of all buses can be calculated from nonlinear power flow equations as described in many literatures. In this paper, a backward/forward sweep method, which considered to be the best appropriate method for distribution electrical networks, is implemented [17]. Since these equations are nonlinear, many DSM programs optimize the system neglecting the power loss and power constraints. However, in practice, the DSM program should consider the power network

constraints in addition to each customer constraints. The overload of power lines and voltage bus regulation constraints are as follows:

$$I_k(t) < I_{k,max} \quad \forall t, \quad (4)$$

$$V_{min} < V_j(t) < V_{max} \quad \forall t, \quad (5)$$

where $I_k(t)$ is the magnitude of k -th branch current in time t ; $I_{k,max}$ is the k -th branch capacity; V_{min} and V_{max} are the minimum and maximum levels of voltage of the network, respectively. Furthermore, each customer has some individual constraints. First, their task should be finished before the desired time, so the starting time should be selected as follows:

$$t \leq t_{0,ik} < t_{end,ik} - t_{d,ik} \quad \forall k, \quad (6)$$

where t is the present time interval, and $t_{end,ik}$ is the desired finishing time of i -th customer's k -th appliance. Second, each customer has a specific maximum allowable demand. Therefore, the total consumption of i -th customer in each time interval should satisfy the following constraint:

$$\left(P_{ie,i}(t) + \sum_{k=1}^{n_{e,i}} P_{e,ik}(t) \right) + \left(Q_{ie,i}(t) + \sum_{k=1}^{n_{e,i}} Q_{e,ik}(t) \right) \leq S_{max,i}^2 \quad \forall t, \quad (7)$$

where $Q_{ie,i}(t)$ is the inelastic reactive power of the i -th customer in time t ; $Q_{e,ik}(t)$ is the reactive power of the i -th customer's k -th elastic appliance in time t ; and $S_{max,i}$ is the maximum allowable apparent power of i -th customer. Consequently, the mathematical model of the RTP-based indirect DSM program using the Cournot oligopoly competition model is as follows:

$$\begin{aligned} \text{Min}_{t_{0,ik}} \text{Obj} = & \sum_{k=1}^{n_{e,i}} P_{e,ik}(t) \cdot S \left(\sum_{i=1}^n \left(P_{ie,i}(t) + \sum_{k=1}^{n_{e,i}} P_{e,ik}(t) \right) + P_{loss}(t) \right) \\ & + \sum_{k=1}^{n_{e,i}} \sum_{t=t_{0,ik}, \tau=t+1}^{t_{0,ik}+t_{d,ik}} P_{e,ik}(\tau) \cdot \pi^p(\tau) \end{aligned}$$

s. t.

$$P_{loss}^{pe} = \sum_{i=1}^m \sum_{k=1}^m |V_i^e| \cdot |V_k^e| \cdot |Y_{ik}| \cdot \cos(\delta_j - \delta_k - \theta_{ik}), \quad (8)$$

Power Flow equations [21],

$$I_k^e(t) < I_{k,max} \quad \forall k, \forall t,$$

$$V_{min} < V_j^e(t) < V_{max} \quad \forall k, \forall t,$$

$$t \leq t_{0,ik} < t_{end,ik} - t_{d,ik}, \quad \forall k, \forall t,$$

$$\left(P_{ie,i}(t) + \sum_{k=1}^{n_{e,i}} P_{e,ik}(t) \right) + \left(Q_{ie,i}(t) + \sum_{k=1}^{n_{e,i}} Q_{e,ik}(t) \right) \leq S_{max,i}^2 \quad \forall t.$$

where $\pi^p(\tau)$ is the predicted energy price for future times. The equilibrium point (real-time price) of the network can be calculated from solving the above optimization problem by each customer, simultaneously. In order to solve this optimization problem, each customer should predict its own consumption for the future times and estimate other customers' consumptions in the present time and future times. Furthermore, this is a nonlinear non-convex multi-objective optimization problem with many variables, and it

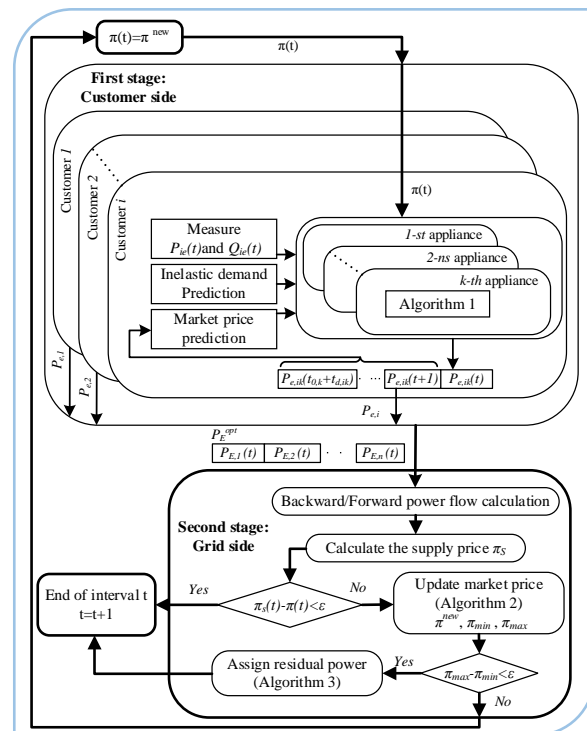


Figure 1. The proposed method to solve the RTP-based indirect DSM

cannot be solved in this form. In the next Section, a heuristic two-stage iterative method to quickly calculate the Nash equilibrium point of the network is proposed.

III. THE TWO-STAGE HEURISTIC METHOD

This Section presents a heuristic two-stage iterative method to solve the RTP-based indirect DSM program optimizing problem in (8). In this method, a modified optimization problem, which neglects the network constraints and the dependency of price to other customers' decisions, is solved in the first stage by each customer. The second stage calculates the whole network states and compensates the modification of the first stage using an iterative algorithm to approach the equilibrium. Figure 1 illustrates the mechanism of the proposed method.

A. First Stage: Customer Side

In the first stage, customers minimize their cost regarding the local constraints in a given price. In this case, the optimization problem of (8) converts to (9) as follows:

$$\begin{aligned} \text{Min}_{t_{0,ik}} \text{Obj} = & \sum_{k=1}^{n_{e,i}} \sum_{t=t_{0,ik}}^{t_{0,ik}+t_{d,ik}} P_{e,ik}(t) \cdot \pi_d(t) \\ \text{s. t.} & t \leq t_{0,ik} < t_{end,ik} - t_{d,ik}, \quad \forall k, \\ & \left(P_{ie,i}(t) + \sum_{k=1}^{n_{e,i}} P_{e,ik}(t) \right) + \left(Q_{ie,i}(t) + \sum_{k=1}^{n_{e,i}} Q_{e,ik}(t) \right) \leq S_{max,i}^2. \end{aligned} \quad (9)$$

where $\pi_d(t)$ is a given market price, which is updated for time interval t by the second stage to consider the dependency of each customer to other customers and network constraints. Although, the optimization problem of (9) is much easier to solve than (8) and some of the existing optimization methods can be used to solve this problem, this paper propose a heuristic method to quickly find the optimum solution of (9). As our method only use the simple mathematical operation, it can be implemented in simple computing devices such as smart meters.

In order to accelerate the calculation process, the proposed technique schedules each appliance separately. The algorithm orders the plugged elastic appliances of i -th customer in time t from the appliance with the smallest to the largest desired finishing time, and then the starting time of each appliance is selected sequentially so that the cost becomes minimum. In other words, the algorithm gives a higher priority to the appliance that should finish its task sooner than others and has fewer options. In order to determine the starting time ($t_{0,ik}$), the electricity cost of the task for different starting times are calculated and the cheapest one that satisfies (7) is selected. Algorithm 1 details the first stage of the proposed heuristic method to solve (9).

B. Second Stage: Grid Side

In the first stage, the optimum consumption of each customer in the given demand price (π_d) is calculated. In the second stage, the supply price (π_s) for the total power of the network is calculated and if the prices are not same, the price of the first stage is updated to approach the equilibrium point.

Generally, in a rational power market, a supply curve is a non-decreasing function and a demand curve is a non-increasing function; and the Nash equilibrium point is the intersection of these two curves (as shown in Figure 2.a). In this case, if π_s is greater than π , the price of the equilibrium point (π^*) is also greater than π , and vice versa.

The proposed algorithm uses this idea and bisects the difference between these two prices ($\pi_s - \pi_d$) to find the equilibrium point. Algorithm 2 details the process of finding the new price (π^{new}) for the next iteration. In this algorithm, π_{min} and π_{max} are the upper and lower limits of the equilibrium price, respectively. In order to satisfy the network constraints, a controlling price is added into π^{new} to control the consumption of each bus.

In the indirect method, since each customer wants to minimize its own cost, they may make a similar decision and

Algorithm 1: First stage – Minimizing customer cost (9)

- 1: Order the i -th customers' elastic appliances from the smallest $t_{end,ik} - t_{d,ik}$ ($k=1$) to the largest $t_{end,ik} - t_{d,ik}$ ($k=n_{e,i}$).
 - 2: For $k=1$ to $n_{e,i}$ do
 - 3: Calculate cost $\sum_{t=t_{0,ik}}^{t_{0,k}+t_{d,ik}} P_{e,ik}(t) \cdot \pi(t)$ for $t_{0,ik} \in (t, t_{end,ik} - t_{d,ik})$.
 - 4: Check constraint: $(P_{ie,i}(t) + \sum_{l=1}^k P_{e,il}(t))^2 + (Q_{ie,i}(t) + \sum_{l=1}^k Q_{e,il}(t))^2 \leq S_{max,i}^2$ for all t .
 - 5: Select the cheapest costs that satisfy the constraint.
-

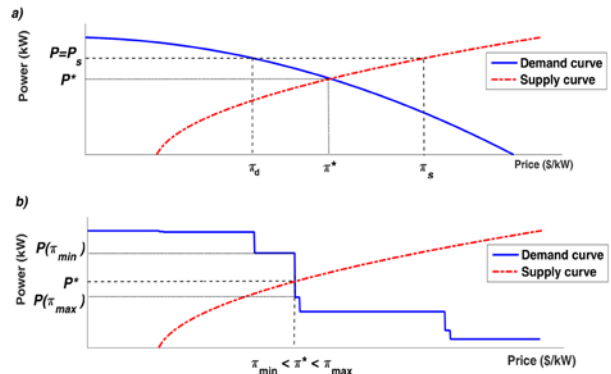


Figure 2. The demand and supply curve in a rational power market; a) a general form; b) when customers decide similar

Algorithm 2: Second stage - part 1, calculating $\pi^{new}, \pi_{min}, \pi_{max}$

- 1: If $\pi_d < \pi_s$ then $\pi_{min} = \max(\pi_{min}, \pi_d)$ else $\pi_{max} = \min(\pi_{max}, \pi_d)$
 - 2: $\pi^{new} = (\pi_{min} + \pi_{max}) / 2$.
-

collectively cause sudden changes in the demand curve as shown in Figure 2.b. In this case, although the proposed bisectional method converges to the equilibrium price ($\pi_{min} \approx \pi_{max}$), the consumption power cannot be calculated from the demand curve due to the sudden changes in this curve. The algorithm calculates the consumption power from inverse supply curve and assigns the difference between P^* and $P(\pi_{max})$, called the residual power, to some random customers by changing their price from π_{max} to π_{min} . This little change has no effect on the market price but changes their power consumption. In a real system with different appliances and different consumption behavior of customers, the occurrence probability of this problem is very low. Still, the proposed algorithm can be used to handle the problem. Algorithm 3 details the proposed method to handle this problem.

IV. CASE STUDY

A. Simulation Setup

For our simulation, the IEEE-37 bus test system is selected. Figure 3 shows the single line diagram of this system and the line data and the maximum power of each bus is taken from [18]. We generate the load profiles based on homes with different appliances and customer behavior modeled in [19]. For this purpose, a group of different home profiles (without wet appliances) are created by the simulator given in [20] as inelastic loads; then the adequate number of them, randomly, is assigned to each bus to consume the same maximum power reported as in [18]. This procedure results in 1491 customers connected to the different buses consuming about 14.5 MWh in each day. This high-consumption inelastic profile helps us to show the effectiveness of the proposed method in a power system under stressed.

Algorithm 3: Second stage-part 2, allocating residual power

- 1: Select π_{max} as π^* .
- 2: Calculate $P(\pi_{max})$ from Algorithm 1.
- 3: Calculate P^* from supply curve.
- 4: $P_{res} = P^* - P(\pi_{max})$
- 3: **While** $P_{res} > 0$ **do**
- 4: Select a customer randomly, change its price to π_{min} , and calculate $\sum P_{e,ik}(\pi_{min})$.
- 5: $P_{res} = P_{res} - (\sum P_{e,ik}(\pi_{min}) - \sum P_{e,ik}(\pi_{max}))$

We consider two different elastic appliances: dish washer and clothes washer with tumble dryer. The average consumption profiles of them is shown in Figure 4. These profiles are the hardest profiles to handle for the proposed algorithm due to a long time consumption period and a high difference of energy consumption during the period. When these appliances start to operate, they should operate until the task is completed. However, the price may change in future time intervals and this can become a source of error in the proposed method. Still, the simulation results in the next Section show that the proposed method can still manage this problem well.

It is assumed that customers use the dish washer with the probability of 50 % in each day and they turn it on between 8 and 10 am and the task needs to be done before 6 to 9 am of the next day with the uniform distribution. The clothes washer is plugged into the network between 10 and 12 am with probability of 50% and the task needs to be done before 10 to 12 am of the next day with the uniform distribution. These elastic appliances add about 5.5 MWh to total energy consumption of the network.

As shown below in (10), the supply function is calculated so that the average price for off-peak and on-peak time of inelastic loads equal to 4 and 17 ¢/kW according to [21].

$$S(P_{total}) = 3.77E - 7.P_{total}^2 + 1.41E - 4.P_{total} + 5.32E - 2, \quad (10)$$

where P_{total} is the total input power of the network including power loss. In this simulation the error of inelastic power prediction and price forecasting is modeled by a normal distribution with standard deviation equals to three per cent.

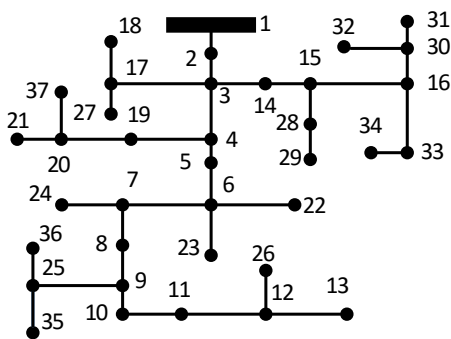


Figure 3. The IEEE-37 bus test system

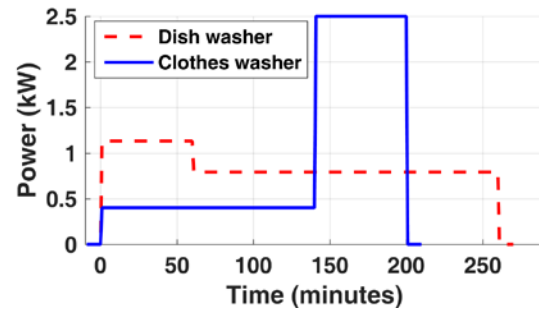


Figure 4. The average consumption profile of elastic appliances

B. Simulation Results

The proposed two-stage method solving the RTP based indirect DSM program is implemented in MATLAB platform using a computer with an 8-core 2.3 GHz CPU and 8 GB RAM. We consider different cases as listed below:

- Case 1: The network without elastic loads.
- Case 2: The network with the elastic loads and without DSM program (i.e., flat rating program).
- Case 3: The network with the elastic loads and with TOU based DSM program [21].
- Case 4: The network with the elastic loads and with the proposed RTP based indirect DSM program.

Figure 5 shows the total active power and the marginal cost of energy production in different cases. The system without elastic loads is shown in case 1 (details are shown in Figure 6). In this case, the demand peak is equal to 1045 kW and the maximum marginal cost is equal to 0.32 \$/kW. Without DSM program (case 2), each appliance consumes the power as soon as it connects to the network. In this case, a demand peak (1908 kW), which is much higher than the inelastic demand peak is created around noon and increases the maximum marginal cost to 1.16 \$/kW. The TOU based DSM program (case 3) has low energy tariff during off-peak periods, which attracts the elastic loads to consume power in these periods. In this case, a new rebound peak is generated as shown in Figure 5. The rebound peak in this case is equal to 1654 kW and the maximum marginal cost is 0.85\$/kW. Table I compares the peak power, the energy loss during each day, the maximum marginal cost, the total energy cost, and the minimum bus voltage in different cases.

Figure 6 shows the total active power of elastic appliances in the proposed method. Customers, in order to avoid expensive electricity price, schedule their elastic loads when the real-time price is low. As a result, none of the elastic loads consumes energy between the hours of 17 and 23. This strategy leads the peak power of network and the maximum marginal cost of the production to remain constant although the energy consumption increased by 38%. Table I shows that the total cost of energy supplied in the proposed method (2849 \$) is about half of the total cost of energy supplied in the flat rate (5617 \$) or TOU based (5250 \$) program.

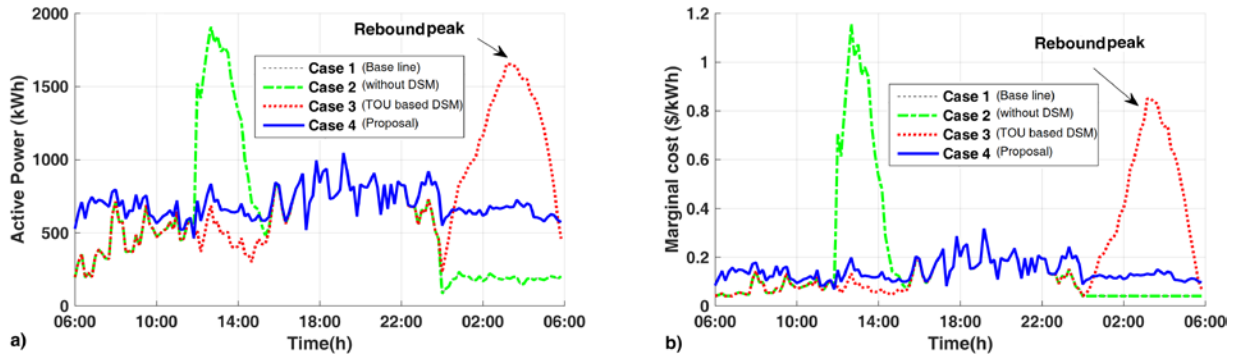


Figure 5. Comparison between cases 1-4: (a) total active power, b) marginal cost

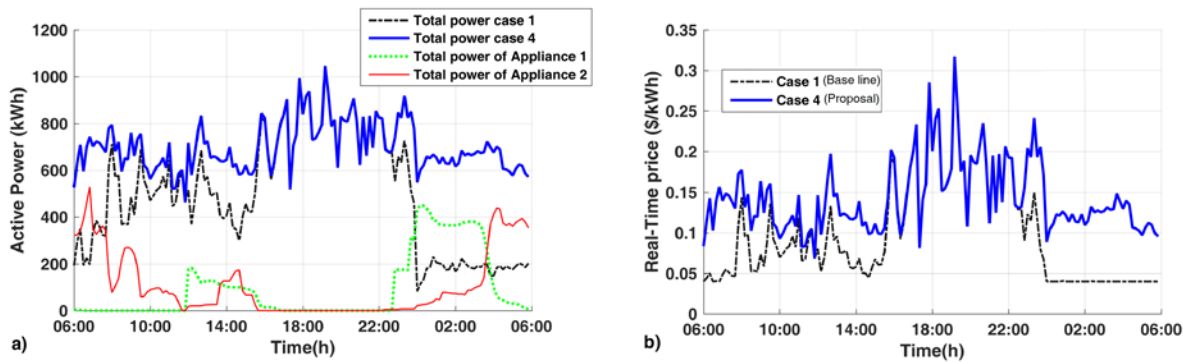


Figure 6. Comparison between the proposed method (case 4) and inelastic loads (case 1): a) total active power, b) the real time price

TABLE I. PERFORMANCE COMPARISON OF DIFFERENT CASES

	Peak power (kW)	Energy loss (kWh)	Maxi price (\$/kW)	Total energy cost (\$)	Mini voltage (%)
Case 1 (Base line)	1045	262	0.317	1710	95.1
Case 2 (Without DSM)	1908	583	1.156	5617	90.2
Case 3 (TOU based DSM)	1654	559	0.850	5250	91.3
Case 4 (Proposed)	1045	443	0.317	2849	95.1

The results show that the total elastic power consumption has some small local peak. These local peaks are happen because the method is an indirect one and each customer decides independently, and we consider the worst load profiles, which have a large operating period. Using load profiles, which has less dependency during time, such as water heaters or electrical vehicles, can improve the results even more.

Figure 7 shows the worst voltage profiles of different cases. In cases 2 and 3, because system has a high peak demand, the voltage of some buses drop lower than 95%, while the proposed method (case 4), has voltage profile exactly same as case 1 due to the peak load control. In cases 1 and 4, the worst voltage drop occurs on bus 26 at 19:20'.

The number of iterations and the calculation time for each time interval are shown in Figure 8. As each customer optimizes its consumption, the proposed method can quickly

find the equilibrium point. In this implementation, each time interval is assumed equal to 10 minutes long, which is a practical assumption in SGs. However, the proposed algorithm can be employed for time intervals less than one minute due to fast calculation.

V. CONCLUSION

The environmental concern and shortage in fossil fuel is increasing the penetration level of renewable energy sources in the electrical grids. The uncontrollable nature of output power produced by renewable source makes a DSM program more imperative in the modern power grid. In this paper, a new RTP-based indirect DSM program using an imperfect competition market in smart grids is proposed. The indirect DSM program gives the decision authority to customers and can attract more customers to participate in the program, while the imperfect competition market model prevents the rebounding peak and satisfies the power system constraints. Although, the indirect demand control in an imperfect competition market leads to a complicated nonlinear non-convex multi-objective optimization problem, this paper proposes a heuristic two-stage iterative method to quickly solve the problem. The method is implemented in MATLAB on the IEEE 37-bus test system to analyze the effectiveness of the method. The test system includes about 1500 customers with actual load profiles and different elastic appliances. The results show that the proposed method solves the problem quickly enough for real-time application and it decreases energy cost of individual customers and

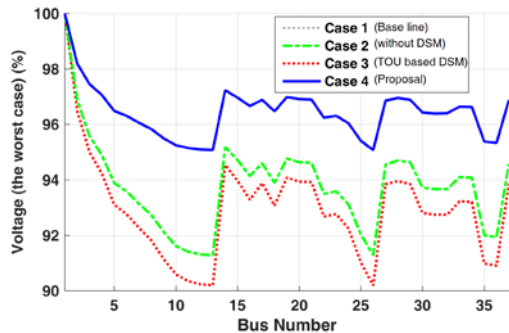


Figure 7. The worst voltage profiles

power loss, and also maintain power system constraints, such as voltage regulation, within their limits.

ACKNOWLEDGMENT

This research was funded by the MSIP (Ministry of Science, ICT and Future Planning), Korea, under the "ICT Consilience Creative Program" (IITP-2015-R0346-15-1007) supervised by the IITP (Institute for Information & communications Technology Promotion) and under the "Basic Science Research Program" (2013R1A1A10104 89, 2015R1C1A1A01053788) through the NRF (National Research Foundation).

REFERENCES

[1] "Benefits of demand response in electricity markets and recommendations for achieving them. A report to the United States Congress pursuant to section 1252 of the Energy Policy Act of 2005," ed. US Washington, DC: US Washington, DC: Department of Energy.[https://www.smartgrid.gov/files/Benefits_Demand_Response_in_Electricity_Markets_Recommendati_200608.pdf] (20 Jun 2016).

[2] M. Alizadeh, X. Li, Z. Wang, A. Scaglione, and R. Melton, "Demand-side management in the smart grid: Information processing for the power switch," *Signal Processing Magazine, IEEE*, vol. 29, Issue.5, 2012, pp. 55-67.

[3] J. S. Vardakas, N. Zorba, and C. V. Verikoukis, "A Survey on Demand Response Programs in Smart Grids: Pricing Methods and Optimization Algorithms," *Communications Surveys & Tutorials, IEEE*, vol. 17, Issue.1, 2015, pp. 152-178.

[4] M. Parvania and M. Fotuhi-Firuzabad, "Demand response scheduling by stochastic SCUC," *Smart Grid, IEEE Transactions on*, vol. 1, Issue.1, 2010, pp. 89-98.

[5] S. Braithwait, "Behavior modification," *Power and Energy Magazine, IEEE*, vol. 8, Issue.3,2010, pp. 36-45.

[6] A. W. Berger and F. C. Schweppe, "Real time pricing to assist in load frequency control," *Power Systems, IEEE Transactions on*, vol. 4, Issue.3, 1989, pp. 920-926.

[7] A. Safdarian, M. Fotuhi-Firuzabad, and M. Lehtonen, "A distributed algorithm for managing residential demand response in smart grids," *Industrial Informatics, IEEE Transactions on*, vol. 10, Issue.4, 2014, pp. 2385-2393.

[8] T.-H. Chang, M. Alizadeh, and A. Scaglione, "Real-time power balancing via decentralized coordinated home energy scheduling," *Smart Grid, IEEE Transactions on*, vol. 4, Issue.3, , 2013pp. 89-98.

[9] P. McNamara and S. McLoone, "Hierarchical Demand Response for Peak Minimization Using Dantzig-Wolfe Decomposition," *Smart Grid, IEEE Transactions on*, vol. 6, Issue.6, 2015, pp. 2807-2815.

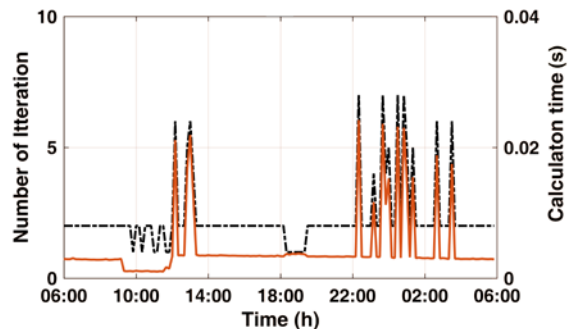


Figure 8. The numebr of iterations and the calculation time for each time interval

[10] T. Logenthiran, D. Srinivasan, and T. Z. Shun, "Demand side management in smart grid using heuristic optimization," *Smart Grid, IEEE Transactions on*, vol. 3, Issue.3, 2012, pp. 1244-1252.

[11] M.S. Kuran, A.C. Viana, L. Iannone, D. Kofman, G. Mermoud, and J.P. Vasseur, "A Smart Parking Lot Management System for Scheduling the Recharging of Electric Vehicles," *Smart Grid, IEEE Transactions on*, vol. 6, Issue.6, 2015, pp. 2942-2953.

[12] Z. Wang and R. Paranjape, "Optimal residential demand response for multiple heterogeneous homes with real-time price prediction in a should be a spacemultiagent framework," *IEEE Trans. Smart Grid* 2015, 10.1109/TSG.2015.2479557

[13] D.S. Kirschen, G. Strbac, "Fundamentals of Power System Economic". John Wiley & Sons: West Sussex, UK, 2004

[14] Q.D. La, Y.W.E.Chan, B.-H. Soong, "Power management of intelligent buildings facilitated by smart grid: A market approach," *IEEE Trans. Smart Grid* 2016, 7, 1389-1400.

[15] T. Namerikawa, N. Okubo, R. Sato, Y. Okawa, and M. Ono, "Real-Time Pricing Mechanism for Electricity Market With Built-In Incentive for Participation," *Smart Grid, IEEE Transactions on*, vol. 6, Issue. 6, 2015, pp.2714-2724.

[16] J. G. Grainger and W. D. Stevenson Jr, *Power System Analysis*. India McGraw-Hill Education, Dec 1, 2003

[17] G. Chang, S. Chu, and H. Wang, "An improved backward/forward sweep load flow algorithm for radial distribution systems," *Power Systems, IEEE Transactions on*, vol. 22, Issue.2, 2007, pp. 882-884.

[18] A. Al-Hinai, K. Sedhisigarchi, and A. Feliachi, "Stability enhancement of a distribution network comprising a fuel cell and a microturbine," presented at the Power Engineering Society General Meeting, 2004. IEEE, Denver, colorado,USA, June, 2004.

[19] I. Richardson, M. Thomson, D. Infield, et al., "Domestic electricity use: A high-resolution energy demand model," *Energy and Buildings*, vol. 42, Issue. 10, 2010,pp. 1878-1887.

[20] Richardson, I.T. Domestic electricity demand model-simulation example. Availabe online: <https://dspace.lboro.ac.uk/dspace-jspui/handle/2134/5786> (19 May 2016).

[21] SmartGridCity pricing plan comparison chart. Availabe online: <http://smartgridcity.xcelenergy.com/media/pdf/SGC-pricing-plan-chart.pdf> (19 May 2016)

Simulation of Electric Vehicle Battery Behaviour for Frequency Regulation Use: Profitability Versus Mobility Constraints and Grid Needs

Lamya Abdeljalil Belhaj^{1,2}, Antoine Aubineau¹,
Antoine Cannieux¹, Salomé Rioult¹,

¹Institut Catholique d'Arts et Métiers, Icam
Carquefou, France

²Institut de Recherche en Energie Electrique de Nantes
Atlantique
Saint Nazaire, France
e-mail: lamya.belhaj@icam.fr

Isabel Praça, Zita Vale

GECAD – Research Group on Intelligent Engineering and
Computing for Advanced Innovation and Development,
Institute of Engineering, Polytechnic of Porto (ISEP/IPP),
Porto, Portugal
e-mail: {icp, zav}@isep.ipp.pt

Abstract—Electric Vehicles Batteries are particularly adapted for frequency regulation service regarding their features and their availability. Many parameters have an important impact on the service profit like the grid needs, the driving patterns, the battery wear, the investments and the service remuneration. The aim of this study is to propose an algorithm in view of dynamic simulation taking into account grid requests, vehicles driving patterns and the electricity prices. The proposed tool can use real Electric Vehicles and grid data as well as simulated ones. It allows apprehending the profitability for various markets situations, mobility patterns and charging schedules. It also allows following the gains during the day in view of gains communication to the Electric Vehicle or fleet owner and for a dynamic decision about the service delivery depending on the profit and the battery availability.

Keywords-Vehicle to Grid; Frequency regulation; Profitability calculation; Dynamic simulation; Regulation market remuneration.

I. INTRODUCTION

Nowadays, the widespread use of Electric Vehicles (EVs) faces many difficulties due to their high prices and their limited autonomy compared to vehicles that use fossil fuels. However, with the foreseen advancements in storage technologies, EV will be an important tool under the context of smart grids to improve efficiency and sustainability of power systems. Indeed, it may be a very relevant means to provide grid services in order to better manage, with the uncertainty of renewable generation, grid congestions as well as using the batteries energy for other grid services. In fact, the vehicles are used 5% of the time for mobility and are available for other purposes during the remaining time [1]. Consequently, a good storage potential will be available according to the development of EV. On the one hand, the EV battery can support the intermittent renewable sources of energy by absorbing the production when there are no consumption needs in the grid. At the same time, the used energy for mobility will come from green sources ensuring the low carbon footprint of the EV.

On the other hand, the EV battery can help the grid for balancing production and consumption and ensuring power

quality. In fact, the available energy can be used for ancillary services like frequency regulation or peak shaving.

In the context of Vehicle to Grid (V2G), an EV fleet acting like a generation unit is an interesting actor in the energy markets like in Germany and Sweden [2], California [3] or France [4]. Studies also proved that a single EV is able to provide ancillary services under real-time conditions [5] in the PJM market, which coordinates electricity in 13 states in USA and the District of Columbia.

Some studies [6] highlighted that the peak power management corresponding to power injection in the grid during high consumption periods is more suitable with hybrid vehicle regarding the high amount of needed power versus mobility constraints and battery wear. Nevertheless, other ancillary services are very suitable for EVs batteries in particular frequency regulation [7] [8] characterized by low amount of energy requests many times during the day.

Studies show gains between 100€ per year per vehicle in the French context [4] and 2000€ in the American one [3]. The EV battery is profitable for frequency regulation service because the initial capital cost of the battery purchased for driving may not be totally assigned to the V2G [1]. Besides, the battery response time is quick [1] [3] and the low quantity of energy induces shallow cycling and thus extended life cycles [9]. However, the profitability for several actors like the DSO, EV aggregator and EV owner must be ensured and is variable depending on the context. The profitability may concern EV owner or EV fleet aggregator. For the EV owner, the service may be profitable at his level if a single-vehicle is able to provide the service under real-time conditions in the regulation market. Otherwise, his gain will be shared with an EV fleet aggregator able to offer a higher level of power to the grid.

This paper aims to present an interesting tool allowing the simulation of the dynamic behaviour of an EV Battery (EVB) while ensuring, mobility and frequency regulation service. The proposed algorithm calculates the service availability and the net profit for each request of the grid.

The first part of this article describes the frequency regulation service and some regulation markets in the world. The second one presents a detailed description of the profitability calculation methodology by request. The third part presents the algorithm allowing simulating the EVB behaviour during one day including the availability and the profitability. It also presents the used algorithm to generate the driving patterns that are one of the main inputs of the frequency regulation simulation. The other parameters and inputs are also described. Finally, realistic case studies compare the profitability for various situations. They illustrate the possibility of using the proposed tool in any context to simulate the EV behaviour under mobility and services constraints. It can also integrate real EV data to calculate the service profitability and to decide about the service delivery.

II. FREQUENCY REGULATION

The grid power quality is dependent on the real time balance between the electric consumption and the production while maintaining, for instance, rated voltage, frequency and harmonics level. Regarding the frequency regulation, it is dependent on the balance of active power in the grid. In fact, the frequency decreases if the consumed active power exceeds the generated one, thus, there is a need of “regulation up”. Contrariwise, if the generation exceeds the consumption, frequency rises and a “regulation down” is necessary. In order to achieve these operations, three frequency reserves exist: the primary and the secondary reserves, which are generally automatic, and the tertiary reserve or long-term reserve, which is triggered manually.

The primary reserve is for an instantaneous adjustment (seconds) and activated automatically. Today, this regulation is implemented via the speed regulation of the production groups and the frequency of use is high. Obviously, as EVBs can offer the primary regulation, they are also able to offer secondary and tertiary ones. However, this study will concentrate on the primary regulation.

Regarding the high amount of needed power at grid level compared to each EV battery capacity, new actors like EV aggregators will allow optimizing EV resources as storage. For the fleet manager, one of the main issues is the real available power for the service. In fact, EVBs may not be plugged in or not with the right State of Charge (SOC). In this context, various studies on the stochastic behaviour of EVs stated the reliability of the frequency regulation service despite the mobility constraints [10].

A. Markets

Regarding the regulation market, we talk about Automatic Generation Control Market (AGC) in most of the countries. In the smart grid context, new grid components offer regulation services in the regulation market like controllable loads or electric storage. For instance, CAISO Market allowed Non-Generator Resource (NGR) such as batteries and flywheels, to bid in the regulation market [11].

Batteries are well positioned in the AGC market by nature because the time response of the electric storage is fast and adapted to high quality primary frequency regulation. The California Energy Commission stated that the storage resources are at least twice as effective as a combustion turbine for the grid regulation purposes [11].

The payment of regulation services is represented by various prices depending on the markets [12]. Most of them take into account capacity price for the energy made available for the service and service price for the effective supplied energy. For instance, in the ISO New England (ISO-NE), the payment includes capacity price and service price [13]. Some of the markets use only one of the two remunerations as in France where the primary reserve payment is provided by a fixed tariff and the payment is limited to a capacity price whereas secondary reserve includes both of the capacity and service prices [4].

The regulation market functioning is highly dependent on the electric grid features. It mainly depends on the geographical location, the renewables’ penetration, the EVs presence. Besides, it is also impacted by the advancements in the smart grid installations with possibilities of grid services offers based on storages, load management and other means. Many markets are under development or are currently changing depending on the grid situations.

III. PROFITABILITY CALCULATION

In this part, the annual net profit calculation [3] is extended to profitability calculation per grid request.

A. Per request revenue calculation

In the case of V2G used for frequency regulation, the capacity payment is for power being available in kW-h to support the grid. Whereas the energy payment is for the energy in kWh exchanged in real time. The per request revenue is calculated using the following equation:

$$R_{\text{reg-r}} = R_{\text{el-r}} + R_{\text{cap-r}} = (p_{\text{el}} Q_{\text{request}}) + \left(p_{\text{cap}} P \frac{h_{\text{plug}}}{T_{\text{day}}} \right) \quad (1)$$

For the remunerated produced energy per request $R_{\text{el-r}}$, the delivered energy Q_{request} in kWh is multiplied by the electricity price p_{el} , which is the market selling price of electricity in €/kWh.

Besides, the capacity payment $R_{\text{cap-r}}$ is calculated using:
 - p_{cap} , the capacity price, which is in €/kW-h. It is the price for the service availability, it means the remuneration fixed by the contract for the participation to the service when the battery is plugged in and available. There is a remuneration even if there is no service.

- P is the contracted capacity available for the V2G, in kW. It is the smallest value between vehicle power P_{veh} and the line power P_{line} because both of them limit the power. P may also be limited by the performance represented by the response ramp dynamic. The ability of ramping limits the total amount of power capacity in some markets like PJM [14]. Nowadays, 95% of the charging stations are slow charging for instance

in France 3kW [15]. For V2G participation, fast charging is more interesting. We assume a value of 15kW with adapted installation [3].

- T_{day} is the number of transfers per day.
- h_{plug} is the number of hours during the day when the EV is plugged in and available for the service.

In regulation down, we assume that the operation is always financially positive because the battery will have to be charged for mobility purposes. In fact, if the SOC matches with the demand, the regulation down is achieved, and the gain corresponds to the stored energy E_{sc} (kWh) multiplied by the price of buying the electricity c_{pe} (€/kWh) at the charging moment. The gain represents the charging cost if it had been realized using the grid.

B. Per request cost calculation

The cost for regulation up is defined as follows:

$$C_{\text{reg-r}} = C_{\text{el-r}} + C_{\text{c-r}} = c_{\text{en}} Q_{\text{request}} + \frac{c_{\text{ac}}}{T_{\text{day}} d_{\text{plug}}} \quad (2)$$

Regarding the energy cost $C_{\text{el-r}}$ calculation:

- c_{en} is the cost per energy unit in €/kWh, which includes: the cost of electricity, losses, plus battery degradation cost. It is calculated as follows:

$$c_{\text{en}} = \frac{c_{\text{pe}}}{\eta_{\text{conv}}} + c_{\text{d}} \quad (3)$$

Where c_{pe} is the cost of purchased electricity for recharging in €/kWh. η_{conv} is the two-way electrical efficiency and is around 73% [3].

c_{d} is the cost of battery degradation calculated using :

$$c_{\text{d}} = \frac{c_{\text{bat}}}{3 L_{\text{c}} E_{\text{s}} \text{DOD}} \quad (4)$$

- L_{c} is the number of cycles fixed to 2000 cycles for Li-ion battery at 25°C [9].

We assume that shallow cycling has less impact on battery lifetime than deep cycling [3] [7]. Thus, factor 3 is used for the number of cycles.

- DOD is the maximum Depth of Discharge in % fixed to 80% [9].
- c_{bat} is the total battery replacement cost in €, calculated using:

$$c_{\text{bat}} = (E_{\text{s}} c_{\text{b}}) + (c_{\text{l}} t_{\text{l}}) \quad (5)$$

Where c_{b} is the cost of the battery in €/kWh assumed to be $c_{\text{b}} = 300\text{€/kWh}$ [15].

c_{l} is the cost of labour in € and t_{l} the labour time required for battery replacement. They are fixed to the average of the labour cost, in 2015 in Europe it was 35€/h [16] and a replacement labour time of 8 hours [3].

- E_{s} in kWh is the energy of the battery fixed to 22 kWh, which represents 65% of EVs in France in 2013 [15].

For the capital cost calculation $C_{\text{c-r}}$:

- c_{ac} is the annualized capital cost for additional equipment needed for V2G calculated using:

$$c_{\text{ac}} = c_{\text{c}} \text{CRF} = c_{\text{c}} \frac{d}{1 - (1 + d)^{-n}} \quad (6)$$

- c_{c} is the capital cost i.e., the one-time investment assumed to be 1800€ including on board metering, adapted power electronics for V2G, wireless communication system, and wiring costs [3].

- CRF is the capital recovery factor calculated using d , which is the discount rate in % and n the amortization duration in years thus the lifetime of the V2G hardware fixed to 10% and 10 years [4].

- d_{plug} is the the number of days in the year when the EV is plugged in and available for the service.

The cost from regulation down is assumed to be null because there is no need of additional equipment and it is considered as always interesting because it is free charging.

IV. SIMULATION ALGORITHMS

The frequency regulation simulation algorithm is implemented in Matlab. To make it available under SEAS Shared Intelligence Platform (SEAS-SI), developed by GECAD for SEAS project [17], inputs and outputs templates, as well as specific web services, needed to be developed accordingly. SEAS-SI platform allows algorithms sharing without confidentiality concerns. Those algorithms may be executed on-line, alone, sequentially or combined differently. The EV behaviour algorithm outputs are used for the frequency regulation simulation.

A. EV behaviour algorithm

Electric Vehicle Scenario Simulation tool (EVeSSi) has been actively developed since 2011 [18] with the goal of supporting the development of realistic case studies that include scenarios with EVs, eliminating the need to create manually each individual vehicle profile.

EVeSSi includes several modules: scenario and input configuration, SUMO simulation, SUMO output data importer, electric grid creator, and an intelligent grid allocator. In the first stage, EVeSSi is used essentially as a parameterization tool to introduce the input data for the simulation in SUMO. These inputs can be summarized as follows: the first step is to generate/load the road network (load a real road network or generating a “virtual” one by introducing specific parameters), a second step is related to the creation of EVs and its parameters, and then it is necessary to specify the charging points or use a random generation to do it. Finally, an algorithm can perform the daily activities and generate the necessary trips, which are then simulated by SUMO engine (the actual traffic simulation results). The data importer module reads the files generated by SUMO application and then filters, treats and analysis the necessary data to be executed by the subsequent developed algorithms. The grid creator can generate an electric grid taking into account the dimensions of the road network. This creates a grid with intelligently distributed electrical buses and respective branches. This algorithm is used only if the user does not specify a local real grid. If the user loads the

respective real grid the mentioned generation is skipped. After this step, the intelligent grid allocator finds the corresponding electric bus where EV can connect, depending on the location, i.e., the street of the arrival or where it is parked.

The traffic model allows evaluating the chaotic behaviour of traffic, which is affected by several factors, including the road network topology, the number of cars and their routes, the types of vehicles, traffic lights and the users' driving behaviour, which is hard to predict. The influence of traffic patterns in travel times can be analysed, and the energy consumption measured. The integration of the traffic model with EVeSSi enables to bridge the road network and the electricity grid, therefore, overcoming the existent gap in current applications [19]. In fact, there is a huge potential in applications with EVeSSi, for instance, evaluating performance of electric public transports, analysing optimal location of charging points and charging stations, estimating electricity network impacts, testing different control strategies like smart charging and V2G approaches, predicting traffic patterns and user behaviour, among others.

B. Frequency regulation algorithm

There are three main loops in the frequency regulation algorithm (FreqReg). The first one decides about the EV availability for the service mainly according to mobility and charging constraints. The second one deals with frequency up requests and the third one with the frequency down requests. During all the simulation, the SOC is calculated according to the delivered services, the mobility and the charging. However, for a real EV, the SOC may be given by the EV Battery Management System using adequate communication solutions when possible. ISO 15118-2015 defines the bidirectional communications protocol for the Vehicle to Grid communication interface. It prepares a standardized context for EV integration to the power grid. For instance, communication requirements for energy demand/response information (local and grid) as well as vehicle charge status are defined. In our simulation, the algorithm inputs are described in Fig.1.

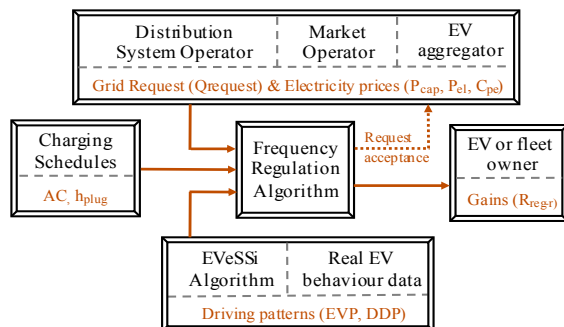


Figure 1. Frequency regulation algorithm interactions

1) Availability for the service request:

The algorithm decides about the availability of the EV for frequency regulation service:

If the EV is not used for mobility and if it is plugged in and not charging, the EV is available for the service, thus, the capacity payment R_{cap-r} and the capital cost C_{c-r} are calculated.

- In case of mobility use, using the vehicle driving efficiency η_{veh} in (kwh/km) and the travel distance (km).
- In case of charging, according to the charger features.

2) Frequency regulation up/down:

If the EV is available and the grid demand is to supply/store energy, the request is for frequency regulation up/down. The loops calculation is as follows:

- The available energy E_{sa} /storage capacity E_{sc} is calculated using the last calculated value of the SOC:

$$\begin{cases} E_{sc} = E_s (1 - SOC) \\ E_{sa} = E_s (SOC - (DRB + (1 - DOD))) \end{cases} \quad (7)$$

DRB is the distance range corresponding to the EV owner needs for mobility. Daily trips in Europe and USA are around 40 km [4]. Thus, for a typical working day, the average driven distance “home to work” is about 20 km. Nonetheless, people will probably overestimate their needs [15].

- If the battery SOC matches the demand, the service is realized, thus, the energy payment R_{el-r} and the energy cost C_{el-r} are calculated.
- If the battery capacity does not match the demand, an offer is made with the available energy / storage capacity and the EVB is waiting for a new grid request.
- The new SOC is calculated after the service delivery.

3) Simulation inputs:

All the algorithm inputs are vectors with length i representing the number of requests per day.

a) Driving pattern:

The inputs describing the EV behaviour are:

- The vector “EV Plugged in” is: $EVP = [EVP_1 \dots EVP_i]$
 $EVP_i = 1$ if the EV is plugged in and $EVP_i = 0$ if the EV is on the road or parked but not plugged in.
- Driven Distance per Period in km: $DDP = [DDP_1 \dots DDP_i]$

EVeSSi outputs are the EV status regarding mobility with the consumed energy, the driving hours and the connection to each bus. Thus, it is useful to define EVP and DDP vectors.

The data-set generated using EVeSSi contains 1800 realistic EVs and PHEVs with a 24h-period scenario and a step time of 1h. It is available as “Case with 1800 EVs / GECAD” in IEEE-PES Working Group on Intelligent Data Mining and Analysis [20]. There are 180 EVs and we are focusing on three representative types of vehicles:

- Type 1: 1h of daily trip with a round trip and a total of around 20 km. It represents the average of 40% of the 180 EVs of the database. For the simulation, we use EV n° 39 – Bus n°30;
- Type 2: 2h of daily trip with two travels and an average of 20 km per travel. It represents a typical working day in Europe and USA [4]. For the simulation, we use a total of 46 km – EV n°19 – Home (Bus n°7) – Work (Bus n°11);

- Type 3: 2h of daily trip with high mobility needs with two travels. For the simulation, we use a total of 165 km – EV n°179 – Home (Bus n°3) – Work (Bus n°22).

b) *Charging:*

The charging vector is called “Availability to Charge”: $AC = [AC_1 \dots AC_i]$; $AC_i = 0$ for EVB not available for charging and $AC_i = 1$ for EVB available for charging. In our case studies, the EV is charged during the low electricity price hours depending on the mobility constraints. Otherwise, the algorithm allows integrating any smart charging schedule.

c) *Grid requests:*

The energy needs, at each request, are:

$$- Q_{request} = [Q_{req1} \dots Q_{reqi}]$$

The DSO fixes its needs in kWh for frequency regulation up and down. Our simulation can be realized for any grid needs. Our studies highlighted a slight annual profit difference of 21 € per year between summer (2015/07/19) and winter (2015/02/25). Thus, the results are presented for winter day to investigate the parameters impact. The data is available on RTE (French DSO) data base [21]. Requests are given for each half an hour thus 48 requests are simulated per day. The inputs may also be recuperated in real time through the right communication devices with the DSO or the aggregator. In our approach, we assume 100 000 EVs under contract and carrying out the half of the frequency regulation demand.

d) *Remuneration and prices:*

- $P_{cap} = [P_{cap1} \dots P_{capi}]$. We use a constant capacity price $P_{capi} = 0,017€/kW-h$, representing of the French market. However, the remuneration level will certainly change in the next years and may become variable [4];

- $P_{el} = [P_{le1} \dots P_{eli}]$. We assume a constant price of $P_{eli} = 0.05€/kWh$. It is a mean value of the electricity price in EPEX database in 2015 (average for one day by season) [36]. This value is mainly dependent on the regulation market and may vary during the day;

- $C_{pe} = [C_{pe1} \dots C_{pei}]$ is the electricity price for charging the battery fixed to EPEX values [22].

V. CASE STUDIES

A. *Mobility*

Fig. 2 represents the grid requests for one EV and for the 25th February 2015. It represents regulation up requests with positive values and regulation down ones with negative values.

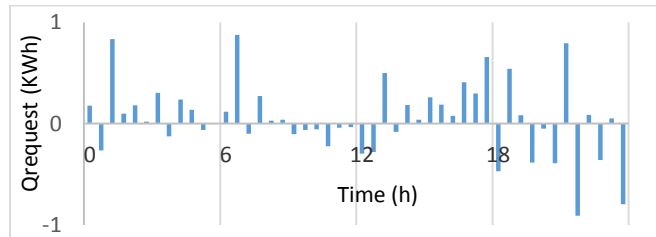


Figure 2. Grid requests for one EV, 2015/02/25.

Fig. 3 represents the batteries of the three types of vehicles submitted to grid requests, mobility and charging.

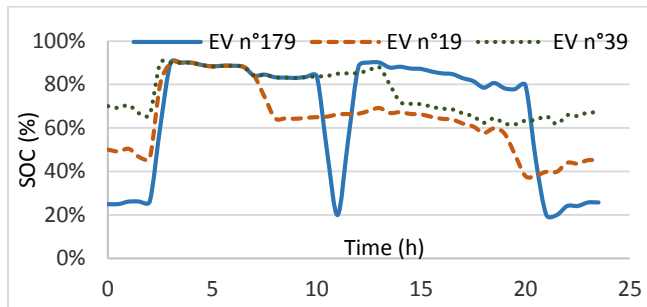


Figure 3. EVs batteries State of Charge (SOC) variation, 2015/02/25

Regarding the EV n°39 (20km) and n°19 (46km), the SOC decreases according to the mobility of the day. Otherwise, the EVB is available for frequency regulation service except during the charging scheduled during the night taking advantage of low electricity price period. Fig. 3 shows that the regulations up and down have very low impact on the SOC regarding the low amount of energy and the compensation of the two kinds of requests. We notice that there is no need of charging during the day to allow the EV owner to ensure its requirements regarding mobility.

The net profits for one day are as follows:

- For EV n°39: 4,4 € per day (1 606 € extended to 1 year).
 - For EV n°19: 4,2 € per day (1 533€ extended to 1 year).
- The net profits are very close. The main part of the gain is coming from the capacity remuneration (around 80%), which is impacted by the EV availability to offer the service. This conclusion is true under the adopted remuneration conditions, however it may be completely different in other contexts where the capacity price is low or does not exist.

The EV n° 179 has more important mobility needs. Consequently, charging is necessary during the day to ensure the second trip of the day and is scheduled after the end of the first trip. The EV offers frequency regulation during the rest of the day and as for the previous cases, the service impact has low impact on the EV SOC. The net profit per day is around 3,7€ (1 350€ extended to 1 year). The benefit is lower than for the other EVs because of the lower availability of the EV due to the charging period and the mobility constraints; however, the gain is still very interesting.

B. *Charging and V2G equipment*

EV owners may plug the EVB at home on their primary EV Supply Equipment (EVSE) or at work on their secondary EVSE. Nevertheless, EVSE may not be available at work. Besides, even if the EV owner decides to participate to the regulation market through V2G investment at home, he is not ensured to have this possibility everywhere.

Thus, we consider two scenarios for the same grid requests in Fig. 4:

- C1: EV n°19 with EVSE at home and at work.
- C2: EV n°19 with EVSE only at home.

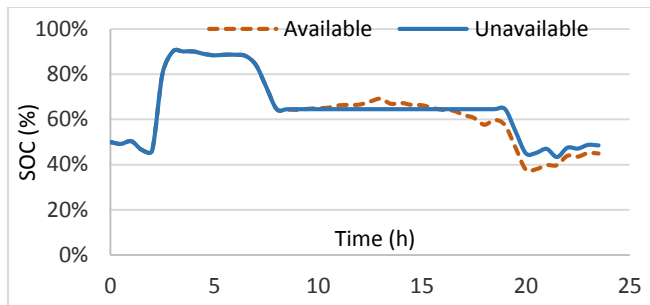


Figure 4. EV n°19 battery State of Charge (SOC) variation 2015/02/25.

Notice that because the EV is not plugged in or because the V2G service is not possible, EVB SOC is not affected when the driver is at work. Fig. 3 also highlights the low impact of the service on the SOC. However, this situation has an important impact on the profit, which is about 1,43€/day (522€/year). In fact, the driver cannot offer the service at work, thus the plugged in time is low inducing no capacity payment and thus the net profit drop.

VI. CONCLUSION

The proposed algorithm is an interesting tool allowing simulating the frequency regulation service offered by Electric Vehicle Battery. In fact, it allows the dynamic calculation of the service availability as well as the net profit taking into account the service cost, the service remuneration, the grid needs and the mobility constraints for each request during the day. The simulation approach takes into account the mobility patterns obtained thanks to the simulation algorithm EVeSSi. Otherwise, the real EV SOC can be obtained using adapted communications means with the Battery Management System when possible. Besides, the algorithm allows varying the market remuneration conditions during the day; therefore, it is adaptable to various energy markets conditions. The results highlight that the service profitability is interesting even with high needs of mobility. In fact, in a regulation market where the capacity price exists, one of the most important parameter is the availability of the EV. In contrary, if it is low or does not exist, the electricity price becomes more important in the net revenue. One of the main parameters that may affect the frequency regulation net revenue is the unavailability of the adapted EV Supply Equipment. The regulation markets are very different in the world and the smart grid context changes them. The proposed simulation tool is helpful to predict the dynamic net profits evolutions according to the varying prices and the EV owners' behaviours.

Finally, the algorithm outputs can be used to make the EV or fleet owner aware of the gains through adequate interfaces in order to support the incentive nature of such participation. They can also be used for the communication with the grid in order to decide about the service availability depending on the SOC level and/or the profitability. Forthcoming studies aim to include smart charging schedules in the simulation to apprehend their impact on the frequency regulation

profitability. Besides, in the real time context, it will be interesting to investigate the algorithm functioning including all the estimations and optimizations that could be interesting to add in order to achieve various V2G services.

ACKNOWLEDGMENT

This work was supported by SEAS Project (nr 12004), EUREKA - ITEA2.

REFERENCES

- [1] W. Kempton and J. Tomić, "Vehicle-to-Grid Power Implementation: From Stabilizing the Grid to supporting Large-Scale Renewable Energy", *Journal of Power Sources*, vol. 144, issue 1, 2005, pp. 280-294. Elsevier
- [2] S. L. Andersson, et al., *Plug-in Hybrid Electric Vehicles as Regulating Power Providers: Case Studies of Sweden and Germany*, *Energy Policy*, vol. 38, issue 6, 2010, pp. 2751-2762. Elsevier
- [3] J. Tomić and W. Kempton, "Using Fleets of Electric-Drive Vehicles for Grid Support", *Journal of Power Sources*, vol. 168, issue 2, 2007, pp. 459-468. Elsevier
- [4] M. Petit and Y. Perez, "Vehicle-to-Grid in France: What Revenues for Participation in Frequency Control?", *10th International Conference on the European Energy Market*, 2013, pp. 1-7. IEEE, Stockholm
- [5] W. Kempton, et al., *A Test of Vehicle-to-Grid (V2G) for Energy Storage and Frequency Regulation in the PJM System*, Results from an Industry-University Research Partnership, vol. 32, 2008
- [6] W. Kempton and T. Kubo, *Electric-Drive Vehicles for Peak Power in Japan*, *Energy Policy*, vol. 28, issue 1, 2000, pp. 9-18. Elsevier
- [7] A. Hoke, et al., "Electric Vehicle Charge Optimization Including Effects of Lithium-Ion Battery Degradation", *IEEE Vehicle Power and Propulsion Conference*, 2011, pp. 1-8. IEEE, Chicago IL
- [8] S. Han, S. Han, and K. Sezaki, "Economic Assessment on V2G Frequency Regulation Regarding the Battery Degradation", *Innovative Smart Grid Technologies IEEE PES*, 2012, pp. 1-6. IEEE, Washington DC
- [9] S. Han and S. Han, "Economics of V2G Frequency Regulation in Consideration of the Battery Wear", *3rd IEEE PES International Conference*, pp. 1-8, IEEE, Berlin (2012)
- [10] A. Manjunath, "Reliability assessment of frequency regulation service provided by V2G", *North American Power Symposium*, 2015, pp. 1-5. IEEE, Charlotte NC
- [11] H. Bevrani, *Robust Power System Frequency Control*, Second edition, Springer, USA, 2014
- [12] KEMA, *Research Evaluation of Wind Generation, Solar Generation, and Storage Impact on the California Grid*, Prepared for the California Energy Commission, 2010. Available from: <http://www.energy.ca.gov/2010publications/CEC-500-2010-010/CEC-500-2010-010.PDF/> 2016.05.30
- [13] Dynapower EMS, *5 Things to Know about the ISO-NE Frequency Regulation Market*, Dynapower corporation, 2015. Available from: <http://www.dynapowerenergy.com/dpems-blog/5-things-to-know-about-the-iso-ne-frequency-regulation-market/> 2016.05.30
- [14] Forward Market Operations, *PJM Manual 11, Energy & Ancillary Services Market Operations*, PJM, 2012. Available from: <http://www.pjm.com/~media/documents/manuals/m11-redline.ashx/> 2016.05.30
- [15] P. Codani, M. Petit, and Y. Perez, "Participation d'une Flotte de Véhicules Electriques au Réglage Primaire de Fréquence"

- [Participation of an Electric Vehicle fleet to primary frequency control], Symposium de Génie Électrique, Hal, Cachan, 2014
- [16] Coe Rexecode, Labor cost indicators in Europe, 2015. Available from: www.coe-rexecode.fr/public/Indicateurs-et-Graphiques/Indicateurs-du-cout-de-l-heure-de-travail-en-Europe/ 2016.05.30
- [17] SEAS Shared Intelligence. Available from: <http://www.sip.gecad.isep.ipp.pt/> 2016.05.30
- [18] J. Soares, et al., "Electric Vehicle Scenario Simulator Tool for Smart Grid Operators", *Energies*, vol. 5, no. 12, 2012, pp. 1881–1899
- [19] J. Soares, et al., "Realistic traffic scenarios using a census methodology: Vila real case study", PES General Meeting, Conference & Exposition, 2014 IEEE, 2014, pp. 1–5
- [20] Intelligent Data Mining and Analysis, Electric Vehicles. Available from: <http://sites.ieee.org/psace-idma/data-sets/> 2016.05.30
- [21] RTE. Available from: <http://clients.rte-france.com/> 2016.05.30
- [22] EPEX SPOT. Available from: <https://www.epexspot.com/fr/> 2016.05.30

Outsourcing Electric Vehicle Smart Charging on the Web of Data

Maxime Lefrançois*, Guillaume Habault[†], Caroline Ramondou[‡], and Eric Françon[‡]

*École Nationale Supérieure des Mines,
FAYOL-ENSMSE, Laboratoire Hubert Curien,
F-42023 Saint-Étienne, France
Email: maxime.lefrancois@emse.fr

[†]IMT/TELECOM Bretagne,
IRISA, Rennes, France,
Email: guillaume.habault@telecom-bretagne.eu

[‡]Compagnie Nationale du Rhône,
69004 Lyon, France,
Email: {c.ramondou, e.francon}@cnr.tm.fr

Abstract—This paper describes the results of a joint work between partners in ITEA2 12004 Smart Energy Aware Systems (SEAS) project, which aims at developing an ecosystem of distributed services that target energy efficiency. This paper particularly focuses on Electric Vehicle (EV) need for smart charging, which is made possible with Internet-of-Things (IoT) capabilities and smart grid deployment. A use case is proposed by Compagnie Nationale du Rhône (CNR) to tackle the emerging need for electric mobility. In this CNR scenario, a new player, named Smart Charging Provider (SCP), exposes a charge plan optimization algorithm on the Web. This service can be used by any Charging Station Operator (CSO) over the world in order to optimize their charge plans. These optimizations are computed with respect to economical or environmental criteria, while ensuring the satisfaction of constraints expressed by EV Drivers and CSOs. Apart from describing the actual implementation and deployment of this service as a RESTful Web service, this paper also overviews three of the main contributions of SEAS project that were used together to achieve this goal: (1) SEAS Reference Architecture Model, designed to enable real-time interconnection of any energy actors; (2) SEAS ontology, used throughout SEAS ecosystem to quantify systems and their interconnections; (3) SPARQL-Generate language and protocol, implemented to ensure semantic and syntactic interoperability at low cost in SEAS ecosystem.

Keywords—Smart Charging; Electric Vehicle; Distributed Architecture; Web of Data; Ontologies

I. INTRODUCTION

Lately, the number of Electric Vehicle (EV) has been constantly increasing and it is expected to grow even more in the coming years. However, [1] estimated that EV charging may have a significant impact on electricity peak demand, at the level of giga watts, and at specific time and location. Indeed, EVs are charged at a constant amount of power as soon as they are plugged in. Hence according to [1], 90% of the charging is going to take place in the late mornings when drivers arrive at their office, or in the evenings when drivers come back home. This constant charging will therefore occur during already existing electricity demand peaks, leading to important fluctuations in energy consumption. Such situation will cause tremendous undesired effects for the distribution grid – power peaks, voltage drops, expensive generation and grid reinforcements, finally ending up with increased electricity costs.

However, in most cases, these EVs stay parked for sev-

eral hours. Therefore, it would be possible to coordinate the charging during such period. This concept is known as smart charging. [2] defines smart charging as follows:

Smart charging of an EV is when the charging cycle can be altered by external events, allowing for adaptive charging habits, providing the EV with the ability to integrate into the whole power system in a grid and user-friendly way.

Smart charging targets the following benefits for:

- Customers: it might reduce their electricity costs;
- DSOs (i.e., Distribution System Operators): it could assist grid management with control signals;
- The society: it could avoid grid and generation investments;
- The environment: it may facilitate integration of renewable energies (e.g. self-consumption of electricity with solar power and electric vehicles);
- Service providers and retailers: it would give them opportunity to provide customers with innovative products and services.

In a broader perspective, these benefits are also targeted by ITEA2 SEAS project, which aims at designing a global ecosystem to help manage and optimize energy consumption, production and storage. This will be made possible by providing innovative services designed for various energy stakeholders and energy-aware systems. Apart from smart charging services, SEAS ecosystem includes a large spectrum of services, as depicted in Figure 1, which all contribute to better manage energy availability and needs.

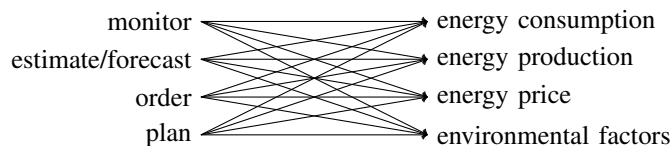


Figure 1. General services envisioned in SEAS ecosystem

The rest of this paper is structured as follows. Section II describes a Compagnie National du Rhône (CNR) Use Case (UC) that involves the concept of smart charging. The paper then focuses in Section III on CNR algorithm used to provide

a smart charging service. Then, an overview of three of the main contributions of SEAS project follows: a SEAS ecosystem architecture (Section IV); an energy domain based ontology (Section V); and SPARQL-Generate protocol that drastically lowers the costs for SEAS partners to become semantically interoperable (Section VI). These contributions were used together to design an implementation of CNR smart charging service, whose deployment within SEAS ecosystem is described in Section VII. Finally, Section VIII concludes and presents how this work can be generalized in SEAS project.

II. CNR SMART CHARGING SCENARIO

This section describes the first contribution of this paper: the definition of an innovative UC for smart charging. It overviews the architectural, representational and interoperability needs arising from this UC, which are then answered in the following sections of this paper.

A. Roles Description

A charging station is an equipment comprised of one or several *Electric Vehicle Service Equipment* (EVSE). Each EVSE has a meter (m) to monitor any charging process and is connected to an electric junction via a metering place. This CNR UC targets private charging stations, which may be owned and used by : 1) households, to charge ones vehicle at home; 2) companies, to charge cars from corporate fleet at a workplace. Figure 2 illustrates this CNR Smart Charging UC.

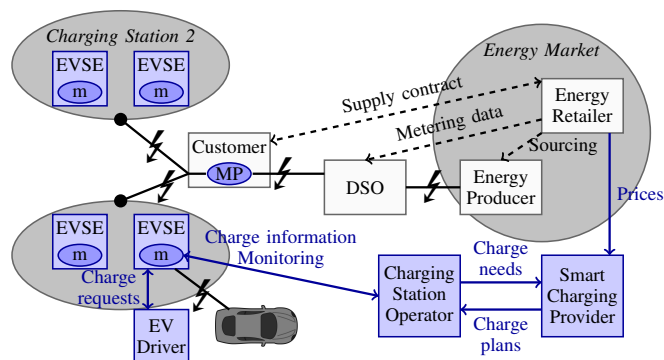


Figure 2. Illustration of CNR Smart Charging UC

Let us overview the main players of this scenario. The charging station is owned by a *Customer*, who pays electricity supply for the area to its *Energy Retailer* based on a *Metering Point* (MP) usually operated by a *DSO*. The charging station is used by *EV Drivers* – either a resident of an household or an employee of a given company – who plug their vehicles to an available EVSE. A charging station is controlled by a *Charging Station Operator* (CSO), which is responsible for monitoring and applying charge plans (which include switching on and off EVSE, but also charging with a limited power). The CSO entrusts a new actor, the *Smart Charging Provider* (SCP), with the establishment of an optimal charge plan for each EV based on information provided. The SCP may request additional information – e.g. Electricity Tariff – from other actors – e.g. an *Energy Retailer* – in order to define such charge plans.

B. Interactions of the smart charging process

In Figure 2, the power distribution is represented by a black line with a lightning bolt. Communications specific to this UC are represented by blue arrows, whereas other communications are represented by dashed arrows.

An EV Driver is authorized to use a charging station connected to the grid, and managed by a given CSO. When this EV Driver plugs its EV to an available EVSE, it first has to communicate with the CSO. The communication is made available either directly – via its smartphone or a web application – or through the charging station, in order for the EV Driver to specify the charging requirements : energy needs (related to battery situation) and preferences (in a given maximum charging time). This can boil down to the estimated departure time, but it may also include other information such as the price he is willing to pay, or whether he wants to consume only local green energy production.

The CSO takes these pieces of information into account along with several other parameters such as power constraints (limitation of maximum instantaneous power at the delivery point, energy requested by other EV Drivers connected to the same area) and asks the SCP for an optimized charge plan.

SCP combines the received information with other data such as prices information (e.g. dynamic hourly price of energy) and control signals (e.g. maximum power demand). It then runs optimization algorithms to settle the EV charge plan, which is a series of consecutive blocks of maximal power value (Pmax) for defined time periods.

The CSO, receiving the resulting charge plan from SCP, applies this plan and monitors the charging station in accordance. The EV controls the actual power delivered by the charging station to the battery, which should be lower than the Pmax defined by the charge plan – according to the mode 3 charging process (international standard IEC 61851 and IEC 62196).

At any time, an EV Driver can change its charging needs. For instance, he might request an immediate battery charging, if he actually need its battery fully charged in a short amount of time. Therefore, the charge plan may be re-optimized by the SCP on CSO requests and at any time during the charging process – especially if new EV charging events occurs (plug/unplug), or if an EV Driver modify its requirements but also and above all, if a modification of available power is notified.

Concretely, some incentives can be used to make EV Drivers accept the smart charging service: they can be economical (the charging will be cheaper), or environmental (the charging will save CO₂ emissions).

C. Decoupling Roles in the UC

Actually, CNR *virtually* already implements this UC for its charging stations. We use the term *virtually*, because CNR currently plays all the roles within this UC. Indeed, CNR is:

- The customer: CNR owns several charging stations located at its head office in Lyon (France) and at different energy production sites along the Rhône river. These charging stations are used by employees to charge CNR's EV fleet.

- The energy supplier: charging stations consume electricity supplied by CNR. Even if the electricity is delivered by the grid, CNR is the electricity supplier for each metering point, and has to balance supply with its renewable production.
- The CSO: charging stations are controlled remotely from the CNR’s head office.
- The SCP: CNR uses its own Energy Management System that embeds optimization algorithms in order to provide optimized charge plans.

In order for any customer to use this smart charging service, it has been necessary to decouple each role. It has been a complex task and the methodology used was to progressively externalize roles from the original implementation by answering questions such as:

- How would it work if the EV user was not an employee of the CNR ?
- How would it work if the charging station was located in Turkey ?

As a consequence, any actor should be able to play any of the aforementioned roles. Yet, this modularity is not direct. Nevertheless, all of the information needed to run CNR’s charge plan optimization algorithm is produced, modeled, exchanged, and processed internally in CNR Information System. Hence, any change of actor who plays a given role in the UC would require important integration efforts, which means important conception and development costs.

Sections IV to VI hence overview work that target seamless interoperability between actors, at the lowest possible cost. First, let us describe the charge plan optimization algorithm.

III. THE CHARGE PLAN OPTIMIZATION ALGORITHM

It is incontestable that smartgrid and energy management would benefit from smart charging. [1] conducted a survey on the effects of e-mobility in autumn 2014, which also lists all its potential and benefits. In addition, the literature includes many studies related to the problem of coordinated EV charging and discharging in a smart grid, to cite but a few, [3]–[8]. The various optimization approaches presented in these papers are based on either single or multi-objective optimization, according to solely current information, or including forecast-based solutions.

CNR is an hydroelectricity producer which has developed an electricity mixed renewable production (wind power, solar power, small hydro-power). CNR has therefore become an expert in managing an intermittent energy, by forecasting, optimizing, marketing and supervising production. CNR uses its own algorithm in order to optimize EV consumption according to several strategies. The smart charging strategy tested in CNR UC is based on forecast and day-ahead electricity prices, the available power at the metering point, the real-time connection of the vehicles at the charging station and the EV Driver requirements.

The goal of this optimization approach is to minimize the charging cost without negotiating the charging needs, as the customer satisfaction and the reliability of the charging service have higher priority than the system operating cost. It then integrates static and dynamic information related to:

- EV Drivers: their charging needs (maximum delay for charging completion);
- EV: minimal and maximal charging power, and battery State of Charge (SoC);
- Charging station: minimal and maximal charging power;
- Consumption place: network access tariff and load curve;
- Electricity contract with the Energy Retailer based on time-varying prices (e.g. spot prices);
- Forecast and day-ahead electricity prices.

Note that the aim in this paper is not to review the existing optimization algorithms, neither is to compare the CNR algorithm to the existing algorithms. Instead, we are interested in describing a methodology to make such an algorithm available, a) in a real deployment, b) at low cost, and c) to any actual CSO (via the Web). The result is the deployment of CNR SCP that runs a charge plan optimization algorithm. Any node on the Internet requiring a charge plan can contact this SCP for any types of EVs and EVSEs.

IV. ARCHITECTURE

One important task for SEAS project was to define an architecture to enable real-time interconnection of any energy actors. This interconnection will then help actors offer energy dedicated services to SEAS entities. Therefore, this architecture should meet some general requirements such as: a) being scalable, adaptable and dynamic; b) offering plug-and-play solutions (having as less manual configuration as possible); and c) providing secure communications and privacy of information.

Different UCs have been defined to demonstrate SEAS benefits on different domains (EV, House, Building, Microgrid, etc.). All these UCs have then been used to define functions and communication requirements that such an architecture should address. Several architectures exist such as [9] but none of them address all SEAS project requirements. That is the reason why SEAS partners define their own architecture, named *SEAS-Reference Architecture Model (S-RAM)*.

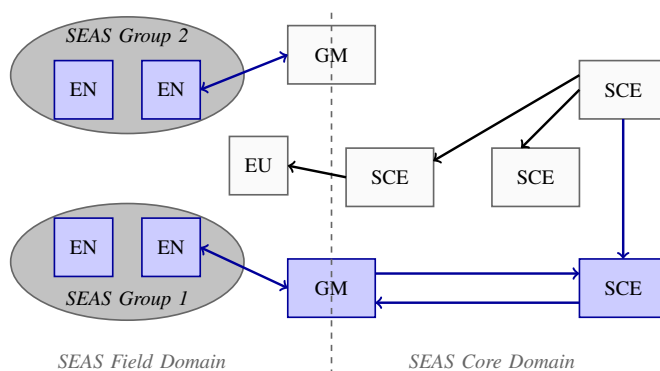


Figure 3. Illustration of SEAS Reference Architecture Model

Figure 3 is an illustration of S-RAM for CNR Smart Charging UC as presented in Section II. As depicted in Figure 3, S-RAM is divided in two domains, Field Domain (SFD) and Core Domain (SCD). Entities within SFD monitor and/or help control local load and generation. For instance, in CNR scenario, both EVSE’s meter – called End Node (EN) in S-RAM — and Customer — called End User (EU) — help CSO

monitor and control any charging process. In addition, SFD could be divided in SEAS Groups (SGs) in order to facilitate energy management and optimization. Each group is therefore managed or operated by a Group Manager (GM). This manager – the CSO in CNR UC – is aggregating data coming from all entities willing to participate in the group energy management. GMs might analyze data collected in the field in order to make a decision to better manage the energy of their SGs. GMs being at the edge between SCD and SFD, their decisions can also be taken considering information (informative or control) coming from outside the group. Indeed, SEAS Core Entities (SCE) within SCD might both send energy demands to SGs and/or provide information or services to help SGs in their energy management — for instance, SCP in CNR smart charging scenario. With this architecture, any node in SFD or any SG, via its GM, can participate in a Demand- Response (DR) system and so, help have better global energy consumption plan.

As any communication architecture, S-RAM requires to be secured so that information is not shared with untrustworthy entities. S-RAM relies on its security service that helps authenticate all entities participating in this architecture. Moreover, Internet Protocol (IP) is widely present in current objects deployed for energy related topics. And as it is assumed that it will be even more present in the future, SCD relies on IP and secured web protocols such as HTTPS. S-RAM SCD can therefore be seen as an overlay of IP/HTTPS.

The SEAS project being an European project, it has several partners and is not dedicated to only one domain of energy management. Instead, it focuses on any energy management domain. Data representation is therefore crucial. In fact, it is important that all these potential actors can understand each other and use common services without having to configure each possible case manually. Furthermore, the structure of energy networks is changing, and the current structure may not be the reference in coming years. This has to be taken into consideration in smart grid development, and, as mentioned previously, the SEAS project wants its architecture to be dynamic and adaptable, and so, auto-configurable. Therefore, S-RAM requires to rely on data standard providing a) links and relationships; b) abstraction in demands; and c) a common language. That is the reason why the Resource Description Framework (RDF) [10] formalism has been chosen as an abstract data model in S-RAM.

Within S-RAM, a charging station is a SG operated by a CSO. As mentioned previously, CNR smart charging service relies upon an algorithm that defines the charge plan based on information provided by the CSO and the Energy Retailer. CNR SCP is an SCE providing a smart charging service. S-RAM choices – especially with the usage of a common language based on ontologies – help any SEAS Entities discover, understand and have access to this service.

V. ONTOLOGIES

This section overviews one of the ontologies that has been developed in SEAS project, namely the SEAS ontology [11]. This ontology is used throughout SEAS ecosystem to ensure inter-operability. But first, let us recall some basics about Knowledge Representation and Semantic Web.

A. Overview of the Semantic Web Stack

In the domain of Smart Grids, a huge amount of knowledge is available and produced in heterogeneous and distributed manner. Knowledge Engineering and Semantic Web actually aim at answering generic needs that arise from the production of such knowledge. One wants to represent, manipulate, exchange, query, reason with, update, and validate the knowledge.

The World Wide Web Consortium (W3C) standardized a full stack of standards for Semantic Web on top of Unicode and Universal Resource Identifiers (URIs) standards. The first step towards inter-operationalization of data is to unambiguously name things with an URI. The second step uses RDF in order to describe anything in terms of a set of triples (*subject, predicate, object*). RDF is therefore an abstract data model (a directed acyclic graph), and has multiple concrete syntaxes such as RDF/XML [12], Turtle [13] or JSON-LD [14]. For instance, the Turtle snippet from Figure 4 serializes an RDF Graph with exactly five triples. This example describes the geolocation of a charging station.

```
@prefix rdfs: <http://www.w3.org/2000/01/rdf-schema#> .
@prefix geo: <http://www.w3.org/2003/01/geo/wgs84_pos#> .
@prefix seas: <http://purl.org/NET/seas#> .
@base <http://data.mycsocompany.org/rest/> .

<cs/10001> a seas:ChargingStation ;
  rdfs:comment "CSO Charging Station with id 10001."@en ;
  geo:location [ geo:lat 45.763084 ; geo:long 5.692196 ] ;
```

Figure 4. Turtle example describing the geolocation of a charging station.

There are multiple RDF *vocabularies* on the Web that can be used, each defining its own set of URIs. For instance, `geo:location` is a prefixed URI, whose expanded form is `http://www.w3.org/2003/01/geo/wgs84_pos#location`. URIs `geo:location`, `geo:lat`, `geo:long` are defined within the W3C Basic Geo (WGS84 lat/long) Vocabulary. Then, `<cs/10001>` is a relative URI, that needs to be resolved against some base URIs, which in this case is `http://data.mycsocompany.org/rest/`. These URIs are not chosen randomly. Indeed, except for the dummy CSO company website and the SAREF ontology, all URIs mentioned in this paper actually leads to some document. Moreover, The Linked Data principle defines four simple principles to publish RDF knowledge on the Web [15]: (1) Use URIs as names for things; (2) Use HTTP URIs so that people can look up those names; (3) When someone looks up for an URI, provide useful information, using the standards (RDF, SPARQL); and (4) Include links to other URIs, so that they can discover more things.

For reasoning with RDF, one must choose some formal semantics, and build inference engines (or reasoners) to understand such axioms and infer new knowledge (or reason) with RDF graphs. Among other, [16] define semantics for RDF and RDFS. [17] grounds the Web Ontology Language (OWL) constructors (e.g., `allValuesFrom`) and axioms (e.g., `subClassOf`) on the First Order Logics (FOL). In this way, RDF enables to represent knowledge about things that are identified by URIs, and ontologies enable to capture the semantics of this knowledge and to reason. For example, using OWL 2 direct semantics, the RDF Graph and the logical formula below are equivalent.

```
saref:Currency owl:oneOf ( om:euro om:United_States_dollar
om:pound_sterling );
(∀x)[Currency(x) ⇒ (x = EUR) ∨ (x = USD) ∨ (x = GBP)]
```

This example illustrates a clear design issue in the current SAREF ontology. It also illustrates that extra care has to be taken when reusing existing ontologies.

B. The SEAS Ontology

Another important task in SEAS project was therefore to design ontologies to represent and reason with knowledge related to energy domain. We followed a three-step knowledge engineering methodology [18]: (1) agree on a conceptualization of the domain; (2) develop the ontology for the domain, formally grounded on an appropriate knowledge representation formalism; (3) operationalize it for the domain.

The first step has been achieved by organizing interviews between knowledge engineering researchers and energy domain experts during a dedicated workshop [19]. It helped us unveil the importance of representing knowledge such as time series, aggregated values, and quantity integration and derivations for the energy domain. Yet, there exists no ontology on the Web to represent this knowledge. Furthermore, the FOL formalism behind OWL is not appropriate to reason with time series and sums.

The result of the second step is an extension of the joint W3C-OGC Semantic Sensor Network (SSN) ontology [20]. This extension enables to describe processes such as sensing, actuating, forecasting, planning. All of these processes take as input and output estimations of qualities of a) concepts *systems*; b) *connections* between these systems; and c) *connection points* of a system where connections may occur. Inputs and outputs are described using the W3C Data Cube ontology [21].

Figure 5 illustrates the core of the SEAS ontology:

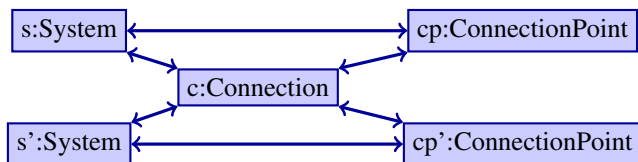


Figure 5. The core of the SEAS Ontology

The SEAS ontology also contains a module that defines classical qualities for systems, connections and connection points in the energy domain, as illustrated in Figure 6.

EnergySystem ConsumptionPower ProductionPower StoragePower TotalIncomingPower TotalOutgoingPower ...	EnergyConnectionPoint IncomingPower IncomingEnergy ...	EnergyConnection TransferringPower TransferredEnergy ...
---	--	--

Figure 6. Extract of qualities defined for SEAS feature of interest.

This module is automatically generated from a JSON configuration file retrieved from SEAS GitHub repository [22]. And every expert in the SEAS project can contribute to this

file. The SEAS ontology can also be reused for any other domain (e.g., water or waste management), provided that a new JSON configuration file is written for that domain. Among other, the SEAS ontology enables to describe time series, aggregations of quantities, derivations and integration of quantities.

As a result, this ontology is used to model the input and output of CNR SCP service: EVs and EVSEs are connected energy systems, whereas the need and the plans are commands or observations of the energy connections between these systems. It especially describes the TransferringPower measure with respect to the Time dimension.

VI. SEMANTIC AND SYNTACTIC INTEROPERABILITY

As previously mentioned, RDF is an abstract data model. Much like in communication models, the transmitter node must encode the RDF graph in a serialized form that next is sent to the receiver node, which must decode the message. The everlasting issue is then to ensure that the receiver “understands” the message exactly as the transmitter expected. This is almost impossible with human communication, but we want machines to do so.

With RDF, one trivial solution to this issue is to choose one of the concrete RDF syntaxes, and to impose every node to be able to encode and decode messages with respect to this syntax. Yet, this method is not practical for two reasons. First, SEAS partners want to keep on using their legacy system. Indeed, they are used to exchanging messages with their legacy partners in CSV, XML or JSON, and it would be too expensive for them to completely switch to RDF. Second, using RDF will increase message payload and resource required to process them. In fact, it would be irrelevant for simple messages sent by resource constrained SEAS nodes (e.g., simple time series of consumption values) to be sent in RDF syntaxes.

As a consequence, one crucial piece of work in the SEAS project was to drastically lower the cost in order to adapt existing systems to RDF. The result of this work is to use a new RDF-based solution, namely SPARQL-Generate [23], which is both a language and a protocol.

The language part of SPARQL-Generate is an extension of SPARQL 1.1, which enables to declaratively describe how messages (in XML, CSV, JSON, or any other format) may be interpreted in RDF. This language is more expressive than SPARQL 1.1 itself, and is already implemented on top of Apache Jena [24].

The protocol part of SPARQL-Generate enables the two following scenarios:

- an HTTP client sends its request in a legacy format to a server *along with a SPARQL-Generate query*, thus the server may interpret the message properly in RDF using SPARQL-Generate.
- an HTTP server answers in a legacy format to its client *along with a SPARQL-Generate query*, thus the client may interpret the message properly in RDF using SPARQL-Generate.

CNR SCP implementation makes use of such SPARQL-Generate protocol: it sends a SPARQL-Generate query along

with CNR legacy XML format information. As a result, it allows any client to properly interpret any response in RDF using SPARQL-Generate.

VII. IMPLEMENTATION OF CNR SCP ENTITY WITHIN SEAS PROJECT

The smart charging service offered by CNR SCP is implemented and deployed as a RESTful Web Service. This service defines two interactions with other SEAS Entities:

- 1) Requests for the execution of SCP algorithm. The requesting node sends an XML document with static information about the charging station, the EVSEs, and charging needs as formulated by EV Drivers. CNR SCP sends back an acknowledgment, that provides the location where the algorithm result will be retrievable.
- 2) Requests for an SCP algorithm execution result at a given location. If available, CNR SCP sends back an XML document containing the optimized charge plan, along with a link to a SPARQL-Generate query that can be used to interpret this XML document as RDF, according to SEAS ontologies.

This service is available for testing, and documented on the Web [25]. Moreover, the code is openly available on GitHub and other partners in SEAS project already started using it to implement their own service [26].

VIII. CONCLUSIONS AND PERSPECTIVES

This paper reported a joint work between partners in ITEA2 12004 SEAS project, which aims at developing an ecosystem to help entities better manage, coordinate and optimize energy consumption, production and storage. This ecosystem enables to deploy distributed services that target energy efficiency. This paper particularly focuses on CNR EV Smart Charging UC, which tackles the emerging need for electric mobility.

In this CNR scenario, an SCP offers to any entities in SEAS ecosystem the possibility to obtain EV charge plans. These plans are computed based on different collected information (economical or environmental). It has been made possible thanks to SEAS project contributions a) S-RAM, designed to enable real-time interconnection of any energy actors; b) the SEAS ontology, used to quantify systems and their interconnections; and c) the SPARQL-Generate language and protocol, designed to ensure semantic and syntactic interoperability at low cost.

Finally, we described the actual implementation and deployment of CNR SCP as a RESTful Web service. Its code is openly available on SEAS project GitHub. As a consequence, this UC can now be instantiated anywhere, and any SEAS entity can entrust CNR with the role of the SCP.

Further work includes the interconnection of this service with other energy optimization services, or data generation services. Furthermore, CNR SCP service – as any other RESTful HTTP Web service – can be made secure using HTTPS, but it also can be monetized.

ACKNOWLEDGEMENT

This work has been partially funded by the ITEA2 12004 SEAS project - <http://the-smart-energy.com>.

REFERENCES

- [1] “Smart Charging: steering the charge, driving the change,” Eurelectric, Eurelectric paper D/2015/12.105/7, March 2015, last accessed 2016-05-20. [Online]. Available: http://www.eurelectric.org/media/169888/20032015_paper_on_smart_charging_of_electric_vehicles_finalpsf-2015-2301-0001-01-e.pdf
- [2] E-Mobility Coordination Group (M/468) and CEN-CENELEC-ETSI Smart Grid Coordination Group (M/490), “Smart Charging of Electric Vehicles in relation to smart grid,” CEN-CENELEC, WG Smart Charging Report, May 2015, last accessed 2016-05-20. [Online]. Available: <ftp://ftp.cen.eu/EN/EuropeanStandardization/HotTopics/ElectricVehicles/SmartChargingReport.pdf>
- [3] S. Deilami, A. S. Masoum, P. S. Moses, and M. A. Masoum, “Real-time coordination of plug-in electric vehicle charging in smart grids to minimize power losses and improve voltage profile,” *Smart Grid, IEEE Transactions on*, vol. 2, no. 3, 2011, pp. 456–467.
- [4] O. Sundström and C. Binding, “Flexible charging optimization for electric vehicles considering distribution grid constraints,” *Smart Grid, IEEE Transactions on*, vol. 3, no. 1, 2012, pp. 26–37.
- [5] Y. Cao, S. Tang, C. Li, P. Zhang, Y. Tan, Z. Zhang, and J. Li, “An optimized ev charging model considering tou price and soc curve,” *Smart Grid, IEEE Transactions on*, vol. 3, no. 1, 2012, pp. 388–393.
- [6] M. A. Ortega-Vazquez, F. Bouffard, and V. Silva, “Electric vehicle aggregator/system operator coordination for charging scheduling and services procurement,” *Power Systems, IEEE Transactions on*, vol. 28, no. 2, 2013, pp. 1806–1815.
- [7] E. L. Karfopoulos and N. D. Hatziargyriou, “A multi-agent system for controlled charging of a large population of electric vehicles,” *Power Systems, IEEE Transactions on*, vol. 28, no. 2, 2013, pp. 1196–1204.
- [8] A. Zakariazadeh, S. Jadid, and P. Siano, “Multi-objective scheduling of electric vehicles in smart distribution system,” *Energy Conversion and Management*, vol. 79, 2014, pp. 43–53.
- [9] The Telecommunication Technology Committee, “oneM2M Technical Specification Functional Architecture,” oneM2M Working Group, Technical Specification, February 2016, last accessed 2016-05-20. [Online]. Available: http://www.ttc.or.jp/jp/document_list/pdf/j/TS/TS-M2M-0001v1.13.1.pdf
- [10] R. Cyganiak, D. Wood, and M. Lanthaler, “RDF 1.1 Concepts and Abstract Syntax, W3C Recommendation 25 February 2014,” W3C, W3C Recommendation, Feb. 25 2014. [Online]. Available: <http://www.w3.org/TR/2014/REC-rdf11-concepts-20140225/>
- [11] M. Lefrançois, “The SEAS ontology,” Apr. 2016, last accessed 2016-07-17. [Online]. Available: <https://w3id.org/seas/>
- [12] D. Beckett, “RDF/XML Syntax Specification (Revised) W3C Recommendation 10 February 2004,” W3C, W3C Recommendation, Feb. 10 2004. [Online]. Available: <http://www.w3.org/TR/2004/REC-rdf-syntax-grammar-20040210/>
- [13] E. Prud’hommeaux and G. Carothers, “RDF 1.1 Turtle - Terse RDF Triple Language, W3C Recommendation 25 February 2014,” W3C, W3C Recommendation, Feb. 25 2014. [Online]. Available: <http://www.w3.org/TR/2014/REC-turtle-20140225/>
- [14] M. Sporny, G. Kellogg, and M. Lanthaler, “JSON-LD 1.0 - A JSON-based Serialization for Linked Data, W3C Recommendation 16 January 2014,” World Wide Web Consortium (W3C), W3C Recommendation, Feb. 25 2014. [Online]. Available: <http://www.w3.org/TR/2014/REC-json-ld-20140116/>
- [15] T. Berners-Lee, “Linked Data - Design Issues,” 2006. [Online]. Available: <http://www.w3.org/DesignIssues/LinkedData.html>
- [16] P. Hayes and P. F. Patel-Schneider, “RDF 1.1 Semantics, W3C Recommendation 25 February 2014,” W3C, W3C Recommendation, Feb. 25 2014. [Online]. Available: <http://www.w3.org/TR/2014/REC-rdf11-nt-20140225/>
- [17] B. Motik, P. F. Patel-Schneider, and B. Cuenca-Grau, “OWL 2 Web Ontology Language Direct Semantics W3C Recommendation 27 October 2009,” W3C, W3C Recommendation, Oct. 27 2009. [Online]. Available: <http://www.w3.org/TR/2009/WD-owl2-semantics-20091027/>
- [18] B. Bachimont, “Engagement sémantique et engagement ontologique: conception et réalisation d’ontologies en ingénierie des connaissances,” in *Ingénierie des connaissances, évolutions récentes et nouveaux défis*,

- J. Charlet, M. Zacklad, G. Kassel, and D. Bourigault, Eds. Eyrolles, 2000, ch. 19.
- [19] M. Lefrançois and P. Bourguignon, "SEAS Workshop - Boost the Knowledge Model and the Pilot development," Dec. 2015, last accessed 2016-07-17. [Online]. Available: <http://data.the-smart-energy.com/workshop/2015/12>
- [20] K. Taylor, K. Janowicz, D. Le Phuoc, and A. Haller, "Semantic Sensor Network Ontology," World Wide Web Consortium (W3C), W3C First Public Working Draft, May 16 2016. [Online]. Available: <http://www.w3.org/TR/2016/WD-vocab-ssn-20160531/>
- [21] R. Cyganiak and D. Reynolds, "The RDF Data Cube Vocabulary, W3C Recommendation 16 January 2014," World Wide Web Consortium (W3C), W3C Recommendation, Jan. 16 2014. [Online]. Available: <http://www.w3.org/TR/2014/REC-vocab-data-cube-20140116/>
- [22] M. Lefrançois, "The sources of the SEAS ontology website on GitHub," Mar. 2016, last accessed 2016-07-17. [Online]. Available: <https://github.com/thesmartenergy/seas>
- [23] S. Harris and A. Seaborne, "SPARQL 1.1 Query Language - W3C Recommendation 21 March 2013," W3C, W3C Recommendation, Mar. 21 2013. [Online]. Available: <https://www.w3.org/TR/sparql11-query/>
- [24] M. Lefrançois, N. Bakerally, and A. Zimmermann, "The SPARQL-Generate demonstration website," Apr. 2016, last accessed 2016-07-17. [Online]. Available: <https://w3id.org/sparql-generate>
- [25] M. Lefrançois, E. Françon, and N. Benzine, "The CNR pilot Smart Charging Provider demonstration website," Apr. 2016, last accessed 2016-07-17. [Online]. Available: <http://cnr-seas.cloudapp.net/scp/>
- [26] M. Lefrançois, "The CNR pilot Smart Charging Provider demonstration website source code," Apr. 2016, last accessed 2016-07-17. [Online]. Available: <https://github.com/thesmartenergy/CNR-SmartChargingProvider>

Hypergraph of Massive Digital Traces as Representation of Human Activities: A Way to Reduce Energy Consumption by Identifying Sustainable Practices

Eddie Soulier
 Tech-CICO
 University of Technology of Troyes (UTT)
 Troyes, France
 email: eddie.soulier@utt.fr

Philippe Calvez
 Crigen – Digital Lab
 ENGIE
 Saint-Denis, France
 email: philippe.calvez1@engie.com

Abstract— On one hand, the ecological transition and sustainable development issues are today a reality that can not be ignored given the negative impacts of human activities on their environments. On the other hand, an increasingly important digitization of these environments results in the generation of massive volumes of digital traces, which are all signs of actors’ activities. A significant challenge is to understand the ins and outs of environmental impact due to activities and considering Energy Impact (EI) as a key indicator and how this indicator can strongly change from an activity to another. Our approach considers the Practices recognition on the basis of these digital traces generated by human and non-human entities during specific activities. Practice (instantiation of activity) uses more or less resources (physical and virtual) during their existence. Being able to identify which one is more resources dependent would help to better understand how to promote ecological transition. Promoting, or at least identifying on the basis of indicators (i.e., Energy Impact), practices that have a low impact on the environment could be an innovative approach. These practices, defined as coordination of multiple heterogeneous entities in time and space, can be formalized in the form of multidimensional activities structures – Activities’s Hypergraph – using the Assemblage Theory (“Agencement” in French) and using a set of mathematical tools (Simplicial Complexes, Hypernetworks). This research attempts to model the phenomenon of human and non-human activity based on the characterization of the context (massive contextual data). These Assemblages are represented and computed in a research platform (IMhoTEP), which aims to build these complex structures not based on a priori entities’ classification, but by focusing on the relationships they maintain in several dimensions. The main goal is to offer a decision tool, which supports actors’ ecological transition by understanding activities inducing consumption or production of resources. This academic research in the field of computer science is based on continuous digitization of physical and virtual spaces, particularly highly connected urban areas (Smart City, Internet of Everything).

Keywords— Activities; Assemblage; Digital Traces; Energy Impact; Simplicial Complex; Theory of Graph; Theory of Practice.

I. INTRODUCTION

It is observed that daily human activities have an increasingly impact – mostly negative – on the environment. They are mainly not sustainable due to excessive consumption and uncontrolled using of multiple resources (mostly non-renewable). Electrical energy (Figure 1) is a leading resource in human activities.

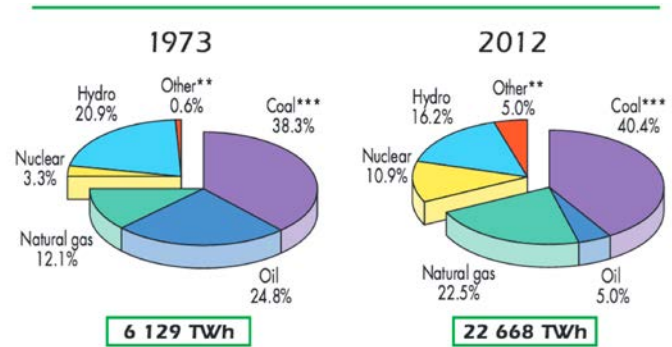


Figure 1. 1973 and 2012 fuel share of electricity generation.

Energy companies, institutional, provide several indicators to measure electric energy consumption including the “Energy Impact”. We consider that each human activity has an Energy Impact (in French Emprise Energétique or EmE). We have chosen to use this indicator (EI) as a measure of electrical energy consumption in human activities. EI is the only indicator that takes into account the indirect consumption (not visible to the final consumer) in addition to the direct consumption visible to the final consumer. EI concept is based on research work of Pourouchottamin [1] and Figure 2 describes it.

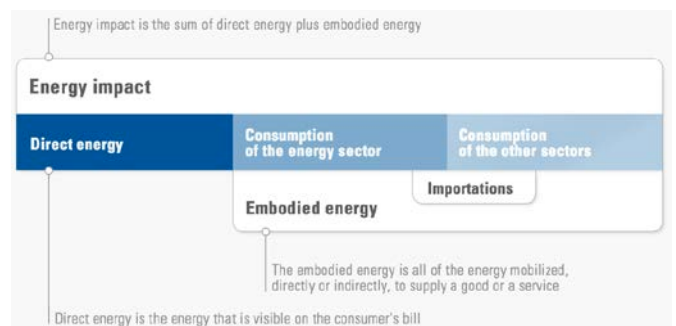


Figure 2. Energy Impact (Emprise Energétique (EmE)).

Direct energy refers to the energy visible to consumers, i.e., their fuel bills for individual vehicles, electricity, gas and other fuels for housing, etc. Direct energy corresponds to the final energy consumed by households. Embodied energy is the energy necessary for the provision of property or the service offering to the end consumer. Embodied energy is needed to manufacture and delivery of equipment at home, or produce food, energy required to the construction of the house, etc. It is also called content of energy for goods and services. This embodied energy must itself be decomposed according to its

use. Embodied energy of the non-energy sectors means that it is used by economic actors in France and in the world to imagine, test, produce, and transport goods and services ultimately consumed by households. Embodied energy of direct energy corresponds to the share of energy required to develop, produce the “final” energy from natural resources and make it available to the consumer. The process requires extraction, conversion, transportation, manufacturing plants and infrastructures, etc.

Today, the calculation of energy impact is not based on the actual activities of people. It is difficult to identify what human actors really do for daily activities. Besides the question of measuring of energy impact, the functional representation of these activities do not correspond to the image the people have of their own activities. This makes it difficult to build a supervisory activity system that would help to reduce the consumption of energy by managing activities. There is in this sense a real need to answer this lack. This classic definition of human activities based on statistical study bring two basic problems:

- The first problem is that there is no overlap between the functional separation and real activities of people.
- The second problem is that the data used, are only primarily the result of statistical surveys that provide aggregated results from data, which are not directly related to activities.

Human activity is a very complex phenomenon to be observed except:

- In the case of very trivial activity (or for which semantics is well controlled)
- When it is based on pre-defined categories or declarative items.

In all other cases, we are confronted to an activity recognition problem.

Activity Recognition in computer science is a research area in strong development [2].

In this research field, there are two main approaches:

- Activity Recognition based on Vision
- Activity Recognition based on Sensor and two types of algorithms/representation:
- Machine Learning
- Representation of knowledge.

We consider that these approaches do not allow to solve the problem as we consider it. Indeed, the computational approach of the recognition of activities do not take full account of the context of activities. For environment, lifestyles (context) significantly affect how activities are performed. That is why we have chosen to rely on specialized research work, which considers the influence of lifestyle on human activities. In particular, we study the academic work of Spaargaren [3-5], Røpke [6-8] and Shove [9-14]. Their conclusion is that changing the behavior of agents can not come from individual incentive micro level (micro) or institutional macro level (i.e., laws, ...). The basic and core assumption of our approach is that the behavior in the activity is determined by practice, in which activities are embodied (shown in Figure 3).

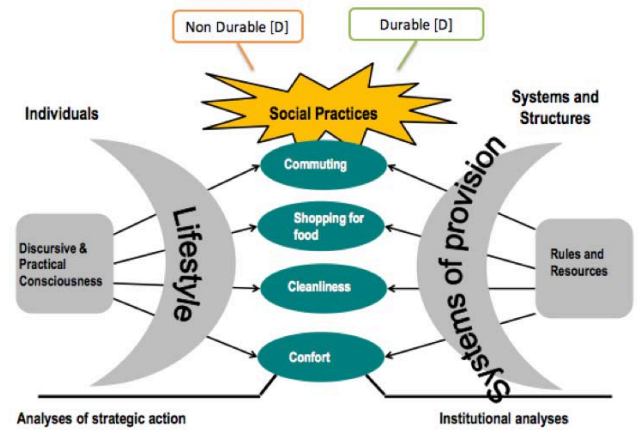


Figure 3. Influence of Lifestyle and System of provision on Social Practices [15].

Practice is one of the main theoretical artefacts of our approach and one of our key contribution is to develop a modeling framework of practices and/or building a computer system (IMhOTEP Platform) to calculate the energy impact (EmE) related to these practices based on massive digital traces (Big Data) related to human activities.

The main problematic of our research work is how to identify (automatically and within computer science), in highly digitized environments, actors’ practices in which activities are encapsulated. How to recommend low environment impact practices without using a priori or declarative lists?

II. FUNCTIONAL MODEL FOR BUILDING STRUCTURES OF HUMAN ACTIVITIES

We present our research model and our hypotheses in Figure 4.

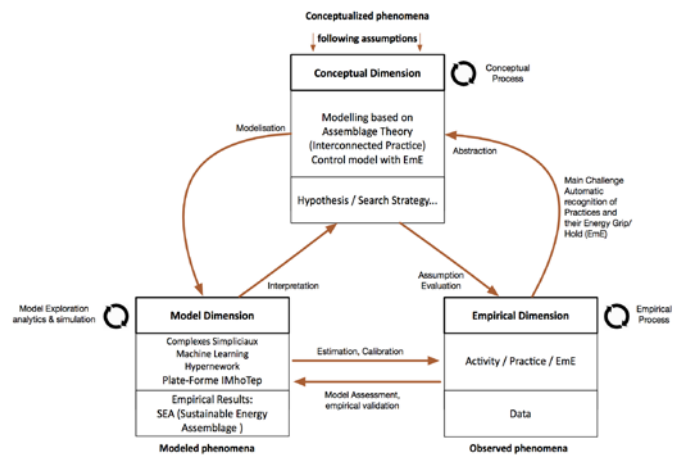


Figure 4. Global Research Model for building Sustainable Energy Assemblage (SEA).

The Empirical dimension of our model is related to the phenomenon observed, it is to say, activities and practices. Specifically, the observed phenomenon is an interconnected set of practices of various fields (housing, transportation, leisure...) and their energy impact (EmE). In this area, it seeks to observe and measure the phenomenon, by taking advantage of

aggregating heterogeneous digital traces. It is in this empirical dimension that we establish a first form of the observed facts (basic activities) presented later in this work. We consider practice as the core conceptual artefact of our approach. Practice is defined by Reckwitz [16] as “a routinized type of behavior which consists of several elements, interconnected to one other: forms of bodily activities, forms of mental activities, ‘things’ and their use, a background knowledge in the form of understanding, know-how, states of emotion and motivational knowledge. A practice – a way of cooking, of consuming, of working, ...”

Our hypothesis is that practices are interconnected. For this key assumption, we suggest the concept of Assemblage (“Agencement” in French) based on previous academic works of Soulier with Delalonde [17], and with Bugeaud [18][19].

Assemblage is a methodological tool [18] for the study of any phenomenon consisting of:

- a large number of heterogeneous entities, autonomous and active,
- multidimensional network of relationships in which they associate,
- forms of organization and ability to act that emerge from their interactions.

In our field, we define a Sustainable Energy Assemblage (Agencement Energétique Soutenable [AED] in French), which is a multidimensional structure of entities in relationship in one or more dimension. In this structure – view as a Hypergraph – we aim to identify a cluster that represents Practice (group of heterogeneous entities in interaction). These practice have, as defined previously, an energy grip/hold (EmE).

The conceptual dimension of our research Model, helps us to characterize relevant factors of the observed phenomenon of the empirical dimension. That is why we consider significant concept for our approach such as Activity, Practice, Energy Impact.

We assume that an Assemblage is a multidimensional connectivity system and that we we could calculate this system and the connectivity of heterogeneous elements of a practice in several dimensions. For this we use the mathematical tool of Simplicial Complex developed by Atkin [20, 21] and generalized by J. Johnson [22] as Hypernetworks.

The last part of our model describes the model dimension. In this area, we seek to operationalize previous cited dimension of our model, through a consistent and unambiguous formal system. In our case, this formal system is based on mathematical tools that are Simplicial Complex that help operationalize the structure as SEA in a specific information system platform called IMhOTEP (sustaInable MObility and Energy social-Practices inside Smart Cities), which we developed as a proof of concept to build and represent the dynamic structures of activities. This area of the model should confirm or not our theories from the conceptual dimension (theory of sustainable practices / Sustainable Energy Assemblage through the Energy Impact model) and confirm as well observation from the empirical dimension (Practice and Influence Energy). At this point, we transform our previous model into the model shown in Figure 5, in order to display our three core concept such Energy grip/hold (EmE), Practice and Assemblage.

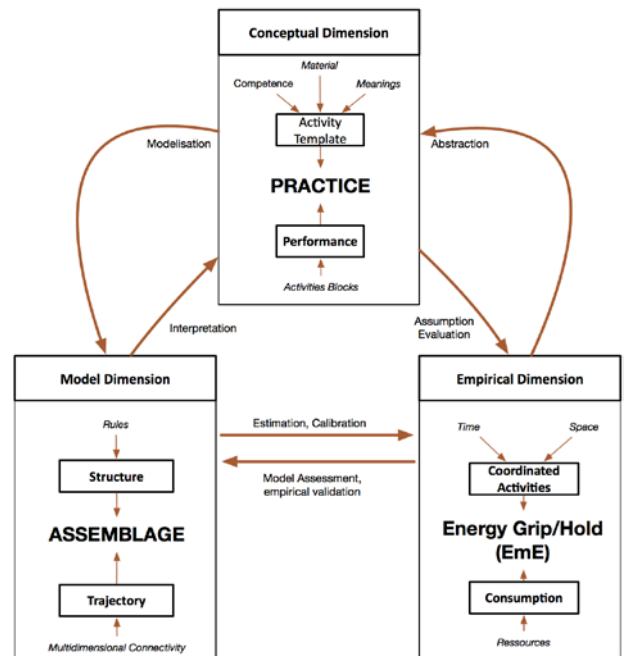


Figure 5. Research Model with Core Concept of the approach.

III. BUILDING STRUCTURES OF PRACTICES FROM DIGITAL TRACES

Calculating the Energy grip/hold (EmE) of practice from massive digital traces of activities (Big Data) generate many problems in data acquisition, data processing and modeling.

Digital traces are modeled based on ActivityStream protocol developed by Messina [23], recently upgraded in a new version of protocol by Snell [24]. We consider multiple dimensions of digital traces, as shown in Figure 6. All these dimensions aim to define more accurately characteristics of human activities.

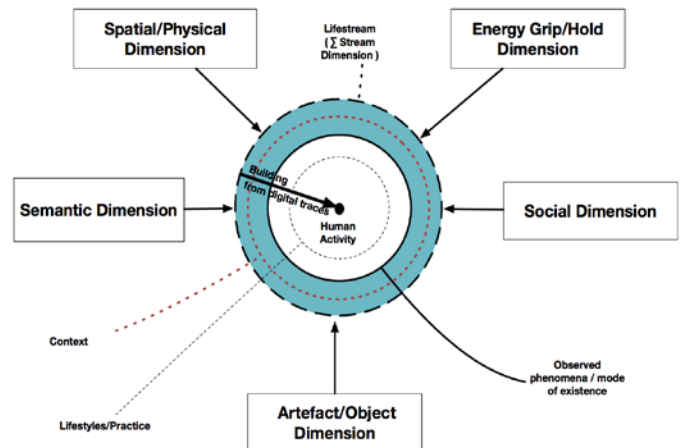


Figure 6. Digital Dimension of Human Activities.

The conceptual model takes into account the activity, location and mobility triangle, as shown in Figure 7. Activity can be localized or distributed and independent or dependent.

The key point is the allocation of a category of activities automatically by grouping activities, which are closed. To do this we apply K-Means Algorithm to define clusters of category of activities in which we could later identify Practices. Once these clusters are defined we use graph query to search for specific practice and its Energy Impact evaluation. Figure 10 show the structure of activities.

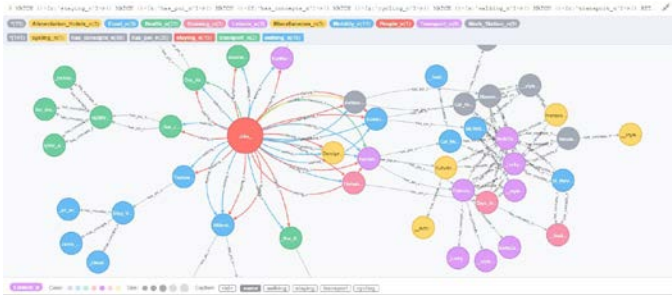


Figure 10. Structure of Activities – Practice searching based on Graph Queries.

The scale of the following experiment was limited to 3 people over one month, mostly due to limitation of Smartphones using a data/sensor for following people over time, and location and the willingness of people to share their constant spatial position during a long period of time. The mobile application energy consumption of the battery, due to work all day long and push every Lat/Lon position and other data every minute, was clearly a disadvantage at this point of the experiment. Regarding the acquisition of data from different context sources (Tweets, Google Place...), it depends on how many “activities” (defined stops over 5 minutes and considered as activity) are done by user. The average volume of data per day, per user, if we consider all digital traces needed for the IMhOTEP approach acquired for this period of time, reached 12 Mo of data/per user/per day. This could be considered as relatively low. But if we scale up to hundreds or thousands of people, the volume could lead to a computational challenge, especially when considering to manage a large graph with hundreds, thousands, even millions of nodes with multidimensional relationships.

This implementation of IMhOTEP was experimental in order to acquire data to build an Hypergraph of activities. Computational challenges were present, for instance to connect all open source tools (mobile application, Database, code to extract data, API access). This element was a heavy constraint because when you want to access to API like Twitter or Google, or others such Yelp, you only get a specific amount of query from the API. Moreover test and implementation suffer due to API’s limits.

Another limit directly linked to the Matrix Calculation (Incidence and Adjacency) was the time required to calculate the experiment. It was not a huge problem at this point, but size of matrix (for hypergraph calculation / Simplicial Complex) could lead to combinatorics computation challenge.

A data, collected every minute for Geo Position, starts to be acquired when someone stops doing activities. This “starting” point leads to aggregation of data. As already written, we came

to an average of data per day per user of 12 Mo. We can imagine that if you acquire more data to better characterize the context of an activity and build a representation with Simplicial complex, you will have to scale and move to a probably more resilient infrastructure (such TitanDB/SPARK, which we are actually testing).

Regarding computational challenge, it will depend mostly on the objective of the approach and use cases. Because collecting real time or/and predictive activity directly from a user and his mobile phone will represent a huge challenge (computing / hardware, i.e battery). If the ultimate goal is to produce a daily dashboard, computational challenge will still be present but definitively in a different scale.

Based on our Energy Control Model, and the IMhOTEP platform, we have a 63% accuracy for identifying practices with the right categorization. When we ask people who participate to the experimentation if the practice found by the IMhOTEP platform has the right category and reflect what they did, they answer positively to more than 6 of 10. Regarding the initial objective to identify almost automatically complex practices, this intermediary result is relevant.

V. CONCLUSION

Our approach is based on massive digital traces aggregation and how from these pieces of heterogeneous information, we are able to build automatically and backward a structure of human activities. The other objective was to identify practice related to person without an a priori categorization of practices analyzed. Recognition rate could be improved by being able to better localize people in space and time and use more advanced machine learning algorithm to infer over the time lifestyles of people. IMhOTEP provides a new way of building large multidimensional Hypergraph to represent dynamic structures of heterogeneous entities. Perspective and next research should focus on how to manage large amount of users, which can lead to combinatory calculation limits due to large incidence and adjacency matrices.

REFERENCES

- [1] P. Pourouchottamin, C. Barbier, L. Chancel and M. Colombier, “New representations of energy consumption,” IDDRI, UMR 8568 CIRED, EDF R&D, 2013.
- [2] L. Chen and I. Khalil, “Activity recognition: Approaches, practices and trends,” *Activity Recognition in Pervasive Intelligent Environments*, Springer, 2011, pp. 1-31.
- [3] G. Spaargaren and B. Van Vliet, “Lifestyles, consumption and the environment: The ecological modernization of domestic consumption,” *Environmental Politics*, vol. 9, no. 1, 2000, pp. 50-76. R. Nicole, “Title of paper with only first word capitalized,” *J. Name Stand. Abbrev.*, in press.
- [4] G. Spaargaren, “Theories of practices: Agency, technology, and culture: Exploring the relevance of practice theories for the governance of sustainable consumption practices in the new world-order,” *Global Environmental Change*, vol. 21, no. 3, 2011, pp. 813-822. M. Young, *The Technical Writer’s Handbook*. Mill Valley, CA: University Science, 1989.
- [5] G. Spaargaren, “Sustainable consumption: a theoretical and environmental policy perspective,” *Society & Natural Resources*, vol. 16, no. 8, 2003, pp. 687-701.
- [6] I. Røpke, “The dynamics of willingness to consume,” *Ecological Economics*, vol. 28, no. 3, 1999, pp. 399-420.

- [7] I. Røpke, "Theories of practice—New inspiration for ecological economic studies on consumption," *Ecological Economics*, vol. 68, no. 10, 2009, pp. 2490-2497.
- [8] I. Røpke, "New technology in everyday life—social processes and environmental impact," *Ecological Economics*, vol. 38, no. 3, 2001, pp. 403-422.
- [9] E. Shove, *The design of everyday life*, Berg Publishers, 2007.
- [10] E. Shove, H. Chappells, L. Lutzenhiserc and B. Hackettd, "Comfort in a lower carbon society," *Building Research & Information*, Volume 36, Issue 4, 2008.
- [11] E. Shove, "Beyond the ABC: climate change policy and theories of social change," *Environment and planning. A*, vol. 42, no. 6, 2010, pp. 1273.
- [12] E. Shove, M. Watson and M. Pantzar, *The dynamics of social practice: Everyday life and how it changes*, SAGE Publications Limited, 2012.
- [13] E. Shove and G. Walker, "Governing transitions in the sustainability of everyday life," *Research Policy*, vol. 39, no. 4, 2010, pp. 471-476.
- [14] E. Shove, "Converging conventions of comfort, cleanliness and convenience," *Journal of Consumer Policy*, vol. 26, no. 4, 2003, pp. 395-418.
- [15] G. Spaargaren and C.S.A.K. Koppen, "Provider strategies and the greening of consumption practices: Exploring the role of companies in sustainable consumption," *The new middle classes*, 2009, pp. 81-100.
- [16] A. Reckwitz, "Toward a Theory of Social Practices A development in culturalist theorizing," *European journal of social theory*, vol. 5, no. 2, 2002, pp. 243-263.
- [17] E. Soulier, C Delalonde and O Petit, " Subjectivation and singularizing process in the perspective of situated learning and actor network theory," *International congress AREF*, 2007.
- [18] F. Bugeaud, "Isamsara: for an engineering-based services and systems mereology hypergraphs ", *Troyes*, 2011.
- [19] E. Soulier, F. Rousseaux, F. Bugeaud, J. Legrand and H. Neffati, "Modeling and simulation of new territories projects using agencements theory, mereological principles and simplicial complex tool," *Proc. 2011 IET International Conference on Smart and Sustainable City (IET ICSSC2011)*, Shanghai, China July, 2011, pp. 6-8.
- [20] R.H. Atkin, *Combinatorial Connectivities in Social Systems: an application of simplicial complex structures to the study of large organizations*, Birkhäuser - 3764309121, 1977.
- [21] R.H. Atkin, *Mathematical structure in human affairs*, Heinemann Educational London - 0435820257, 1974.
- [22] J. Johnson, "Hypernetworks of Complex Systems," *Complex Sciences*, 2009, pp. 364-375.
- [23] M. Atkins, et al., "Atom Activity Streams 1.0," *Abgerufen am*, vol. 22, no. 08, 2011, pp. 2013.
- [24] J. Snell, "JSON activity streams 2.0," 2014.

SWIM: Social Welfare Maximizing Incentive Mechanism for Smart Meter Data Aggregation

Duin Back^{1,2}, Bong Jun Choi^{1,2}

¹Department of Computer Science, The State University of New York (SUNY) Korea, Korea

²Department of Computer Science, Stony Brook University, United States

Email: ^{1,2}{duin.back, bjchoi}@sunykorea.ac.kr

Abstract—In spite of many benefits, e.g., energy and communication cost efficient data aggregation, in-network data aggregation network in the smart meter network involves some smart meters acting as relays. Unlike wireless sensor networks (WSNs), the aggregator in the smart meter network cannot assign smart meters as a relay at its will, unless it properly rewards them. Therefore, to encourage users to contribute their smart meters to be used as relays, we introduce an incentive mechanism for the smart meter data aggregation. Unlike the existing incentive mechanisms where the value of completing a requested task is assumed to be fixed regardless of who takes the requested task, we formulate the winner selection problem by incorporating an additional value that depends on who takes the task. Based on the additional value, called “derivative value”, we propose a Social Welfare Maximizing Incentive Mechanism (SWIM) for the smart meter data aggregation. SWIM not only encourages users to contribute their smart meters to be used as relays by rewarding them with incentives, but also enhances overall satisfaction of participating smart meters by maximizing the social welfare of the system. Simulation results show that SWIM achieves better social welfare of the system and utility of the aggregator compared with the existing incentive mechanisms.

Index Terms—Smart Meter; Incentive; Data Aggregation; Social Welfare.

I. INTRODUCTION

Among many important components of the smart grid, the smart meter is one of the most fundamental and essential component in the smart grid system. It digitally records the amount of resource consumption, e.g., electric energy, gas, and water and delivers the recorded data to the main grid, which enables many critical functions of the smart grid, such as load monitoring and billing. Through load monitoring and billing, Demand-Response (DR), or Demand-Side (DS) management can be realized, which enables a demand-supply balance between users and the grid to ultimately reduce the excessive power generation and green gas emission [1].

As the smart meters emerge as the key component of the smart grid, the number of the smart meters installed all over the world has been drastically increasing. For example, there are more than 50 million smart meters installed in the US as of July, 2014 and the number is expected to grow continuously [2]. However, along with the quantitative growth of the smart meters, the ever-increasing volume of the smart meter data and the energy consumption of the smart meter networks emerge as new challenges. Therefore, how to efficiently aggregate the smart meter data has attracted much research attention from the academia and industries. To address the challenges,

many researchers have taken into consideration the in-network data aggregation in the smart meter network [3] [4]. However, existing works assume that the aggregator can assign any smart meter as a relay at will, which is not so practical in the real smart meter networks. Unlike the sensors in wireless sensor networks (WSNs), the smart meters reflect users’ rationality and selfishness. In the smart meter network, users may not contribute their smart meters to be used as relays to avoid potential loss, unless they are given some form of incentives. In other words, unlike in WSNs, the aggregator in the smart meter network has to incentivize users to contribute their smart meters to be used as relays, rather than just assigning them at will. Therefore, to encourage the users to contribute their smart meters to be used as relays, we introduce an incentive mechanism for the smart meter data aggregation. For the incentive mechanism design, we refer to various incentive mechanisms, especially those from the crowdsourcing. However, the existing incentive mechanisms for crowdsourcing assume that the value of completing a requested task is fixed, no matter which worker takes the requested task. In the smart meter network, though immanent but unperceived, there exists some additional value, e.g., reduced energy consumption depending on which smart meter takes the task (acting as a relay), on top of the fixed value of submitting the data itself.

To the best of our knowledge, this is the first work that considers the additional value that depends on who takes the task. In this work, to incorporate the notion of the additional value into the incentive mechanism for the smart meter data aggregation, we present a novel concept of “derivative value” and further develop it into “competition value”. Additionally, we formulate the overall value in the smart meter network as “social welfare”. Rather than maximizing the utility of the aggregator, our incentive mechanism maximizes the social welfare, in order to enhance the overall satisfaction of participating smart meters. The rest of this paper is organized as follows. In Section II, we present the related works. In Section III, we provide our system model. In Section IV, we introduce the derivative value and competition value for the winner selection process. In Section V, we design SWIM, a social welfare maximizing incentive mechanism. In Section VI, we evaluate our incentive mechanism for the smart meter data aggregation. Finally, we conclude this paper in Section VII.

II. RELATED WORK

A. In-network Data Aggregation

In-network data aggregation was first proposed to combine and deliver the data distributed over and collected from many sensors (sources) to a destination node efficiently in terms of the energy and communication cost. In-network aggregation handles not only how data is aggregated at each sensor node but also how data is delivered through the network, which significantly affects the energy consumption and the overall network efficiency. The in-network aggregation can be categorized into three main approaches: (1) tree-based approach, (2) cluster-based approach, and (3) multipath approach.

- 1) Tree-based approaches build a spanning tree where an aggregator is residing on the root of the tree. Using the hierarchical organization of sensor nodes, a tree-based approach can simplify the data aggregation flowing from the sources to the destination. In the spanning tree, each node delivers the sensing data, combined with the data from its children, to its parent node, which will eventually lead to the delivery of every data in the network to the root node (the aggregator) [5] [6]. However, the tree-based approaches have the robustness problem where the data delivery will fail if the node's parent-node does not operate normally.
- 2) Cluster-based approaches are quite similar to the tree-based approaches. However, cluster-based schemes partition nodes into clusters. In addition, each cluster has a special node, named "cluster head", responsible for the intra-cluster data aggregation and the transmission of the aggregated data to the aggregator. That is, a cluster head acts as a relay node for the other nodes in the same cluster [7] [8]. As in the tree-based approaches, the cluster-based approaches enable the simple data aggregation and also have the robustness problem.
- 3) Multipath approaches were proposed as a solution to the robustness problem of both the tree-based approaches and the cluster-based approaches. In a multipath approach, as the name suggests, a node broadcasts data to a number of neighboring nodes, rather than sending its own data or the aggregated data to a single parent. By doing so, a source node can have multiple data flows to the destination, which enables to achieve higher robustness since the data can be delivered even when some of the multiple flows fail. However, multipath approaches achieve the robustness at the cost of some extra overhead resulting from the excessive data transmission [9] [10].

In the smart meter network, since every smart meter estimates the amount of resource consumption and transmits the data to the aggregator(s), the smart meter network shares some similar characteristics with the wireless sensor network. The similarity has led to various research works that apply in-network aggregation to the smart meter network.

B. Incentive Mechanisms for Crowdsourcing

In recent years, many incentive mechanisms for crowdsourcing have been proposed. Yang et al. [11] present two generic but concrete system model of incentive mechanisms for crowdsourcing: the platform-centric model, and the user-centric model to motivate mobile users to participate in the crowdsensing system. D. Peng et al. [12] propose a quality based incentive mechanism for crowdsensing, where the platform rewards the participants proportionally to their contribution, to motivate the rational participants to perform sensing tasks efficiently. C. Liu et al. [13] propose a Quality of Information (QoI)-aware incentive mechanism for participatory sensing to maximize the quality of information by maximizing the user participation in the system. S. Ji et al. [14] present an incentive mechanism for mobile phones with uncertain sensing time. Lee and Hoh [15] propose a Reverse Auction based Dynamic Pricing incentive mechanism with Virtual Participation Credit (RADP-VPC) to maintain participants and promote dropped users to participate again in order to retain sufficient number of participants for the required service quality. However, the existing works assume that the value derived from completing a requested task is fixed, no matter which provider takes the requested task. In other words, the influence range of completing the requested task is confined to the interaction only between the platform (requester) and the *winner providers* who receive the payment for completing the task. Therefore, technically speaking, which provider is selected as a winner does not affect the other loser providers' utilities. However, in reality, some additional values can be derived from which provider takes the task, besides the value of completing the requested task itself.

III. SYSTEM MODEL

In this section, we present the system model of our incentive mechanism for the smart meter data aggregation. The system structure is in a form of reverse auction where the roles of buyers and providers are reversed. That is, in our system, providers (smart meters) compete to obtain the data aggregation task (acting as a relay) from the buyer (aggregator) and rewards will decrease as the providers compete with each other. In our system model, there are an aggregator, a platform, and a set of N smart meters, $\mathcal{W} = \{1, 2, 3, \dots, i, \dots, N\}$ that act as providers in the smart meter data aggregation. Figure 1 illustrates the relay appointment in the smart meter network. We make following assumptions to reflect the real smart meter network.

- 1) The platform can obtain the location information of every smart meter.
- 2) Each smart meter has a limited capacity to aggregate data. That is, each smart meter has the maximum number of smart meters S_{max} that it can support as a relay.

For the smart meter data aggregation, the aggregator posts a set of M data aggregation tasks, $\mathcal{T} = \{1, 2, 3, \dots, j, \dots, M\}$ on the platform where each task j has the corresponding value, $v_j \in \mathbb{R}^+$ to the aggregator. With the second assumption taken

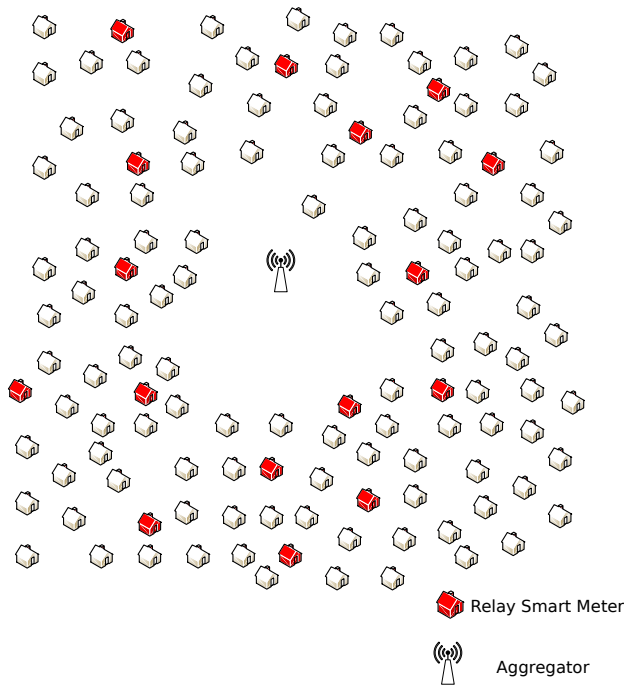


Figure 1. Relay Appointment in Smart Meter Network

into consideration, the aggregator determines the size of the set of tasks, $M \in \mathcal{Z}^+$, which is calculated as

$$M \geq \frac{N}{(S_{max} + 1)}. \quad (1)$$

Given \mathcal{T} , the platform announces the data aggregation task information to all the participating smart meters. In response to the announcement, each smart meter i submits its type information θ_i to the platform. Each type information θ_i consists of smart meter i 's id id_i and bid information b_i . In the process of completing its assigned data aggregation task, smart meter i has an associated cost, $c_i \in \mathbb{R}^+$. Since each smart meter is rationally selfish, each participating smart meter i submits its bid price $b_i \geq c_i$ and decides to work on the requested task only if it is paid with $p_i \geq b_i$. Therefore, when \mathcal{W}_s denotes the set of selected smart meters, the utility of smart meter i is defined as

$$u_i = \begin{cases} p_i - c_i & \text{if } i \in \mathcal{W}_s \\ 0 & \text{otherwise} \end{cases}. \quad (2)$$

Given the set of data aggregation tasks \mathcal{T} and the set of smart meters \mathcal{W} , the platform determines a subset of smart meters which will act as relays for the data aggregation tasks \mathcal{T} and calculates the payment p_j to each relay smart meter of task j . For the aggregator, the payment to the winner smart meters is the cost of completing the data aggregation tasks. Thus, the utility of the aggregator is calculated as

$$u_0 = \sum_{j \in \mathcal{T}} v_j - \sum_{i \in \mathcal{W}_s} p_i. \quad (3)$$

In our incentive mechanism, we aim to achieve the following four desirable economic properties: (1) individual rationality, (2) budget-balance, (3) computational efficiency, and (4) truth-

fulness. The descriptions of each property are provided below.

- **Individual Rationality:** each participating worker has a non-negative utility as $u_i \geq 0$, where u_i is the utility of entity i .
- **Budget-balance:** the budget assigned to the platform can cover all the payment to the winning providers as $\sum_{i \in \mathcal{W}_s} p_i \leq B$.
- **Computational Efficiency:** the winner selection mechanism can be computed in polynomial time.
- **Truthfulness:** no provider can improve its utility by submitting a false cost information. In other words, submitting the true cost information is the dominant strategy for all smart meters.

According to Myerson [16], in order to guarantee truthfulness in a reverse auction system, an auction mechanism should satisfy the following two conditions. First, the winner selection process in the auction is monotone, which means that if provider i wins the auction by bidding b_i , he or she will surely win the auction by bidding $b'_i \leq b_i$. Second, the winner in the auction is rewarded with the critical value, which is defined as the maximum payment a seller can ask, while winning the auction.

IV. DERIVATIVE VALUE AND COMPETITION VALUE

As in the existing incentive mechanisms, the value of submitting the aggregated data itself is fixed. However, on top of the fixed value, we take into consideration some additional value that depends on which smart meter takes the task, called ‘‘derivative value’’. The derivative value matrix of the requested data aggregation task j is defined as

$$\Delta v^j = \begin{bmatrix} \Delta v_{11}^j & \Delta v_{12}^j & \Delta v_{13}^j & \cdots & \Delta v_{1N}^j \\ \Delta v_{21}^j & \Delta v_{22}^j & \Delta v_{23}^j & \cdots & \Delta v_{2N}^j \\ \Delta v_{31}^j & \Delta v_{32}^j & \Delta v_{33}^j & \cdots & \Delta v_{3N}^j \\ \cdots & \cdots & \cdots & \cdots & \cdots \\ \Delta v_{N1}^j & \Delta v_{N2}^j & \Delta v_{N3}^j & \cdots & \Delta v_{NN}^j \end{bmatrix}, \quad (4)$$

where each matrix element Δv_{iq}^j denotes smart meter q 's derivative value when smart meter i is the winner for task j , and $\Delta v_{ii}^j = 0, \forall i \in \mathcal{W}$. When smart meter i is selected as the winner, the derivative value of requested task j is defined as

$$\Delta v_i^j = \sum_{q \in \mathcal{W}} \Delta v_{iq}^j. \quad (5)$$

In other words, assuming smart meter i is the winner for task j , the derivative value of task j is the sum of all the matrix elements in the i -th row. To incorporate the derivative value in the winner selection process, we introduce a ‘‘competition value’’ of smart meter i for task j , which is defined as

$$v_i^j = v_j + \Delta v_i^j, \quad (6)$$

where v_j is the value of submitting the aggregated data of task j itself. In the winner selection process, the smart meter with a higher competition value and a lower bid has a higher probability to win the competition. Additionally, we define

“social welfare” of the system as

$$W(1 \sim N) = \sum_{j \in \mathcal{T}} \Delta v_*^j - \sum_{i \in \mathcal{W}_s} p_i, \quad (7)$$

where Δv_*^j denotes the derivative value of the winner smart meter for task j . That is, the social welfare of the system is the sum of all selected smart meters’ derivative values minus the sum of the payments for them. In this work, rather than maximizing the utility of the platform, we set the objective of the platform as maximizing the social welfare, in order to enhance the overall participating smart meters’ satisfaction.

V. THE DESIGN OF SWIM

In this section, we present SWIM, a Social Welfare maximizing Incentive Mechanism for the smart meter data aggregation to enhance the overall satisfaction of participating smart meters, and prove that the incentive mechanism satisfies all the desirable economic properties. The incentive mechanism consists of two algorithms: (1) k-means clustering algorithm, and (2) winner selection algorithm.

A. k-means Clustering Algorithm

Given the set of data aggregation tasks (\mathcal{T}) and the set of type information from participating smart meters (θ), the platform runs k-means clustering algorithm [17]. As we assumed in the system model, the platform retains the location information of every smart meter. For simplicity, we also assume that data transmission blockage by buildings is negligible. By mapping the identification number of each smart meter to the corresponding location information, the platform can locate each participating smart meter. In this work, we assume that the location information of smart meter i contains a pair of its x-coordinate and y-coordinate. Using this location information, the platform runs k-means clustering algorithm. Since the aggregator has M data aggregation tasks, the platform sets k to M to divide participating smart meters into a set of M clusters, $G = \{G_1, G_2, G_3, \dots, G_j, \dots, G_M\}$ to minimize the intra-cluster distance variance, defined as the sum of square of distance between each smart meter in a cluster and the centroid of the cluster, which is equal to all the energy consumption for the data transmission within the cluster.

B. Winner Selection Algorithm

In the winner selection algorithm, the objective of the platform is to maximize the social welfare of the system. The algorithm is divided into two steps: winner selection step, and payment step.

Step 1 - Winner Selection: To achieve the objective, for each cluster G_j , the platform selects the smart meter with the minimum bid to competition value ratio (b_i/v_i^j) as the candidate for the relay smart meter for data aggregation task j . The winner selection step is the same as the greedy mechanism which selects the smart meter with the minimum bid to competition value ratio as a winner. The mechanism is known to be computationally efficient. Note that in the winner

selection rule, the platform does not determine the winner smart meter, but just the candidate smart meter.

Step 2 - Payment: After selecting a candidate smart meter, the platform decides the payment to the candidate, which is defined as $p_j = \max\{p_j, \frac{b_c}{v_c^j} v_{i^*}^j\}$. Here, the payment p_j in our payment step is the critical value for smart meter i^* when smart meter i^* is the candidate of G_j . According to the winner selection step, when smart meter c satisfies the following chains of inequations

$$\frac{b_c}{v_c^j} \leq \frac{b_1}{v_1^j} \leq \frac{b_2}{v_2^j} \dots \leq \frac{b_{|G_j|-1}}{v_{|G_j|-1}^j}, \quad (8)$$

the platform selects smart meter c as the winner smart meter for G_j . If smart meter i newly joins the cluster G_j and wants to win the auction, it must assign its bid as

$$b_i \leq \frac{b_c}{v_c^j} \times v_i^j. \quad (9)$$

Otherwise, the platform selects smart meter c as the winner smart meter instead of smart meter i according to the winner selection step. After calculating the payment to the candidate smart meter, the platform checks the budget-balance. If the payment is affordable, the platform determines the winner and updates the budget. Otherwise, the platform discards the candidate smart meter and repeats the winner selection rule until it finds the winner in the rest of smart meters or none of the smart meters in the cluster budget-feasible. The detail of the winning requester selection algorithm is presented in Algorithm 1.

Algorithm 1: Winner Selection Algorithm

Input : θ, Γ, B
Output: \mathcal{W}_s

- 1 $\mathcal{W}_s \leftarrow \emptyset, p_{1 \sim M} \leftarrow 0;$
- 2 $G = \text{k-means Clustering}(\theta, |\Gamma|);$
- 3 **for** $G_j \in G$ **do**
- 4 **while** $p_j = 0$ **do**
- 5 $i^* \leftarrow \arg \min_{i \in G_j} \frac{b_i}{v_i^j};$
- 6 $G_j \leftarrow G_j \setminus \{i^*\};$
- 7 $c \leftarrow \arg \min_{i \in G_j} \frac{b_i}{v_i^j};$
- 8 $p_j \leftarrow \max\{p_j, \frac{b_c}{v_c^j} v_{i^*}^j\};$
- 9 **if** $B - p_j \geq 0$ **then**
- 10 $B \leftarrow B - p_j;$
- 11 $\mathcal{W}_s \leftarrow \mathcal{W}_s \cup \{i^*\};$
- 12 **else**
- 13 $p_j \leftarrow 0;$
- 14 **end**
- 15 **end**
- 16 **end**
- 17 **return** \mathcal{W}_s

C. Economic Properties

In this subsection, we provide the proofs for the desirable economic properties of SWIM.

Lemma 1. *SWIM is individually rational.*

Proof. As we assumed in the system model, each participating smart meter i submits its bid price $b_i \geq c_i$ to compensate the associated cost, and decides to work on the requested task only if it is paid with $p_i \geq b_i$. Thus, the utility of winner smart meter i is $u_i = p_i - c_i \geq p_i - b_i \geq 0$. For the loser smart meter, the utility is simply 0. \square

Lemma 2. *SWIM is budget-balanced.*

Proof. In the payment step, given the candidate for the relay smart meter, the platform checks whether the budget can cover the payment to the candidate. If the payment is not affordable by the current budget, the platform discards the candidate and repeats the winner selection rule. This step guarantees that the payment to the winner smart meters is always decided within the budget constraint. \square

Lemma 3. *SWIM is computationally efficient.*

Proof. Except for k-means clustering, the winner selection algorithm takes $\mathcal{O}(MN^2)$ time since the winner selection step and the payment step take $\mathcal{O}(N^2)$ for each cluster G_j and the winner selection algorithm runs for G whose size is M . \square

Lemma 4. *SWIM is truthful.*

Proof. According to [16], we need to prove that our winner selection step satisfies the two conditions, the monotonicity of the winner selection and the critical value based payment to winners. The monotonicity of the winner selection step is obvious, since if smart meter i wins the auction by bidding b_i , he will be surely selected as winner by bidding $b'_i \leq b_i$. For the critical value based payment, the payment step of SWIM calculates the critical value and set the value as the payment. If smart meter i submits $b_i > p_i$, he will lose the auction and be replaced. Therefore, p_i is the critical value. \square

By Lemmas 1 to 4, we have Theorem 1 as follows:

Theorem 1. *SWIM is individually rational, budget-balanced, computationally efficient, and truthful.*

VI. EVALUATION

In this section, we evaluate our incentive mechanism, SWIM, and compare its social welfare to that of the existing incentive mechanism [18] whose winner selection process is also based on the greedy algorithm, while only taking the fixed value of submitting the aggregated data itself into consideration for the winner selection. For evaluation, we use MATLAB.

A. Simulation Setup

We assume that all the smart meters are randomly distributed in a 2000 m by 2000 m region and the aggregator is located at (1000, 2500), when the vertices of the region are (0, 0), (0, 2000), (2000, 0), and (1000, 2500). In the simulation, we define the cost c_i of smart meter i as the additional data transmission energy needed to act as a relay. To set the cost, we adopt the data transmission energy consumption model from [19]. According to the model, the smart meter consumes E_{elec} in a unit of nJ/bit to operate the transmitter or the receiver and E_{amp} in a unit of $pJ/bit/m^2$ to run the amplifier. Then, the amount of energy expended to send l -bit data a distance d is calculated as

$$P_{TX}(l, d) = E_{elec}l + E_{amp}ld^2. \quad (10)$$

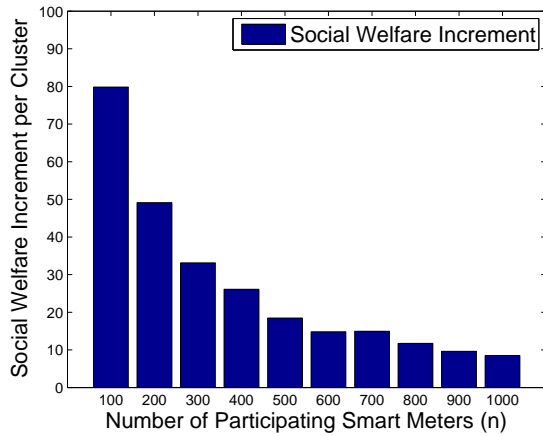
For simplicity, we approximate $P_{TX}(l, d)$ to

$$P_{TX}(l, d) \approx E_{amp} \times l \times d^2, \quad (11)$$

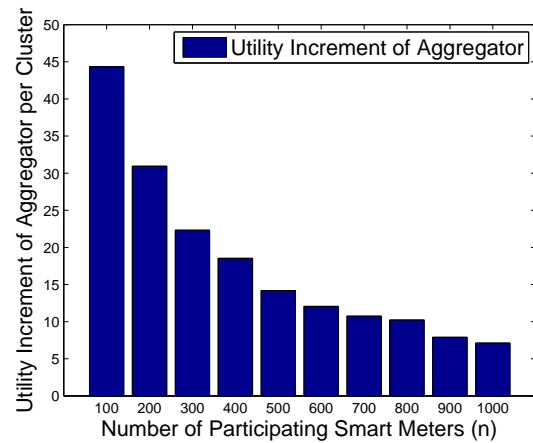
because d affects much more significantly to the transmission energy. In the simulation, we set $E_{amp} = 100$ $nJ/bit/m^2$ and $l = 8000$ bits. For the fixed value of submitting the smart meter data, we set the same value $v = 10$ for every smart meter. That is, v_j , the fixed value of completing the smart meter data aggregation task j for G_j is $|G_j| \times 10$ when the number of smart meters in G_j is the size of G_j . In the simulation, we define the derivative value Δv_{iq}^j as the data transmission energy saving of smart meter q when smart meter i is the winner for task j . As the energy saving is in the unit of J , we convert $10 J$ to the unit value ($v = 1$).

B. Simulation Results

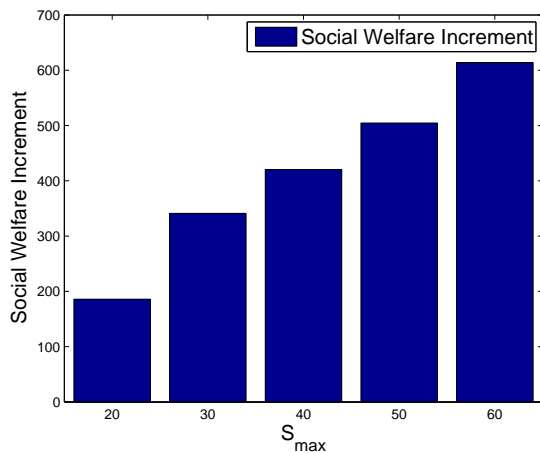
1) *Social Welfare Increment:* Figure 2 shows the social welfare increment by incorporating the derivative value in the winner selection process in comparison with [18]. Figure 2a shows the social welfare increment corresponding to the number of participating smart meters. Results show that regardless of the system size (the number of participating smart meters), the social welfare increment is positive, which means that a higher social welfare is obtained by considering the derivative value in the winner selection process. The higher social welfare results from selecting more profitable (in terms of social welfare) smart meters as relays as well as rewarding them with less payment than [18], while still satisfying the individual rationality of each smart meter. Results also show that as the system size increases, the social welfare increment per cluster decreases. The reason for the decrease in the social welfare increment comes from the density change of smart meters in the simulation region. As the density increases, the difference between the transmission distance to the aggregator and that to a relay smart meter becomes less, which consequently results in the less transmission energy saving. Figure 2b shows the social welfare increments corresponding to the increasing S_{max} . Results show that regardless of S_{max} , a higher social welfare is obtained by considering the derivative value in the winner selection process. The reason for the higher social welfare is the same as that of the system size. Results



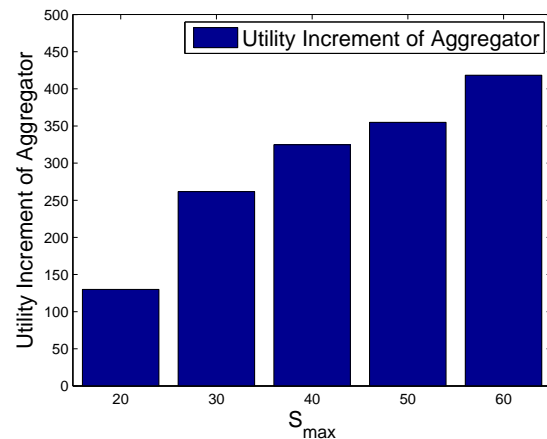
(a) Impact of System Size on Social Welfare ($S_{max}=30$)



(a) Impact of System Size on Aggregator's Utility



(b) Impact of S_{max} on Social Welfare ($n=500$)



(b) Impact of S_{max} on Aggregator's Utility

Figure 2. Social Welfare Increment

Figure 3. Utility Increment of Aggregator

also show the tendency that with higher S_{max} , the system can obtain higher social welfare. Therefore, as S_{max} increases, the aggregator can achieve a larger gap between the derivative value increment and the payment to the winner smart meters. The tendency results from a relatively lower increase rate of the payment corresponding to S_{max} in comparison to that of the derivative value. Assuming one aggregator can cover 500 smart meters, we can achieve an increment of 300 in the social welfare, which amounts to 3000 J . Then, if smart meters transmit data every 15 minutes, we can save 288,000 J per day from 500 smart meters. Applying the calculation result to the number of smart meters installed in the US as of 2014 [2], we can save 28.8 GJ of energy for smart meters in the US. Moreover, if we can deploy smart meters with a higher S_{max} , the smart meter network can achieve even more energy saving.

2) *Utility Increment of Aggregator*: Figure 3 shows the utility increment of the aggregator by incorporating the derivative value in the winner selection process, in comparison with [18]. The simulation settings are the same as those of social welfare increment. Figure 3a shows that regardless of

the system size (the number of participating smart meters), the aggregator achieves the higher utility by considering the derivative value in the winner selection process. According to (3), the utility of the aggregator u_0 is only affected by p_i since v_i for each smart meter has the same value. Thus, unlike the case of social welfare increment, the higher utility of the aggregator only results from achieving narrower gaps between c_i and p_i , $\forall i \in \mathcal{W}_s$ than [18], while still satisfying the individual rationality of each winner smart meter. Results also show that as the system size increases, the utility increment of the aggregator per cluster decreases. The downturn in the utility increment indicates that as the density of smart meters increases, the gap between p_i of SWIM and that of [18] becomes narrower. Figure 3b shows that regardless of S_{max} , the aggregator achieves the higher utility by considering the derivative value in the winner selection process. Results also show that with a higher S_{max} , the aggregator can obtain a higher utility. Such tendency indicates that the aggregator can achieve higher cost-effectiveness by appointing the smart meters with a higher S_{max} as relays. The reason for the tendency is that the reward which will be given to newly appointed smart meters is more expensive than that of the existing relay smart

meters for the increment of data aggregation coverage.

VII. CONCLUSION AND FUTURE WORK

In this paper, we propose SWIM, a social welfare maximizing incentive mechanism for the smart meter data aggregation. SWIM encourages users to contribute their smart meters to be used as relays for the smart meter data aggregation system by rewarding the relay smart meters. In order to enhance the overall satisfaction of participating smart meters, SWIM maximizes the social welfare of the system, rather than maximizing the utility of the aggregator. On top of the fixed value of submitting the smart meter data itself, SWIM incorporates some additional value derived from the data aggregation process, named “derivative value”, in the winner smart meter selection process. We prove that SWIM achieves individual rationality, budget-balance, computational efficiency, and truthfulness. Simulation results show that our incentive mechanism achieves better social welfare of the system and the utility of the aggregator, compared to the existing incentive mechanisms. As a future work, we will consider the data aggregation in the multi-hop heterogeneous relay smart meter network where smart meters have different data transmission distances and S_{max} .

ACKNOWLEDGMENT

This research was funded by the MSIP, Korea, under the “ICT Consilience Creative Program” (IITP-2015-R0346-15-1007) supervised by the IITP and under the “Basic Science Research Program” (NRF-2015R1C1A1A01053788) through the NRF, Korea.

REFERENCES

- [1] Y. Yan, Y. Qian, H. Sharif, and D. Tipper, “A survey on smart grid communication infrastructures: Motivations, requirements and challenges,” *Communications Surveys & Tutorials, IEEE*, vol. 15, no. 1, pp. 5–20, 2013.
- [2] “Smart Electric Meters, Advanced Metering Infrastructure, and Meter Communications: Global Market Analysis and Forecasts,” 2014, URL: <https://www.navigantresearch.com/research/smart-meters/> [accessed: 2016-06-01].
- [3] F. Li, B. Luo, and P. Liu, “Secure information aggregation for smart grids using homomorphic encryption,” in *Smart Grid Communications (SmartGridComm), 2010 First IEEE International Conference on*, Oct. 2010, pp. 327–332.
- [4] F. Li and B. Luo, “Preserving data integrity for smart grid data aggregation,” in *Smart Grid Communications (SmartGridComm), 2012 IEEE Third International Conference on*, Nov. 2012, pp. 366–371.
- [5] C. Intanagonwiwat, R. Govindan, D. Estrin, J. Heidemann, and F. Silva, “Directed diffusion for wireless sensor networking,” *Networking, IEEE/ACM Transactions on*, vol. 11, no. 1, pp. 2–16, 2003.
- [6] S. Lindsey, C. Raghavendra, and K. M. Sivalingam, “Data gathering algorithms in sensor networks using energy metrics,” *Parallel and Distributed Systems, IEEE Transactions on*, vol. 13, no. 9, pp. 924–935, 2002.
- [7] W. B. Heinzelman, A. P. Chandrakasan, and H. Balakrishnan, “An application-specific protocol architecture for wireless microsensor networks,” *IEEE Transactions on Wireless Communications*, vol. 1, no. 4, pp. 660–670, 2002.
- [8] Y. Yao and J. Gehrke, “Query Processing in Sensor Networks,” in *CIDR*, Jan. 2003, pp. 233–244.
- [9] G. P. S. S. Nath, S. and Z. Anderson, “Synopsis diffusion for robust aggregation in sensor networks,” in *Proceedings of the 2nd international conference on Embedded networked sensor systems*, ACM. Worldwide Publisher, Nov. 2004, pp. 250–262.
- [10] S. Moteji, K. Yoshihara, and H. Horiuchi, “DAG based in-network aggregation for sensor network monitoring,” in *International Symposium on Applications and the Internet (SAINT’06)*. IEEE, Jan. 2006.
- [11] D. Yang, G. Xue, X. Fang, and J. Tang, “Crowdsourcing to smartphones: incentive mechanism design for mobile phone sensing,” in *Proceedings of the 18th annual international conference on Mobile computing and networking*. ACM, Aug. 2012, pp. 173–184.
- [12] D. Peng, F. Wu, and G. Chen, “Pay as how well you do: A quality based incentive mechanism for crowdsensing,” in *Proceedings of the 16th ACM International Symposium on Mobile Ad Hoc Networking and networking*, ser. MobiHoc ’15, June 2015, pp. 177–186.
- [13] C. H. Liu, P. Hui, J. W. Branch, C. Bisdikian, and B. Yang, “Efficient network management for context-aware participatory sensing,” in *Sensor, Mesh and Ad Hoc Communications and Networks (SECON), 2011 8th Annual IEEE Communications Society Conference on*, June 2011, pp. 116–124.
- [14] S. Ji, T. Chen, and F. Wu, “Crowdsourcing with trembles: Incentive mechanisms for mobile phones with uncertain sensing time,” in *2015 IEEE International Conference on Communications (ICC)*, June 2015, pp. 3546–3551.
- [15] J.-S. Lee and B. Hoh, “Dynamic pricing incentive for participatory sensing,” *Pervasive Mob. Comput.*, vol. 6, no. 6, pp. 693–708, 2010.
- [16] R. B. Myerson, “Optimal auction design,” *Mathematics of operations research*, vol. 6, no. 1, pp. 58–73, 1981.
- [17] S. Lloyd, “Least squares quantization in pcm,” *IEEE Transactions on Information Theory*, vol. 28, no. 2, pp. 129–137, 1982.
- [18] Q. Liu, T. Luo, R. Tang, and S. Bressan, “An efficient and truthful pricing mechanism for team formation in crowdsourcing markets,” in *Communications (ICC), 2015 IEEE International Conference on*, June 2015, pp. 567–572.
- [19] W. R. Heinzelman, A. Chandrakasan, and H. Balakrishnan, “Energy-efficient communication protocol for wireless microsensor networks,” in *System Sciences, 2000. Proceedings of the 33rd Annual Hawaii International Conference on*, Jan. 2000.

Channel Allocation Plan for DAB and DRM+ Systems in VHF Band III

Youngjae Kim, Sanglim Ju, Kyungseok Kim
Radio & Communications Engineering
Chungbuk National University
Cheongju, Chungbuk, 361-763, Korea

E-mails: kimyj7331@gmail.com, imaward@cbnu.ac.kr, kseokkim@cbnu.ac.kr

Abstract— Recently, analog radio systems are being replaced with digital radio systems. The digital radio can provide high quality services because it is robust to interference and it has a high power efficiency. Thus, an efficient channel allocation plan is needed. This paper proposes a channel allocation plan for Digital Audio Broadcasting (DAB) and Digital Radio Mondiale Plus (DRM+) systems in Very High Frequency (VHF) band III, and presents interference analysis results about this plan. In the channel allocation plan for only DAB system, some local stations lack extra available programs. Accordingly, DRM+ blocks are allocated to the local stations. This paper analyzes the interference between the DAB system and between the DRM+ system. These results will contribute to broadcast network planning of the digital radio.

Keywords-Digital radio broadcast; DAB system; DRM+ system; Channel allocation plan.

I. INTRODUCTION

Recently, most communication systems are changing the digital systems [1] because analog communication systems are sensitive to noise and have a low frequency efficiency. Also many countries are promoting the introduction of the digital radio and some countries are actually providing digital radio service.

Digital radio is robust against interference, has a higher power efficiency than existing systems and can provide additional data service, such as a text message, image, thus it can provide high quality of service that can enhance competitiveness of the radio medium. In particular, it can efficiently use the limited frequency resources because it can multiplex various programs on a single broadcast channel. So, existing broadcasters are able to provide additional services and the listener can obtain a variety of media by introducing new radio operators.

In this paper, we develop a channel allocation plan for the DAB system [7] and DRM+ system [8] in VHF Band III. In this paper, we present the interference analysis simulation results.

This paper content is: In Section 2, the DAB and DRM+ systems are presented. Section 3 describes the DAB and the DRM + channel assignment scheme in the VHF channel. In Section 4, we presents results of the interference analysis simulation. Finally, in Section 5, we present the conclusion.

II. DAB/DRM+ SYSTEMS DESCRIPTION AND FREQUENCY ASSIGNMENT SCHEME

A. DAB and DRM+ systems description

The DAB system can provide a high quality service and excellent mobile reception quality by using audio compression technology based on Moving Picture Experts Group (MPEG) Audio Layer II [2]. Also, it has high efficiency of using frequency because it can transmit multiple programs to an OFDM signal called ensemble. In this paper, 9 programs are transmitted through one ensemble allotted 128kbps bit rate. The transmission method of DAB is Coded Orthogonal Frequency Division Multiplexing (COFDM).

TABLE I. DAB AND DRM+ SYSTEMS FEATURE

	DAB	DRM+
Frequency	Band-I, II, III, IV, L-Band	30MHz ~ Band-III
Transmission	COFDM	COFDM
Modulation	DQPSK	4-QAM 16-QAM
System bandwidth	1.536 MHz	100 kHz
Number of subcarriers	1536	213
Subcarrier spacing	1 kHz	444 Hz
Audio coding	MPEG Audio Layer II	MPEG-4 CELP MPEG-4 HVXC

Broadcast frequency of DRM+ system is extended to 240 MHz also bandwidth is increased to 100 kHz. It uses MPEG-4 Code Excited Linear Prediction (CELP) and MPEG-4 Harmonic Vector excitation Coding (HVXC) in audio coding. The DRM+ system can select one of 4-Quadrature Amplitude Modulation (QAM), 16-QAM modulation according to a service quality and robustness. The transmission method of DRM+ is COFDM and DRM+ system transmits 1 program per 1 block allotted 74.5kbps. Table 1 indicates a summary of the DAB and DRM+ systems [2][3].

B. DAB and DRM+ system frequency assignment scheme

The three DAB ensembles are assigned in VHF channel having a 6 MHz bandwidth. A guard band between each

ensembles is set to 192 kHz. A lower guard band in front of ensemble A is set to 512 kHz, upper guard band beside ensemble C is set to 496 kHz.

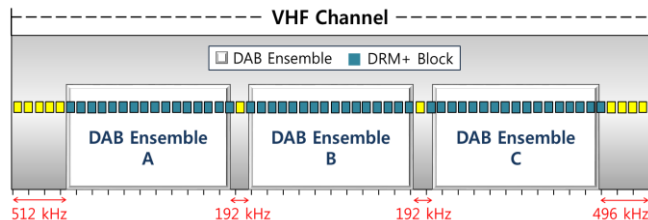


Figure 1. DAB ensembles and DRM+ blocks assignment in VHF channel.

The DRM+ system has a bandwidth of 100 kHz per one block and sets the center frequency interval at 100 kHz. Therefore, it sets a total of 60 blocks in VHF Channel. DAB ensembles and DRM blocks assignment in VHF channel are represented in Figure 1.

III. ALLOCATION PLAN FOR DAB AND DRM+ SYSTEMS

A. Allocation plan for DAB system

Terrestrial Digital Multimedia Broadcasting (T-DMB) in Korea is being transmitted without configuring the SFN (Single frequency Network) in some areas because of the interference effect of the existing analog TV channel. However, we assume SFN area configuration in this paper, since the DTV transition is completed from the analog TV. T-DMB channel of Jeolla-do is divided into three channels. It is integrated into 8 channels. T-DMB channel of Gyeongsangbuk-do that is divided into two channels. It is integrated into 7 channels. T-DMB channel of Gyeongsangnam-do that is divided into two channels. It is integrated into 12 channels. Table 2 shows the integrated channels and the existing the T-DMB channel.

TABLE II. THE RE-ALLOCATION CHANNELS AND THE EXISTING THE T-DMB CHANNEL

Existing T-DMB Channel		Re-allocation channel
Jeollanam-do	8	8
Jeollanam-do (Eastern)	7	
Jeollabuk-do	12	
Gyeongsangbuk-do (Southern)	7	7
Gyeongsangbuk-do (Northern)	9	
Gyeongsangnam-do (Eastern)	12	12
Gyeongsangnam-do (Western)	9	

We were placed in regional DAB ensemble using a derived available channel. The available channels of region are shown in Figure 2. Ensembles of each local station are allocated based on the number of FM broadcasting which is

currently broadcasting. For example, in the case of Seoul, Seoul Tx is broadcasting on 23 FM radio. When FM broadcastings are replaced by DAB ensembles, three ensembles are required. Thus, we allocate ensemble A, B, C of Channel 7. Others also allocate DAB ensembles to another area in the same way shown in Figure 3. FM broadcasting programs are marked with yellow and the allocated DAB ensemble numbers are marked with green in Figure 3. The cases requiring interference analysis for co-channel or an adjacent channel are connected with the arrow and marked in orange. There are 8 cases requiring simulation analysis. The cases are shown in Figure 3.

In the case of Seoul, three DAB ensembles are allocated in Seoul TX and Seoul TX is able to accommodate 27 programs and is broadcasting 23 programs. Therefore, it can transmit further 4 programs. In the same way, extra available programs for each local TX are shown in Table 3.

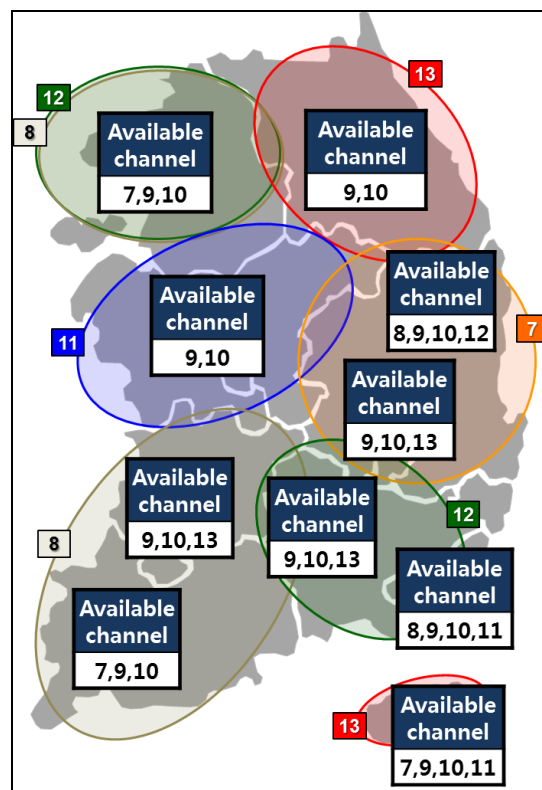


Figure 2. The available channel by region in Korea.

The number of extra available programs is different by region. Cheongju TX cannot introduce a new broadcaster because, in this case, the number of additional available programs is zero. In this paper, in order to solve this problem, we propose an allocation plan for DAB and DRM+ systems in the area with the less than 6 available programs.

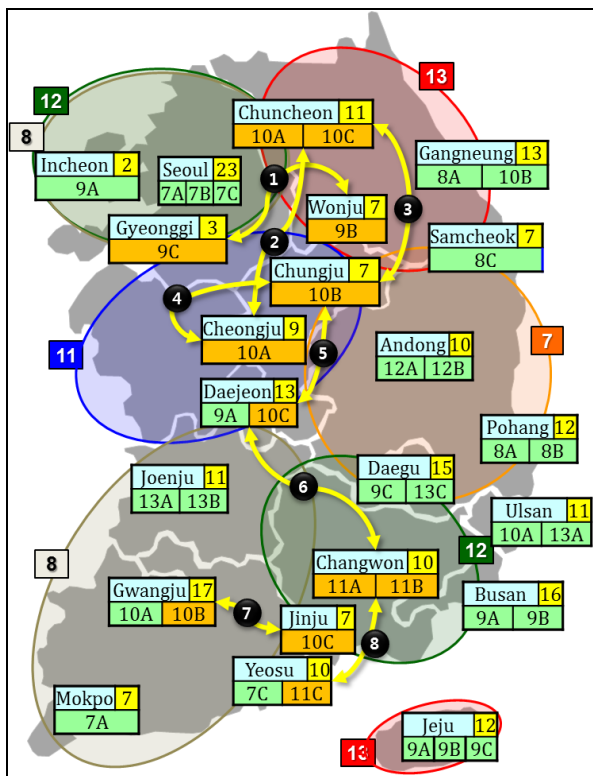


Figure 3. DAB ensemble allocation results by local stations.

B. Mixed allocation plan for the DAB and DRM+ systems

Upper guard band (496 kHz) and lower guard band (512 kHz) are in VHF channel with DAB ensemble. Four DRM+ blocks are allocated in each guard band as shown in Figure 5. Frequency offset between the DRM+ block 4 and DAB ensemble A in lower guard band is 930 kHz. Frequency offset between DRM+ block 57 and DAB ensemble C in upper guard band is 930 kHz.

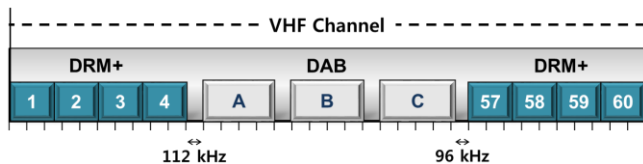


Figure 4. DAB ensembles and the DRM+ blocks allocation in VHF channel.

According to ITU-R standard [4], when the frequency offset between DRM+ block and DAB ensemble is 100 kHz and DAB system is wanted signal, D/U ratio is -36 dB. When Frequency offset between DRM+ block and DAB ensemble is 100 kHz and DRM+ system is wanted signal, D/U ratio is -40 dB. Accordingly, the interference effect between DRM+ block and DAB ensemble is not considered.

TABLE III. EXTRA AVAILABLE PROGRAMS FOR EACH LOCAL TX

Local Broadcasting	Num. of FM program	DAB ensemble (Total available program)	Num. of extra available program
Seoul	23	9A, 9B, 9C (27)	4
Gyeonggi	3	7C (9)	6
Incheon	2	7A (9)	7
Gangneung	13	8A, 10A (18)	5
Wonju	7	7A (9)	2
Chuncheon	11	7B, 10B (18)	7
Samcheok	7	8C (9)	2
Daejeon	13	13A, 13B (18)	5
Chungju	7	10A (9)	2
Cheongju	9	10C (9)	0
Andong	10	12A, 12B (18)	8
Daegu	15	8A, 8B (18)	3
Pohang	12	10B, 10C (18)	6
Changwon	10	8C, 10A (18)	8
Jinju	7	11C (9)	2
Busan	16	11A, 11B (18)	2
Ulsan	11	13A, 13B (18)	7
Joenu	11	10A, 13C (18)	7
Gwangju	17	11A, 11B (18)	1
Yeosu	10	10B, 10C (18)	8
Mokpo	7	9A (9)	2
Jeju	12	12A, 12B, 12C (27)	15

The DRM+ blocks and the DAB ensemble are allocated as shown in Figure 4; the total of 56 DRM+ blocks are secured from VHF channel 7 to 13. We proposed a plan that secures extra available programs in local stations. DRM+ blocks is allocated for the number of lacking extra program. The final result of allocated DRM+ blocks is shown in Figure 5.

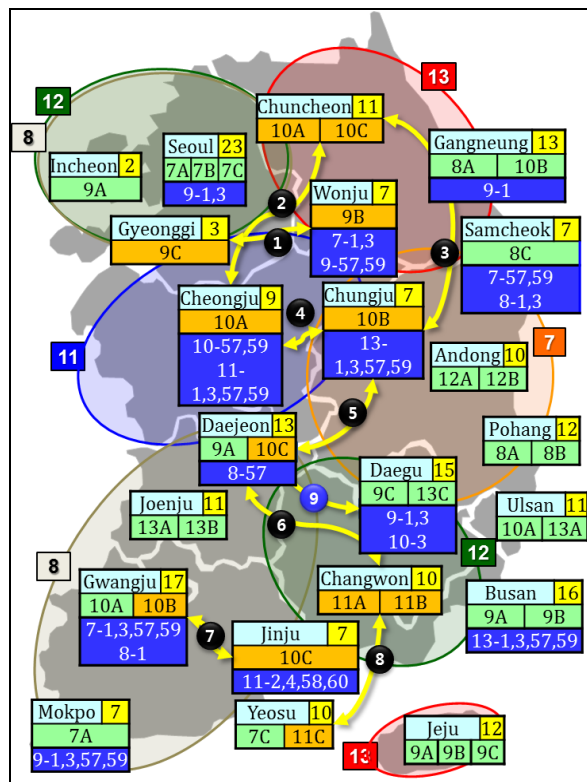


Figure 5. DAB ensemble and DRM+ block allocation results by region broadcasting in Korea.

This plan has the same case considering the interference analysis between DAB ensemble as the only DAB ensemble allocation plan. Frequency offset between DRM+ block of Daejeon and DRM+ block of Daegu is 400 kHz. Hence, we execute an interference analysis for case 9 in Figure 5.

IV. SIMULATION RESULT

We use the Spectrum Management Intelligence system (SMIs) in order to verify the reliability of the derived results. SMIs is a frequency analysis system for broadcast networks that is used to analyze the interference and the field strength of propagation in Korea. This system was offered by the Korea National Radio Research Agency (KNRRA) of Korea Communication Commission (KCC).

Protection Ratio (PR) for DAB system interfered with by DAB system is set by ITU-R standards [4][5]. PR for DRM+ system interfered with by DRM+ system is set by ITU-R standards [4][6]. Each PR is shown in Table 4 and Table 5.

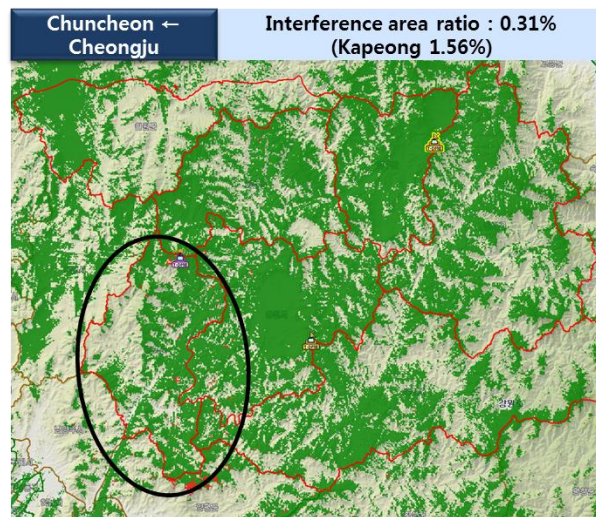
TABLE IV. PR FOR THE DAB SYSTEM INTERFERED WITH BY THE DAB SYSTEM

Channel offset	PR between DAB system
Co-channel	10
Adjacent channel	-37

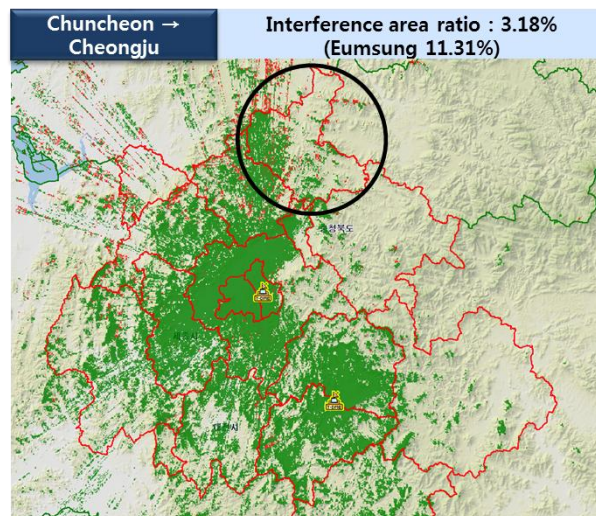
TABLE V. PR FOR THE DRM+ SYSTEM INTERFERED WITH BY THE DRM+ SYSTEM

Frequency offset	PR between DRM+ system
0	4
±100	-16
±200	-40
±400	-63

The interference influence from Cheongju in Chuncheon is shown in Figure 6 (a). The interference area is 0.31% of the coverage area of Chuncheon. The interference area in Kapeong is 1.56% of the total coverage area of Chuncheon. This interference area is 3.18% of the coverage area of Cheongju. The interference area in Eumsung is 11.31% of the total coverage area of Cheongju.

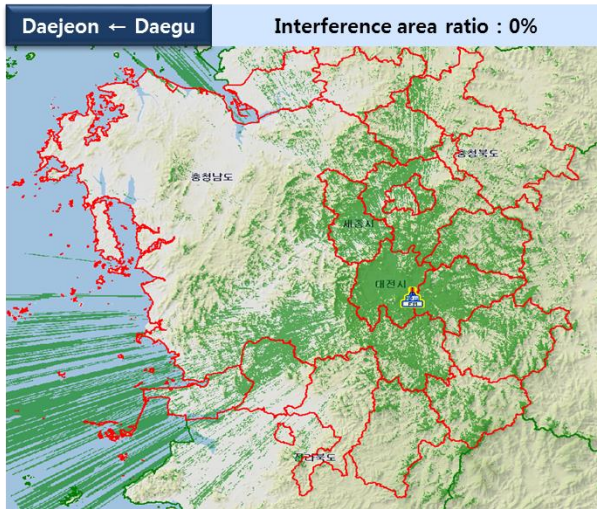


(a) Interference influenced from Cheongju in Chuncheon.

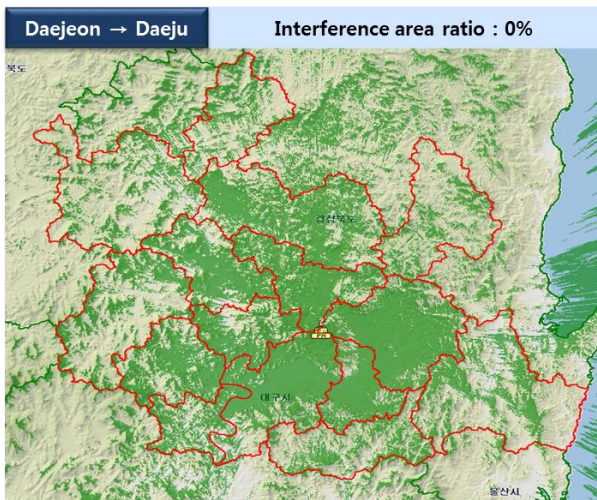


(b) Interference influenced Chuncheon from in Cheongju.

Figure 6. Inteferece analysis result between Chuncheon and Cheongju.



(a) Interference influenced from Daejeon in Daegu.



(b) Interference influenced from Daejeon in Daegu.

Figure 7. Inteferece analysis result between Daejeon and Daegu.

The case 9, interference analysis has confirmed that there is no interference between DRM+ systems. The simulation result is shown in Figure 7. Besides, stations that derived more than 5% interference are organized in Table 4.

As a result of interference analysis, there is no interference between DRM+ block. We derived the results that secure extra available programs without additional interference situation in DAB ensemble allocation plan. The final result is shown in Table 6.

V. CONCLUSION AND FUTURE WORK

When we allocate only DAB ensemble in local stations, some local stations lack extra available programs. In this paper, we proposed a broadcast network plan that allocates DAB system mixed with DRM+ system in order to solve the problem.

TABLE VI. STATIONS THAT OCCURRED MORE THAN 5% INTERFERENCE AREA RATIO

Case	Wanted signal	Interference area ratio	
①	Gyeonggi	.	0%
	Chuncheon	.	0%
②	Chuncheon	Kapeong	1.56%
	Cheongju	Eumsung	11.31%
③	Chuncheon	.	0%
	Chungju	.	0%
④	Cheongju	Eumsung	17.23%
	Chungju	Cheongju	32.92%
⑤	Chungju	Cheongwon	0.73%
	Daejeon	Eumsung	20.75%
⑥	Daejeon	Muju	4.34%
	Jinju	Hamyang	7.25%
⑦	Gwangju	Hadong	11.05%
	Jinju	Hadong	1.82%
⑧	Changwon	.	0%
	Yeosu	.	0%
⑨	Daejeon	.	0%
	Daegu	.	0%

A total of nine cases are derived from allocating DAB ensemble and DRM+ block in each local station. As a result of interference analysis, additional interference case did not occur and local stations that have the extra available programs of less than 6 secure 6 extra available programs. In this paper, the frequency of DRM+ system is allocated with DAB system having no interference. Accordingly, if the DRM+ system is used in guard band in the DAB system, frequency efficiency is improved. The presented results can be used as a basis for broadcast network planning of the digital radio in Korea.

REFERENCES

- [1] M. S. Baek, et al., "Design and Performance Evaluation of Digital Radio Measurement Test Beds for Laboratory Test: DAB, DAB+", and T-DMB Audio, IEEE Transactions on Instrumentation and Measurement, Vol. 62, 2013, pp. 451-459.
- [2] ETSI, Radio Broadcasting Systems; Digital Audio Broadcasting (DAB) to mobile, portable and fixed receivers, ETSI EN 300 401, Rev.1.4.1, 2006.
- [3] ETSI, Digital Radio Mondiale (DRM); System Specification, ETSI ES 201 980, Rev.4.1.1, 2014.
- [4] ITU, Technical basis for planning of terrestrial digital sound broadcasting in the VHF band, Rec. ITU-R BS.1660-6, 2012.
- [5] DSB Handbook, Terrestrial and Satellite Digital Sound Broadcasting to Vehicular, Portable and Fixed Receivers in the VHF/UHF Bands, Edition 2002, ITU Publication Notice No.343-02-cor-02 (May 2002).
- [6] M. S. Baek, et al., "Laboratory Trials and Evaluations of In-Band Digital Radio Technologies: HD Radio and DRM+, IEEE Transactions on Broadcasting", Vol. 62, 2013, pp.1-12.
- [7] ETSI EN 300 401, "Radio broadcasting systems: digital audio broadcasting(DAB) to mobile, portable and fixed receivers," ETSI, Tech. Rep., June 2006, https://www.google.co.kr/url?sa=t&rct=j&q=&src=s&source=web&cd=1&cad=rja&uact=8&ved=0ahUKEwj5oOa1hPPNAhUGHZQKHSMPcMIQFggiMAA&url=http%3A%2F%2Fwww.etsi.org%2Fdeliver%2Fetsi_en%2F300400_300499%2F300401%2F01.04.01_40%2Fen_300401v010401o.pdf&usq=AFQjCNGXB6T193oo1qUJxmJo8P3OfXluFQ&sig2=DWNqTkUsXi5cXYok3m36AQ

[8] ES 201 980, Digital Radio Mondiale (DRM) System Specification, European Telecommunications Standards Institute (ETSI), 2009, V3.1, <https://www.google.co.kr/url?sa=t&rct=j&q=&esrc=s&source=web&cd=1&cad=rja&uact=8&ved=0ahUKEwjwz6fuhPPN>

AhUEn5QKHUkBCAQFggcMAA&url=http%3A%2F%2Fwww.etsi.org%2Fdeliver%2Fetsi_es%2F201900_201999%2F201980%2F03.01.01_50%2Fes_201980v030101m.pdf&usg=AFQjCNG-sKTrr496zRAG4mHyjg7CjOH-Tg&sig2=QmGD6-hT35PoqGoIWDjWAg